

# JUACEP Summer Program 2023 at Nagoya University



Japan-US-Canada Collaborative Education Program

Nagoya University

## Table of Contents

<1> About the Program	----- 3
1-1 Overview	----- 4
1-2 Participants	----- 5
1-3 Schedule	----- 6
<2> Research Achievements	----- 7
2-1 Research Internship: Research Reports	----- 8
2-2 The 27 <sup>th</sup> JUACEP Workshop Presentations	----- 53
<3> Classes and Events	----- 73
3-1 Orientation Sessions	----- 74
3-2 Japanese Course Syllabus	----- 76
3-3 Meet-up for JUACEP Students	----- 78
3-4 Hands-on Workshop	----- 79
3-5 Field Trip	----- 80
3-6 The 55 <sup>th</sup> JUACEP Seminar	----- 81
3-7JUACEP Workshop	----- 82
<4> Participation Essays and Questionnaires	----- 84
4-1 Findings through JUACEP	----- 85
4-2 Questionnaires	----- 92
<5> Appendices	----- 95
5-1 Photo Collection	----- 96
5-2 Building Locations	----- 99
5-3 Mandatory Deliverables	----- 100
5-4 Campus Life Information	----- 101



## <1> About the Program

1-1 Overview ..... 4

1-2 Participants..... 5

1-3 Schedule ..... 6



## 1-1 Overview

### Summer 10-week course 2023 for the students from North Carolina State University and Polytechnique Montréal

*Duration: June 1 – August 30, 2023*

*Research presentations: The 30th JUACEP Workshop on August 9 & 25, 2023*

This program is designed for graduate students from the partner universities in US and Canada, and in 2023 7 students participated. Among them one is from North Carolina State University and 6 are from Polytechnique Montréal.

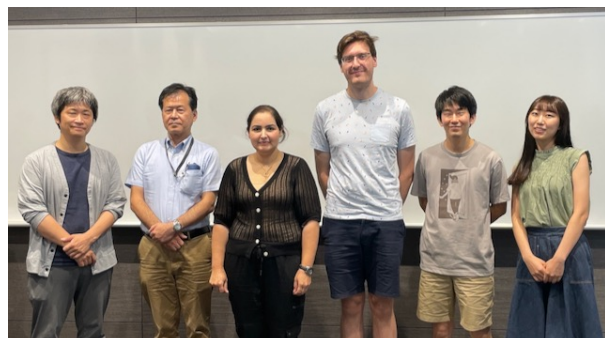
Each participant chose a research laboratory at Nagoya University in accordance with his/her research interest and carried out a research project under the supervisor of the laboratory. Japanese language class for beginner, the hands-on engine-model assembly course and some special events were organized for the program.

During the program period, they took part in the labs' activities such as seminars, sessions, trips, casual parties, and so on. Teaching Assistants (TA) assigned by the program supported the participants not only in research scenes but also in daily life.

At the end of the program, the students submitted their research reports to their respective supervisors and gave the final presentations at the 30th JUACEP Workshop. This workshop was held in the TEL Auditorium of Nagoya University, in a hybrid format with Track A on August 5th and Track B on August 25th.



Workshop on Aug.9



Workshop on Aug. 25

## 1-2 Participants and Nagoya University Staff

	Participants: Name & Affiliation	Adviser & Teaching Assistant at NU
Track A	Catherine DENISOWSKI North Carolina State University Electrical Engineering	Assoc. Prof. Kohei OGAWA TA: Yuki Amemiya Information & Communication Engineering
	Vi RETAULT Polytechnique Montréal Computer Engineering	Prof. Tetsu IWATA TA: Kota KURIBARA Information & Communication Engineering
	Enzo LUCIANI Polytechnique Montréal Aerospace Engineering	Prof. Susumu HARA TA: Ryosuke NAKAMURA Aerospace Engineering
Track B	Arthur BAWIN Polytechnique Montréal Mechanical Engineering	Prof. Toshiro MATSUMOTO TA: Shoketsu TSUTSUMI Mechanical Systems Engineering
	Mohamed MAFTAH Polytechnique Montréal Mathematics for engineering	Assoc. Prof. Tomohiro SOGABE TA: Hepeng WANG Applied Physics
	Hanane TISSIR Polytechnique Montréal Biomedical Engineering	Assoc. Prof. Ryuji KATO TA: Miya KAWASAKI Basic Medical Sciences, Pharmaceutical Science
	Herman MUSUMARI Polytechnique Montréal Civil Engineering	Assoc. Prof. Ryota TSUBAKI TA: Toa KOKURYU Civil Engineering

**Japanese Course Instructor** Ms. Sumie Yasui

### Coordinators of Partner Universities

Ms. Delphine Julien Polytechnique Montréal International (POINT)  
Mr. Tomohisa Koyama Executive Director, NU Tech at North Carolina

### JUACEP Members

Prof. Noritsugu UMEHARA Micro-Nano Mechanical Science and Engineering  
Prof. Toshiro MATSUMOTO Mechanical Systems Engineering  
Prof. Yasumasa ITO Global 30 Automotive Engineering  
Assoc. Prof. Takayuki TOKOROYAMA Micro-Nano Mechanical Science and Engineering  
Assoc. Prof. Reiko FURUYA International Academic Exchange Office  
Lecturer Dina GRIB International Academic Exchange Office  
Tomoko KATO, Administrative staff JUACEP Office

### JUACEP Office

Room #341, Engineering Building II  
Phone +81(0)52-789-2799 or -789-3179

# 1-3 JUACEP Summer Program 2023 Schedule

Day	Day	Date	8:45-10:15	10:30-12:00	13:00-14:30	14:45-16:00	16:15-	
1		June 1 Thu	Arrival, dormitory check-in & self-guided campus tour					
2		June 2 Fri			14:00: Track A: Reception, Stipend and Orientation			
3		June 3 Sat						
4		June 4 Sun						
5		June 5 Mon						
6		June 6 Tue	Research @ each Lab		Research @ each Lab			
7		June 7 Wed	Research @ each Lab		Research @ each Lab			
8		June 8 Thu	Research @ each Lab		Research @ each Lab			
9		June 9 Fri	Research @ each Lab		Research @ each Lab			
10		June 10 Sat						
11		June 11 Sun						
12		June 12 Mon	Research @ each Lab		Research @ each Lab			
13		June 13 Tue	Research @ each Lab		Research @ each Lab			
14		June 14 Wed	Research @ each Lab		Research @ each Lab			
15		June 15 Thu	Research @ each Lab		Research @ each Lab			
16	1	June 16 Fri	Arrival and dormitory check-in		14:00 Track B: Reception, Stipend and Orientation		16:15 Welcome party	
17	2	June 17 Sat						
18	3	June 18 Sun						
19	4	June 19 Mon	Research @ each Lab		Research @ each Lab			
20	5	June 20 Tue	Research @ each Lab		13:45-16:15 Japanese Class① @ E3S-572			
21	6	June 21 Wed	Research @ each Lab		Research @ each Lab			
22	7	June 22 Thu	Research @ each Lab		13:45-16:15 Japanese Class① @ E3S-572			
23	8	June 23 Fri	Research @ each Lab		Research @ each Lab			
24	9	June 24 Sat						
25	10	June 25 Sun						
26	11	June 26 Mon	Research @ each Lab		Research @ each Lab			
27	12	June 27 Tue	Research @ each Lab		13:45-16:15 Japanese Class① @ E3S-572		16:30~ Meet-up	
28	13	June 28 Wed	Research @ each Lab		Research @ each Lab			
29	14	June 29 Thu	Research @ each Lab		13:45-16:15 Japanese Class① @ E3S-572			
30	15	June 30 Fri	Research @ each Lab		Research @ each Lab			
31	16	July 1 Sat						
32	17	July 2 Sun						
33	18	July 3 Mon	Research @ each Lab		13:30 Stipend@JUACEP		Research @ each Lab	
34	19	July 4 Tue	Research @ each Lab		13:45-16:15 Japanese Class① @ E3S-572			
35	20	July 5 Wed	Research @ each Lab		Research @ each Lab			
36	21	July 6 Thu	Research @ each Lab		13:45-16:15 Japanese Class① @ E3S-572			
37	22	July 7 Fri	Research @ each Lab		Research @ each Lab			
38	23	July 8 Sat						
39	24	July 9 Sun						
40	25	July 10 Mon	Research @ each Lab		13:00-16:30 Hands-on workshop @Creation Plaza by JUACEP			
41	26	July 11 Tue	Research @ each Lab		13:45-16:15 Japanese Class① @ E3S-572			
42	27	July 12 Wed	Research @ each Lab		Research @ each Lab			
43	28	July 13 Thu	Research @ each Lab		13:45-16:15 Japanese Class① @ E3S-572			
44	29	July 14 Fri	Research @ each Lab		Research @ each Lab			
45	30	July 15 Sat						
46	31	July 16 Sun						
47	32	July 17 Mon	(Marine day)					
48	33	July 18 Tue	Research @ each Lab		13:45-16:15 Japanese Class① @ E3S-572			
49	34	July 19 Wed	Research @ each Lab		Research @ each Lab			
50	35	July 20 Thu	Research @ each Lab		13:45-16:15 Japanese Class① @ E3S-572			
51	36	July 21 Fri	Research @ each Lab		Research @ each Lab			
52	37	July 22 Sat						
53	38	July 23 Sun						
54	39	July 24 Mon	Research @ each Lab		Research @ each Lab			
55	40	July 25 Tue	Research @ each Lab		Research @ each Lab			
56	41	July 26 Wed	Research @ each Lab		Research @ each Lab			
57	42	July 27 Thu	Excursion by JUACEP					
58	43	July 28 Fri	Research @ each Lab		Research @ each Lab			
59	44	July 29 Sat						
60	45	July 30 Sun						
61	46	July 31 Mon	Research @ each Lab		Research @ each Lab			
62	47	Aug 1 Tue	Research @ each Lab		Research @ each Lab			
63	48	Aug 2 Wed	Research @ each Lab		Research @ each Lab			
64	49	Aug 3 Thu	Research @ each Lab		Research @ each Lab			
65	50	Aug 4 Fri	Research @ each Lab		13:30 Stipend@JUACEP		Research @ each Lab	
66	51	Aug 5 Sat						
67	52	Aug 6 Sun						
68	53	Aug 7 Mon	Research @ each Lab		Research @ each Lab			
69	54	Aug 8 Tue	Research @ each Lab		Research @ each Lab			
70	55	Aug 9 Wed	10:00 30th Workshop I, Special guest talk & Farewell lunch for A&B					
71	56	Aug 10 Thu	Research & Reflection @ each Lab		Deadline of submitting reports			
72	57	Aug 11 Fri	Check out from the dorm & departure		Mountain Day			
58		Aug 12 Sat						
59		Aug 13 Sun						
60		Aug 14 Mon						
61		Aug 15 Tue						
62		Aug 16 Wed						
63		Aug 17 Thu						
64		Aug 18 Fri						
65		Aug 19 Sat						
66		Aug 20 Sun						
67		Aug 21 Mon						
68		Aug 22 Tue	Research @ each Lab		Research @ each Lab			
69		Aug 23 Wed	Research @ each Lab		Research @ each Lab			
70		Aug 24 Thu	Research @ each Lab		Research @ each Lab			
71		Aug 25 Fri	10:00 30th Workshop II					
72		Aug 26 Sat						
73		Aug 27 Sun						
74		Aug 28 Mon	Research & Reflection @ each Lab		Research & Reflection @ each Lab			
75		Aug 29 Tue	Research & Reflection @ each Lab		Research & Reflection @ each Lab			
76		Aug 30 Wed	Research & Reflection @ each Lab		Deadline of submitting reports			
77		Aug 31 Thu	Check out from the dormitory, farewell greetings at each lab and departure					

Track A	Track B
Both tracks	Holiday

## <2> Research Achievements

### 2-1. Research Internship

#### Research Reports

Name	Project topic, <i>Advisor at Nagoya Univ.</i>	Page
Catherine Denisowski NCSU	"Development of an Interactive Real Time Android Communication System" <i>Assoc. Prof. Kohei Ogawa, Information and Communication Engineering</i>	8-16
Vi Retault PolyMTL	"Quantum Circuit of Alzette and Applications" <i>Prof. Tetsu Iwata, Information and Communication Engineering</i>	17-34
Enzo Luciani PolyMTL	"Engineering Educational Research on the Design and Fabrication of a Glider Model" <i>Prof. Susumu Hara, Aerospace Engineering</i>	35-40
Arthur Bawin PolyMTL	"Generation of Unit Curvilinear Meshes in Two Dimensions" <i>Prof. Toshiro Matsumoto, Mechanical Systems Engineering</i>	41 (Undisclosed)
Mohamed Maftah PolyMTL	"Coordination of Drills in Open-Pit Mines: Mathematical & Constraint Programming Formulations" <i>Assoc. Prof. Tomohiro Sogabe, Applied Physics</i>	42 (Undisclosed)
Hanane Tissir PolyMTL	"Investigating Interactions between HUVECs and MSCs in Various Co-culture Configurations" <i>Assoc. Prof. Ryuji Kato, Pharmaceutical Science</i>	43-47
Herman Musumari PolyMTL	"Flow Visualization of Non-Newtonian Fluids - Experimental Approach" <i>Assoc. Prof. Ryota Tsubaki, Civil Engineering</i>	48-52

### 2-2. Presentations

The 30<sup>th</sup> JUACEP Workshop..... 53

# DEVELOPMENT OF AN INTERACTIVE REAL TIME ANDROID COMMUNICATION SYSTEM

Catherine Denisowski

Department of Electrical Engineering, North Carolina State University  
cdeniso@ncsu.edu

Supervisor: Professor Ogawa Kohei

Graduate School of Engineering, Information and Communication Engineering, Nagoya University  
k-ogawa@nuee.nagoya-u.ac.jp

## ABSTRACT

Effective conversations between humans and androids consist of four major components - Speech Recognition, Voice Activity Detection, Response Generation, and Verbal Response. Speech recognition involves the conversion of audio containing human speech into a text transcript, and this converts the speech into a format that the android can understand. Voice activity detection determines whether the (human) user is finished speaking or becomes silent. This allows the android to know when the human is finished speaking so that it can respond with the appropriate timing. Response generation means that an appropriate and logical response will be created to ensure a meaningful conversation. Once the response has been generated, text to speech software is used to produce a verbal response to the human user. In this paper, a system which incorporates these four components will be explored.

## 1. INTRODUCTION

The first system capable of speech recognition was developed in 1952 by Bell Laboratories. This system was capable of recognizing which single digit number (0-9) was spoken [1]. Soon after this, the first Japanese speech recognition system was developed by the Radio Research Lab in Tokyo. This system was developed in 1961 and was capable of recognizing different vowel sounds [2]. Shortly thereafter, increasingly complex ASR (automatic speech recognition) systems were developed in a variety of countries, utilizing different technologies such as speech segmentation, speech clustering algorithms (to make systems speaker-independent), and the hidden Markov model [1]. In the present day, many ASR systems are available for personal and commercial use, such as Google Speech-to-Text, Microsoft Azure Speech-to-Text, and Amazon Transcribe.

The speech recognition tool used in this system is Whisper. This is an open-source ASR system developed by OpenAI. It has two main modes of operation – transcription and translation. Translation will produce a text translation of audio, but currently it is only able to translate non-English languages into English. Transcription will produce a text output based on audio input, and it is available in 97 languages including English and Japanese [3]. This is the mode of operation used in this system.

Whisper is a very robust and versatile tool. It was trained on 680,000 hours of audio data – 438,218 hours of English and 7,054 hours of Japanese [3]. Additionally, Whisper is built with an encoder-decoder transformer architecture. It processes 30 seconds of audio at a time, and this “processing window” moves during processing of the audio file [3]. Please see *Figure 1* for a block diagram of the system architecture.

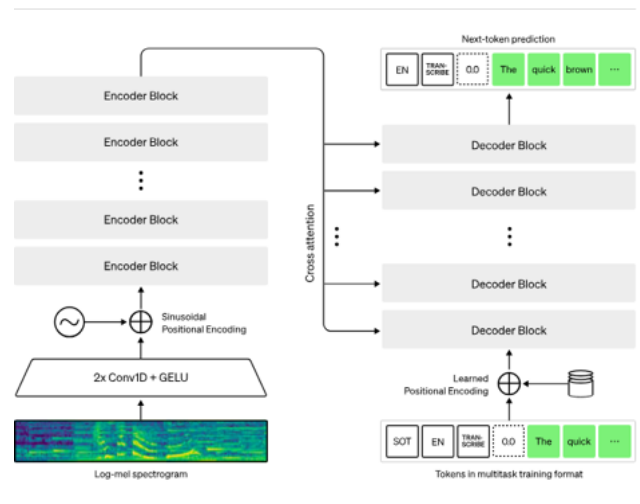


Figure 1 – Encoder-Decoder Transformer Architecture Used in Whisper [4]

Another important feature of Whisper is the many different model sizes available. Please refer to *Table 1* for numerical specifics about each model.

Table 1 – Different Available Whisper Model Sizes [5]

Size	Parameters	English-only model	Multilingual model	Required VRAM	Relative speed
tiny	39 M	tiny.en	tiny	~1 GB	~32x
base	74 M	base.en	base	~1 GB	~16x
small	244 M	small.en	small	~2 GB	~6x
medium	769 M	medium.en	medium	~5 GB	~2x
large	1550 M	N/A	large	~10 GB	1x

Between different model sizes, there is a trade-off between accuracy and speed. For example, the smallest model (*tiny*) is much faster but somewhat less accurate than the largest model (*large-v2*). This effect was measured and the results are presented in *Table 2*. There is a clear relationship between model size (number of parameters) versus amount of time needed to produce a transcript (processing time). Word error rate (WER) is also measured, although there is a very minimal effect as Whisper already has a very high rate of accuracy.

*Table 2 – Effect of Model Size on Processing Time and Word Error Rate*

Model Size	Processing Time (s)	Word Error Rate (%)
tiny	5.0	8.7
tiny.en	5.0	0.0
base	9.8	0.0
base.en	9.6	0.0
small	28.8	0.0
small.en	27.6	0.0
medium	97.8	0.0
medium.en	107	0.0
large	332.2	0.0
whisper-l	329.8	0.0

The majority of Whisper’s model sizes are open-source and completely free, but one model size (*whisper-l*) is under the Whisper API. This model is equivalent in size to the “*large*” model, and costs \$0.006/minute of audio [6]. Since the *tiny* model (which is open-source) was found to be the most effective model size for this system, no API usage was necessary for Whisper.

Whisper was selected for this system because of its ease of use and versatility. Whisper requires very little setup (which will be discussed later in this paper) and works well in both English and Japanese, the two languages needed for this system. Additionally, Whisper’s WER (word error rate, or accuracy) is very low compared to other popular ASR options. When transcribing the Librispeech clean data set, the following WER were measured (*Table 3*):

*Table 3 – Word Error Rate for Different ASR systems under the Librispeech Clean Data Set [7]*

	Word Error Rate
Whisper	2.7%
Google Speech-to-Text	12.1%
Microsoft Azure Speech-to-Text	18.8%
Amazon Transcribe	22.0%

In comparison to three of the major ASR systems that are widely available, Whisper demonstrates a clear advantage in terms of accurate transcriptions.

The other key component for successful human-android conversation is voice activity detection, also known as silence detection. While different VAD systems such as Silero VAD and WhisperX were explored, none of them proved to be compatible with the rest of the system. To combat this, two different approaches were used for detecting voice activity – a manual approach utilizing a button press and an automatic approach using the “pydub” Python package. The manual silence detection method requires the user to press and hold the SPACE key while they are talking and release it when they are done. This manual method allows for the most accurate way for silence to be detected (as it puts that responsibility on the user), but it is also the least advanced way to implement this. The automatic method uses the *split\_on\_silence* function in the “pydub” Python package, which is used to automatically detect when the user has been silent for a configurable amount of time (currently set to 1 second). While this method requires less user input it is less accurate than the manual mode.

The android used in this system is called Android U (nicknamed Yu-chan). This android was developed by the Ishiguro Lab and has the appearance of a human woman, as can be seen in *Figure 2*.





Figure 2 – Android U / Yu-chan

Through the use of text-to-speech software and custom android control software, Yu-chan is able to both verbally respond to users and produce realistic mouth, eye, and head movements. This allows for an effectively simulated conversation between a human and an android.

## 2. SYSTEM ARCHITECTURE

### 2.1 Overview

The system was developed in Python. It consists of the following major components, each of which will be elaborated on in subsequent sections.

Human speech is recorded through a microphone, transcript text is produced using the Whisper speech recognition software, and the full transcript is sent to ChatGPT over TCP once silence is detected (the user stops talking). Once a response has been generated, it will be converted into audio with text-to-speech software and Android U (Yu-chan) will speak with live lip-synching.

This system is divided into two major components – the “Client” and the “Server.” These two components are connected over a TCP socket, and text data is sent between the “Client” and the “Server.” The “Client” refers to the code that records audio, produces a transcript with Whisper, and detects silence to know when the user is finished speaking. The “Server” refers to the code that uses ChatGPT to generate a response, produces an audio response using text-to-speech software, and manages the algorithm used to control Yu-chan’s lip-synching movement. In the remainder of this paper,

“Client” and “Server” will be used to refer to this different functionality.

For a visual representation of the system, please refer to Figure 3.

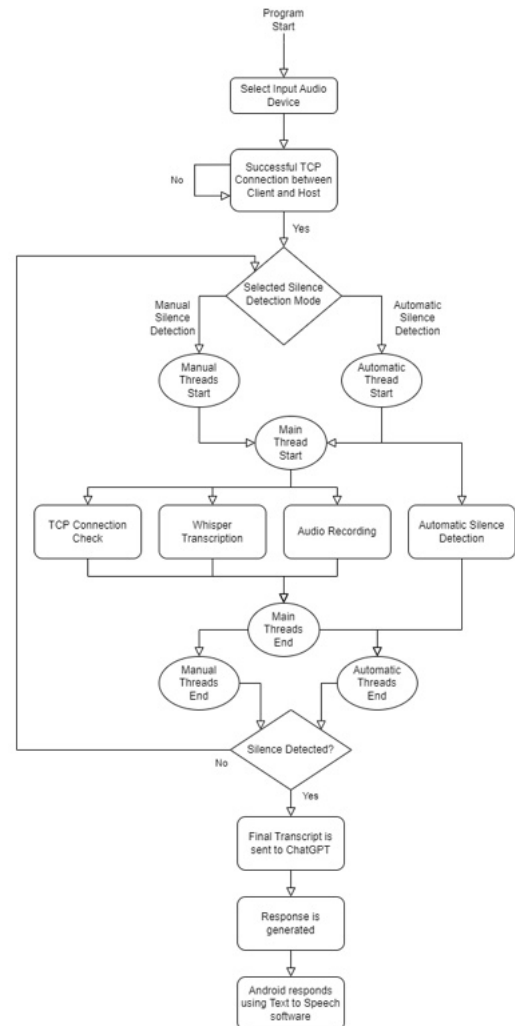


Figure 3 – Flowchart Showing Full System Operation

### 2.2 System Initialization

Upon startup, the system will list all available input audio devices and prompt the user to choose one. This approach was chosen because every user will have different hardware, so it is easiest to ask them to manually select an appropriate device. After this, the TCP socket needed for communication between the Client and the Server will be created. If connection is not possible, the Client will reattempt until socket creation is possible.

Once these initialization steps are completed, the main program loop will be determined by the mode of silence detection set before the program begins. If the manual / “button press” mode is selected, the main mode of operation will begin once the SPACE key is held and pressed. This main mode of operation involves the use of three threads running simultaneously: a TCP connection check, the recording of 5

second audio clips, and transcription of those clips using Whisper.

If the automatic silence detection mode is selected, the main mode of operation begins once any key is pressed. This main mode of operation involves the use of four threads running simultaneously: a TCP connection check, the recording of 5 second audio clips, transcription of those clips using Whisper, and a silence detection thread.

Threading was used to ensure that the conversation was as close as possible to “real-time.” By running multiple processes simultaneously, this reduces the processing time needed from audio recording to a spoken response from Yuchan. Each of these threads will be elaborated on in the subsequent sections.

### 2.3 TCP Connection Check

As mentioned, communication between the Client and Server is done over a TCP connection. Specifically, text data is communicated over a TCP socket from the Client to the Server. Because of this, the first thread is “TCP Connection Check”, and this checks that the TCP connection between the Client and the Server is still active.

To do this, the Client will attempt to send a blank message over the socket to check the connection status. If the transmission is successful, no further action will be taken. If the transmission is unsuccessful, the Client will attempt to reconnect to the Server.

### 2.4 Audio Recording

The second thread in the program is audio recording. Recording is done using the “pyaudio” Python package. The recorded audio is mono / 1 channel and has a sampling rate of 44.1 kHz. As mentioned, audio is recorded in 5 second iterations, and these iterations are saved as WAV files. These filenames contain important information, such as a user-set prefix and both the iteration and dialogue number of the current program run.

#### 2.4.1 Iteration / Dialogue

These two terms are used to refer to different ways to divide the recorded audio segments. “Iteration” refers to one audio recording, which is configured for 5 seconds in the system. “Dialogue” refers to the full audio recording for an entire statement spoken by the user. A “dialogue” is made up of “iterations”, and the number of “iterations” depends on how long the “dialogue” is. For example, 2 seconds of speech would be 1 “iteration” and 1 “dialogue”, while 23 seconds of speech would be 5 “iterations” and 1 “dialogue”. In the remainder of this paper, the terms “Iteration” and “Dialogue” will be used to refer to this distinction.

### 2.5 Speech Recognition

#### 2.5.1 Whisper Transcription

As mentioned previously, OpenAI’s Whisper ASR system is used to produce transcripts of recorded audio. One

important thing to note is that this third thread does not take place until the second time the threads are run. This is because the first time the threads are run, there is no recorded audio to analyse. Because of this, transcription always occurs on the previously iteration instead of the current iteration.

Whisper requires very little syntax or setup to run. Here is the code needed to run this tool with all of the extra parameters included:

```
model = whisper.load_model("tiny")
promptGiven = "Hello, it's so great to meet you!"

transcript_args = dict(
    task = whisper_task,
    temperature = temperature_vals,
    fp16 = False)

transcript_audio = model.transcribe(audio_transcribe,
prompt = promptGiven, **transcript_args)
```

Figure 4 – Code Used in Whisper Transcription

As can be seen from Figure 4, *audio\_transcribe* is the audio file being transcribed, and transcript text is saved in the *transcript\_audio* variable. *model.transcribe* calls Whisper – *model* is the selected model size, and this is currently set to “tiny.” Since speed was the most important constraint to make the conversation as real time as possible and since there were minimal effects to WER/accuracy, the *tiny* model was used in this code.

The remainder of the variables are parameters used for correct Whisper output. While all of these parameters are used to ensure that the system runs as desired, not all of them are inherently required. The only required parameters are *model* and *task* (set to transcribe), and Whisper can successfully run with just these parameters.

*Temperature* is a parameter used to control variability in transcripts produced by Whisper. Essentially, higher *temperature* values will lead to more differences between transcripts produced from the same audio file. In the current system, the *temperature* values are set to (0.0, 0.2, 0.4, 0.6, 0.8, 1.0). For each transcription, each value will be used starting with 0.0, and *temperature* that produces the transcript with the highest confidence value (*avg\_logprob*) will be selected.

*fp16* is a format for floating point numbers to be used in code. To run Whisper on CPU (which was used in this system) *fp32* was required. Because of this, *fp16* was set to False so that transcription could occur.

The *prompt* parameter is set in the code and is used to enforce the desired formatting (such as capitalization and punctuation). In this system, it is currently set to “Hello, it’s so great to meet you!”

#### 2.5.2 Hallucination Filtering

Whisper sometimes detects words that were not spoken, especially during periods of silence. These are often referred to as “hallucinations.” One important consideration when



using Whisper is being able to accurately filter hallucinations out of transcriptions. To help ensure that Whisper transcribes hallucinations as infrequently as possible, some common hallucinations are saved within lists to compare against the transcript.

There are two lists within the code – *suppress\_low* and *suppress\_high*. *suppress\_low* contains phrases such as “Thank you” and “Bye bye!” – phrases which could be normal human speech but are common hallucinations. *suppress\_high* contains phrases such as “Thank you for watching” and “See you next week,” which are extremely common hallucinations and much more unlikely statements from a human. If a transcript which contains one of the hallucinations is detected, its *avg\_logprob* / confidence value will be lowered by 0.20 for *suppress\_low* and 0.5 for *suppress\_high*.

While these comparisons may lower the *avg\_logprob* of a transcription, this does not automatically filter the text in that transcription. After all, it is still possible for phrases in the list to be human speech, even if it is unlikely. Transcription text is filtered out if it meets one of two conditions: *avg\_logprob* < -0.9 or *no\_speech\_prob* > 0.6.

As mentioned previously, *avg\_logprob* represents Whisper’s confidence in its transcription. The closer this value is to 0, the greater the probability that the transcription is accurate. If this value is below -0.9 after adjustment from the *suppress\_low/suppress\_high* lists, the transcript is presumed to be a hallucination and it is filtered out.

The other metric used for filtering is *no\_speech\_prob*. This value is calculated by Whisper during transcription and represents the probability of an audio segment being silent. If this value is above 0.6, the transcript is presumed to be a hallucination and it is filtered out.

### 2.5.3 Transcript Files

After each iteration has been recorded and transcribed, each transcript iteration will be saved to a text (.txt) file. These files contain not only the transcribed text, but also key parameter information such as temperature, *avg\_logprob*, *no\_speech\_prob*, and detected language. Additionally, the prompt set within the code and any filtered hallucination are recorded. These files are not accessed later in the code and mainly exist for debug/record purposes. Transcript text is saved to a global list within the system, and this is the source for the final transcript produced and sent to ChatGPT. Please refer to *Figures 5 and 6* for examples of a valid / non-filtered transcript and an invalid / filtered transcript:

```
Prompt: Hello, it's so great to meet you!

{'text': ' One, two, three, four, five, six.', 'segments':
[{'id': 0, 'seek': 0, 'start': 0.0, 'end': 6.0, 'text': ' One,
two, three, four, five, six.', 'tokens': [50364, 1485, 11, 732,
11, 1045, 11, 1451, 11, 1732, 11, 2309, 11, 2309, 11, 2309, 13,
50664], 'temperature': 0.6, 'avg_logprob': -0.5233765652305201,
'compression_ratio': 1.162162162162162, 'no_speech_prob':
0.2679491937160492}], 'language': 'en'}
```

Figure 5 - Text File Contents of Valid Transcript

```
Prompt: Hello, it's so great to meet you! Prompt: Hello, it's so
great to meet you!
```

```
{'text': ' ', 'segments': [{'id': 0, 'seek': 0, 'start': 0.0,
'end': 5.0, 'text': ' See you next time!', 'tokens': [50364,
3008, 291, 958, 565, 0, 50614], 'temperature': 0.0,
'avg_logprob': -1.4155068397521973, 'compression_ratio':
0.6923076923076923, 'no_speech_prob': 0.46128085255622864}],
'language': 'nn'}
```

```
Output pre-filtering: ' See you next time!'
```

Figure 6 – Text File Contents of Invalid Transcript

One other important note about the Whisper transcription is that text needs to be properly encoded before it is saved to the file. It is especially important to do this when Japanese is used, as Japanese characters are not supported under ASCII character encoding. To resolve this, all files are saved under the UTF-8 character encoding.

## 2.6 Voice Activity/ Silence Detection

### 2.6.1 Manual Mode

The manual silence detection mode is a very simple algorithm which requires the user to tell the system when they are speaking. The method works without requiring an additional thread. After the system has been initialized, the user will be given the following prompt:

```
Once you press and hold SPACE, recording will begin.
When you are done talking, release the SPACE key and a
response will be generated.
To continue the conversation, press and hold the
SPACE key again once a response has been generated.
When you are done with your conversation, please
press and hold the SPACE key and say 'おやすみなさい' or
'Good night' to end the program.
Please press SPACE to begin.
```

Figure 7 – User Prompt Upon Startup in Manual Mode

As the code in *Figure 7* describes, pressing and holding the SPACE key signals to the system that the user is speaking, and when it is released the system knows that the user is now silent. Once this silence has been detected, the system will consolidate all available iteration transcripts, creating a dialogue transcript which can be sent to ChatGPT for response generation. Once a response has been generated and spoken back to the user, the following prompt shown in *Figure 8* will be displayed:

```
Please press and hold the SPACE key to continue your
conversation.
When you are done with your conversation, please
press and hold the SPACE key and say 'おやすみなさい' or
'Good night' to end the program.
Please press SPACE to continue.
```

Figure 8 – User Prompt Between Dialogue in Manual Mode

If desired, the user may begin speaking again after pressing the SPACE key, and this will start the next dialogue. This loop will continue as long as the user desires and will

end when the user's final statement to the android is either 'おやすみなさい' or 'Good night' depending on the language of the conversation.

While this mode of silence detection is the simplest to implement and most accurate, it requires the user to take additional action.

## 2.6.2 Automatic Mode

The automatic silence detection mode is a more complex algorithm which requires an additional thread to be used. After the system has been initialized, the user will be given the following prompt as shown in *Figure 9*:

```
Audio recording will begin as soon as you press
any key.
When you are done with your conversation, please say
'おやすみなさい' or 'Good night.' to end the program.
Press any key to begin.
```

*Figure 9 – User Prompt Upon Startup in Automatic Mode*

Once the user presses any key, the system will automatically start recording and transcribing audio. At the same time, the system will also be checking each iteration to see if there is silence. The method that it uses to do this is the *split\_on\_silence* function in the "pydub" Python package. To detect silence, this function is used on each iteration and if the audio file was split into multiple smaller files, then silence was detected and the user is done speaking.

The two parameters used to split the files are *min\_silence\_len* and *silence\_thresh*. Both of these conditions must be met for a split to occur. *min\_silence\_len* is the minimum amount of time that silence needs to be present in order for a lower level of sound to be determined "silence." This is currently set to 1000 milliseconds (or 1 second), and this time was selected because it is long enough that it is unlikely to be a pause between words, but short enough to not slow down the android's response time unnecessary. The second parameter (*silence\_thresh*) is the level that the sound in the audio file must reach in order to be considered silence. This value is currently set to -55 dBFS, and this was found experimentally. It is important to note that both of these parameters are easily changeable and are highly dependent on the environment (factors such as background noise) and the individual users themselves.

If at least one second of audio at -55 dBFS or lower is detected in an iteration file, the file will be split into subfiles. From there, if multiple audio files are present then it will be determined that the user is done speaking. The system will then consolidate all available iteration transcripts, creating a dialogue transcript which can be sent to ChatGPT for response generation. Once a response has been generated and spoken back to the user, the following prompt shown in *Figure 10* will be displayed:

```
When you are done with your conversation, please
press say 'おやすみなさい' or 'Good night' to end the
program.
Please press any key to continue.
```

*Figure 10 – User Prompt Between Dialogue in Automatic Mode*

If desired, the user may begin speaking again after pressing any key, and this will start the next dialogue. This loop will continue as long as the user desires and will end when the user's final statement to the android is either 'おやすみなさい' or 'Good night' depending on the language of the conversation.

While this mode of silence detection has the potential to be the most convenient, it still has somewhat inconsistent operation. This will be discussed later in this paper, but it was found that the system operation / parameters necessary are highly dependent on the environment and the user.

## 2.7 Response Generation

As mentioned, once silence has been detected in either mode, the iteration transcripts are collected from the global list and consolidated into one larger dialogue transcription. While all available text is now in one place, it must be converted into the proper format for ChatGPT. This format is "UTF-8," and this is necessary to support Japanese characters. After this, only one final check will be made. If the transcript text is found to be either 'おやすみなさい' or 'Good night,' then the program will end as the user has signalled that they are done with the conversation.

Once these steps are completed, the transcript text is sent to the Server over the TCP socket. Before ChatGPT is then called, transcript text and the initial prompt for ChatGPT must be combined to ensure the most appropriate response is generated. Here is the initial prompt (translated from Japanese):

```
"You are a female android developed by Ishiguro
Laboratory, and your name is Android 'U'. Your nickname
is "Yu-chan". Please have a conversation while observing
the following three rules. 1. Respond briefly and keep
your responses as short as possible. 2. Have a frank
conversation like a friend. 3. Occasionally ask a
question. "
```

*Figure 11 – Initial Prompt Given to ChatGPT*

Transcript text included in the prompt for ChatGPT (shown in *Figure 11*) does not only include the most recent user dialogue. It also includes up to the last 4 user dialogues, and maintaining this history allows ChatGPT to refer back to previous points in the conversation. Once all of this information has been combined with the initial prompt, it will be sent to ChatGPT and an appropriate response will be generated.

After a text response has been generated, it will need to be converted into an audio response to allow Yu-chan to "speak" to the user. There are two major components to this: text to speech software and android control software. Text to speech software is fairly straightforward, as it converts text into speech, allowing for Yu-chan to verbally respond to the user. Based on the language, the text-to-speech software used

is either “watanabe\_ver4.0\_22” for Japanese or the “mac\_say” Python package in English which utilizes the “say” command on MacOS. The Android Control Software controls Yu-chan’s physical movements such as mouth movements, blinking, and head movements. This allows for Yu-chan to be lip-synched to the produced speech and for her to produce other natural human movements. By utilizing these two types of software, Yu-chan is able to respond in a fairly natural manner, allowing for a true conversation between a human and an android.

### 3. KEY FINDINGS

Throughout the development of this system, many different approaches and parameters were tested to ensure the best possible system operation. Because of this, many incremental tests were done which demonstrated system performance at different key milestones (Whisper transcription works, Whisper can transcribe live audio, manual silence detection works, etc.). However, since the full system is still relatively new, full system in-depth tests have not yet been completed. However, key patterns regarding system operation have emerged through more casual and realistic conversations. Below are a few key findings.

#### 3.1 Automatic silence detection parameters are highly variable based on environment and speaker.

While manual silence detection (“button press”) was simple to implement and refine, automatic silence detection has presented some difficulties. Once the program logic was determined, the last remaining step was to refine the main parameters: *min\_silence\_len* and *silence\_thresh*. However, this soon proved to be more difficult than initially anticipated.

Initial tests of the automatic silence detection algorithm were done in a quiet apartment. Three different kinds of audio were tested – pure silence, pen clicking (non-speech noises), and human speech. For the pen clicking and human speech tests, audio files were recorded at different distances from the external microphone to test the effect of sound volume on silence detection accuracy. *min\_silence\_len* was kept at 1000 milliseconds for all of these tests.

The results of these tests are listed below in *Table 4*. To summarize, *silence\_thresh* values of -28 dBFS and higher (such as -16 dBFS which is the default function value and -6 dBFS) were found to not be sensitive enough. While silence and pen clicking were recognized correctly at these *silence\_thresh* values, speech was detected as silence. While silence, pen clicking, and speech were correctly detected at -40 dBFS, the transcriptions were not fully accurate as there were errors with repeated words or delayed program operation. Despite this, -40 dBFS was used as the initial *silence\_thresh* value as it showed the most promise due to its relative accuracy and speed of analysis.

*Table 4 – Effect of silence\_thresh on Silence Detection Accuracy (Initial Test)*

Type of Audio	silence_thresh (dBFS)	Successfully identified?
Silence	-6	Yes
Pen clicking	-6	Yes
Human Speech	-6	No
Silence	-16	Yes
Pen clicking	-16	Yes
Human Speech	-16	No
Silence	-28	Yes
Pen clicking	-28	Yes
Human Speech	-28	No
Silence	-40	Yes
Pen clicking	-40	Yes
Human Speech	-40	Yes, with errors

However, later testing was done in a meeting room within the laboratory. When conducting these tests, it was found that -40 dBFS was not a suitable *silence\_thresh* value, as it was not sensitive enough. Further experiments determined that -55 dBFS was a more appropriate value for properly differentiating between silence and speech.

*min\_silence\_len* is also a key parameter in automatic silence detection. While 1000 milliseconds or 1 second was selected for this value, pauses in the middle of human speech can be incredibly variable. This parameter has not been fully fine-tuned yet, as it is easier to control pauses between words than silence levels (especially depending on the environment). More focus has been placed on *silence\_thresh*, so *min\_silence\_len* will need to be explored further in the future.

#### 3.2 Different operating systems lead to different system performance.

Surprisingly, system performance was different based on what operating system was used. This system was initially developed on a Windows computer, so initial testing was done using the Windows operating system. For example, this operating system was used for the initial automatic silence detection tests done in the quiet apartment (*results in Table 4*). However, after this point, testing was done under the MacOS system, as equipment in the lab was more compatible with that operating system.

A key difference between operating systems is how program logic functioned. One example of this is how the initial keyboard prompt functioned. After the user is prompted to select an input audio device upon startup, the user will be given the prompt in either *Figure 7* or *9* depending on the selected silence detection method. However, while the system will wait for a key press for the automatic silence detection mode under the Windows operating system, audio recording begins immediately under

MacOS. Additionally, it was found that file operations (opening, reading, and closing files) were much slower under MacOS than Windows, and this led to delays in system operation. Since a majority of the members of the lab and much of the existing equipment available was better suited for MacOS, the system was modified to prioritize better functionality under this operating system.

### 3.3 There is a clear difference in system effectiveness in English and Japanese.

Initial system development was done in English, so initial tests were done in English. As the system became more advanced and there were components to test, development began in Japanese. This was relatively easy to implement, as the only major differences between the English and Japanese systems were the Text to Speech voice model, the appropriate phrase the user needs to say to end the program, and Yu-chan’s response to this phrase. These phrases are shown below in *Table 5*.

*Table 5 – Differences in Program End Phrases Between English and Japanese)*

	English	Japanese
User:	‘Good night.’	‘おやすみなさい’
Yu-chan:	‘Good night. Sweet dreams! I shut down the system.’	‘おやすみなさい。またお話ししましょうね。システムを終了します’

Despite these minor differences, the English version of the system tended to be more effective than the Japanese version of the system in terms of accuracy and speech. While there is not a definitive explanation for the difference, it is strongly suspected that this is due to the difference in training audio between the English and Japanese versions of Whisper. There is over 60 times more English audio than Japanese audio, at 438,218 hours of English compared to 7,054 hours of Japanese. Aside from using another tool, not much can be done to easily resolve this discrepancy.

## 4. CONCLUSION AND NEXT STEPS

The human-android communication system described in this paper is incredibly robust and capable of developing appropriate responses to a human user by combining Automatic Speech Recognition, Voice Activity Detection, Response Generation, and Text to Speech software. This system allows for real time conversations between a human and an android and has a simple user interface which allows any user to easily communicate with the android. While the current system performance can be variable (especially for automatic silence detection), proper fine-tuning of key parameters should be sufficient for generating more uniform results.

This system has been tested by other lab members and by high school students at events such as the WWL Summer Lecture and Open Campus Events. These experiences allowed the system to be tested in “real-world” situations, and this provided invaluable data on system functionality and capability. Please see *Figure 12* to see system setup for these scenarios.



*Figure 12 – Example System Setup for Human-Android Conversation*

Further work on the system will mainly focus on fine-tuning key system parameters, but investigation will also be done into improving system effectiveness in Japanese. This may involve research into another ASR tool, but refining Whisper’s effectiveness in Japanese will be explored first.

## ACKNOWLEDGEMENTS

I would like to thank the JUACEP program for this valuable research opportunity. Special thanks to Ogawa-sensei and the members of my lab, specifically Amemiya Yuki, Kobayashi Atsushi, Yamaguchi Daichi, and Tumul Kumar for being very welcoming and helpful throughout my time in the lab.

## REFERENCES

- [1] Juang, B. H., and Lawrence R. Rabiner. *Automatic Speech Recognition – A Brief History of the Technology Development*. Oct 2004. [https://web.ece.ucsb.edu/Faculty/Rabiner/ece259/Reprints/354\\_LALI-ASRHistory-final-10-8.pdf](https://web.ece.ucsb.edu/Faculty/Rabiner/ece259/Reprints/354_LALI-ASRHistory-final-10-8.pdf).
- [2] Suzuki, Joji, and Kazuo Nakata. “RECOGNITION OF JAPANESE VOWELS - Preliminary to the Recognition of Speech (1).” *Journal of the Radio Research Laboratories*, vol. 8, no. 37, Apr. 1961, p. 193 – 212, [https://www.nict.go.jp/publication/journal/08/037/Journal\\_Vol08\\_No037\\_pp193-212.pdf](https://www.nict.go.jp/publication/journal/08/037/Journal_Vol08_No037_pp193-212.pdf).
- [3] Radford, Alec, et al. *Robust Speech Recognition via Large-Scale Weak Supervision*. Sept. 2022, <https://cdn.openai.com/papers/whisper.pdf>.

- [4]“Introducing Whisper.” *OpenAI*, 21 Sept. 2022, <https://openai.com/research/whisper>.
- [5]“Whisper.” *GitHub*, <https://github.com/openai/whisper/blob/main/README.md>.
- [6]Brockman, Greg, et al. “Introducing ChatGPT and Whisper APIs.” *OpenAI*, 1 Mar. 2023, <https://openai.com/blog/introducing-chatgpt-and-whisper-apis>.
- [7]“Automatic Speech Recognition (ASR) Systems Compared.” *Medium*, 7 July 2021, <https://medium.com/sciforce/automatic-speech-recognition-asr-systems-compared-6ad5e54fd65f>.

# Quantum Circuit of Alzette and Applications

Vi Retault

Polytechnique Montréal, Montreal, Canada  
vi@retau.lt

Supervisor: Tetsu Iwata  
Nagoya University, Nagoya, Japan  
tetsu.iwata@nagoya-u.jp

**Abstract.** Grover’s search algorithm offers a quadratic speedup in secret key brute-force attacks on symmetric cryptography. It requires the encryption algorithm to be implemented as a quantum oracle. This paper presents an optimized quantum circuit design for TRAX-L-17, a lightweight tweakable block cipher based on the ARX-box Alzette. We provide a comprehensive, step-by-step explanation of the circuit construction process, evaluating the quantum resources needed in terms of gate count, circuit depth and quantum cost. We then estimate the cost of running Grover’s search on it. Our method introduces a novel approach that combines different adder types in order to maximize parallelism in scenarios with a limited number of qubits. Additionally, we introduce `pyqcrypto`, a Python library aimed at facilitating the implementation of classical ciphers as quantum circuits.

**Keywords:** Quantum Computers · Quantum Gates · Grover’s Algorithm · Lightweight Tweakable Ciphers · Quantum Cryptanalysis

## 1 Introduction

Quantum computing poses a significant threat to current cryptographic algorithms [11]. Shor’s algorithm compromises the confidentiality of asymmetric cryptography schemes, such as RSA and elliptic-curve cryptography [3, 15]. Grover’s search algorithm [5] can be used to perform  $n$ -bit key recovery attacks in  $\mathcal{O}(\sqrt{2^n})$  on symmetric cryptographic algorithms. These types of attacks have already been evaluated on block ciphers (e.g., AES [9]) and stream ciphers (e.g., ChaCha [1]).

Before standardizing a new cipher, it is crucial to assess its susceptibility to such attacks. Recent endeavors in cryptography have been directed towards lightweight block ciphers, with the conclusion of the NIST Lightweight Cryptography Standardization Process [20]. Among the final candidates, the permutation SPARKLE and the derived authenticated block cipher scheme SCHWAEMM received a quantum resource estimation [23]. The cipher ultimately selected for standardization, ASCON, was also recently evaluated [13], as did other lightweight block ciphers, including SPECK [8] and GIFT [7].

In this work we developed a quantum circuit implementation of TRAX-L-17, a tweakable lightweight block cipher from the SPARKLE suite, based on the 64-bit ARX-box Alzette [2]. It has a block length of 256 bits, a 256-bit key and a 128-bit tweak and is composed of 17 rounds of TRAX-L. TRAX-L is the largest cipher of the TRAX family which also includes TRAX-S and TRAX-M, respectively operating on 64 and 128 bits. Tweakable block ciphers are particularly well-suited for disk encryption, where each block is encrypted with a distinct tweak.

We carry out a comparative study on the quantum implementation of TRAX-L-17 using various methods. Our findings highlight the significance of selecting suitable adder circuits to balance the trade-off between circuit depth and width. The depth of a circuit refers to the maximum number of sequential gates while the width refers to the number of qubits required. When sufficient ancilla qubits are available, employing carry-lookahead adders in parallel for Alzette and sequentially for the key schedule is recommended to minimize the circuit depth, while to minimize the number of ancilla qubits it is best to arrange all of the adders sequentially. To facilitate this investigation, we develop the `pycrypto` Python library, which streamlines the implementation of quantum circuits for classical cryptography. Leveraging this library simplifies the execution of operations on quantum registers, and automatically evaluates the resulting circuits.

Based on the quantum circuit of TRAX-L-17, we present our estimate of the cost to run Grover’s search on it.

Comparing different implementations of quantum circuits is a challenging task due to the varying metrics employed in different research papers. To address this concern, we employ the quantum cost (QC) metric defined in [12]. To compute the quantum cost of a circuit we decompose it into  $1\times 1$  and  $2\times 2$  gates, with the quantum cost of those primitive gates being 1. We also calculate the circuit depth, number of ancilla qubits and number of NOT, Controlled NOT (CNOT) and Toffoli gates.

The paper is organized as follows. In Section 2, we review the operations on quantum registers, in particular the different types of addition. In Section 3, we describe how to implement TRAX-L-17 and in Section 4, we present Grover’s search and evaluate it in terms of quantum cost, circuit depth, and circuit width. Finally, we conclude the paper in Section 5.

## 2 Quantum Register Operations

Currently, building quantum circuits for classical algorithms such as block ciphers is difficult because there are no straightforward quantum equivalents of fundamental classical operations. For instance, Alzette uses 32-bit addition, rotation and XOR operations which can be implemented easily on a 32-bit processor using built-in instructions on 32-bit registers [2]. In contrast, such register operations are not yet properly defined for quantum computers. Instead, circuits are constructed using basic logic gates applied on one or two qubits. We aim to provide a framework for register operations on quantum computers.

Prior work on this topic includes `Chisel-Q`, a high-level language based on Scala to automatically build quantum circuits from classical algorithms [10]. While this work makes it easier to implement classical operations, the high-level nature of the language doesn't leave room for manual optimization, which is desirable to implement cryptographic algorithms efficiently.

In this section, we present `pycrypto`, a Python library that extends IBM's Qiskit toolchain [22] to operate on  $n$ -bit quantum registers. We selected Python for its popularity among researchers and its user-friendly nature. Our library offers quantum register operations for rotation, NOT, XOR and addition, extending the existing `QuantumCircuit` class from `Qiskit`. Furthermore, it can be easily expanded to include new operations.

## 2.1 Definitions

We define an  $n$ -bit quantum register as a view on  $n$  logical qubits.

$$R = (q_0, q_1, q_2, \dots, q_{n-1}).$$

A quantum register operation `op` is then defined as a mapping between input quantum registers  $R$  and output quantum registers  $R'$ , and a series of quantum gates applied to the qubits of the input. The output qubits are essentially a permutation of the input qubits, grouped as registers.

$$\text{op} : (R_0, R_1, R_2, \dots, R_{p-1}) \mapsto (R'_0, R'_1, R'_2, \dots, R'_{q-1}).$$

In summary, quantum register operations generate new views of the input qubits that will contain the result of the operation after the gates are applied. This construction allows to swap qubits without using any gates.

We propose to leverage the `QuantumRegister` class from `Qiskit` to track the views on qubits. Quantum register operations are then implemented as subclasses of an abstract `rOperation` class which accepts instances of `QuantumRegister` as inputs and outputs. Those operations can be used in the same manner as operations from `Qiskit` by using the `rCircuit` class that extends `QuantumCircuit`. This method enables smooth integration of quantum register operations with the existing procedures in `Qiskit`.

## 2.2 Gate-free Rotation

With these definitions, it is possible to implement a  $k$ -bit left and right rotation operation on an  $n$ -bit quantum register without using any gates.  $\llbracket a, b \rrbracket$  is the set of integers  $\{a, \dots, b\}$  for  $a \leq b$ .

$$\begin{aligned} \text{ROR}_k &: (q_i)_{i \in \llbracket 0, n-1 \rrbracket} \mapsto (q_{i-k \bmod n})_{i \in \llbracket 0, n-1 \rrbracket}, \\ \text{ROL}_k &: (q_i)_{i \in \llbracket 0, n-1 \rrbracket} \mapsto (q_{i+k \bmod n})_{i \in \llbracket 0, n-1 \rrbracket}. \end{aligned}$$

Previous works already mention that it is possible to perform gate-free rotations by reordering the qubits, but they don't explain how to keep track of this order for subsequent operations when implementing the circuit [8, 23].



```

1 X = QuantumRegister(7, name='X')
2 qc = rCircuit(X, name='rotation_circuit')
3 X_rotated = qc.ror(X, 3)
    
```

**Listing 1.** Python implementation of a 3-bit right rotation using `pyqcrypto`

In Listing 1 we perform a 3-bit right rotation on the 7-bit quantum register `X` and store the result in `X_rotated`. This operation does not use any quantum gates. Instead, the rotation operator simply returns a new `QuantumRegister`, which provides a modified perspective on the qubits, reflecting the applied rotation. This rotated `QuantumRegister` can then be used in subsequent calculations.

### 2.3 Bitwise XOR

As mentioned in [23], performing a bitwise XOR operation between two  $n$ -bit quantum registers can be done using  $n$  CNOT gates in parallel, resulting in a circuit depth of 1 and a quantum cost of  $n$ .

$$X \leftarrow X \oplus Y.$$

A bitwise XOR operation between a quantum register of size  $n$  and a constant  $m$  can be performed using  $w(m)$  NOT operations where  $w(m)$  denotes the Hamming weight of  $m$ . The resulting circuit has a depth of 1 for  $m \neq 0$  and a quantum cost of  $w(m)$ .

$$X \leftarrow X \oplus m.$$

These two operations are performed in place onto the first operand and the view on the qubits doesn't change. See Figure 1 for an example of a bitwise XOR circuit.

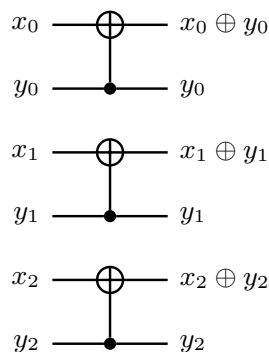


**Fig. 1.** Bitwise XOR circuit between two 3-bit quantum registers

## 2.4 Addition

There are many quantum adders featured in the literature, which can be divided into two main categories: ripple-carry adders and carry-lookahead adders [14].

In Section 3, we demonstrate the significance of selecting the appropriate type of adder to optimize circuit depth and the number of ancilla qubits. Additionally, we show that incorporating different adder types within the same circuit can increase parallelism without requiring additional ancilla qubits. As such, we implemented both types of adders in `pyqcrypto`.

We’re focusing our efforts on in-place  $n$ -bit adders modulo  $2^n$  because they are widely used in cryptographic algorithms, and we only consider circuits that reset the ancilla qubits so that they can be reused.

**Ripple-carry** This type of adder operates by adding the two numbers together bit by bit, propagating the carry between each step. It generally has a higher circuit depth compared to carry-lookahead adders, but requires fewer ancilla qubits.

We selected the ripple-carry adder from [19] because it has a reasonable depth and doesn’t use any ancilla qubits. The output carry computation is skipped to obtain an addition modulo  $2^n$ . This adder was previously used in [8] to implement a quantum circuit for SPECK. It uses  $5n - 6$  CNOT gates and  $2n - 2$  Toffoli gates, has a depth of  $5n - 5$  and a quantum cost of  $15n - 16$ .

**Carry-lookahead** This type of adder computes all carry bits in advance in an ancilla register before performing the simultaneous addition of all bits along with the carry bits. By carefully choosing the order in which to compute the carry bits, it is possible to significantly reduce the depth of the circuit at the expense of using more ancilla qubits.

We implemented the in-place (mod  $2^n$ ) carry-lookahead adder from [4] because it has logarithmic depth and only uses NOT, CNOT and Toffoli gates. It was employed for the implementation of Alzette in [23]. For  $n \geq 5$ , the resulting circuit uses  $10n - 6w(n - 1) - 6\lfloor \log(n - 1) \rfloor - 12$  Toffoli gates,  $4n - 5$  CNOT gates and  $2n - 2$  NOT gates, has a depth of  $2\lfloor \log(n - 1) \rfloor + 2\lfloor \log \frac{n-1}{3} \rfloor + 14$ , a quantum cost of  $56n - 30w(n - 1) - 30\lfloor \log(n - 1) \rfloor - 67$  and requires  $2n - 2 - w(n - 1) - \lfloor \log(n - 1) \rfloor$  ancilla qubits.

## 2.5 Addition with a Constant

The key schedule of TRAX-L requires the addition of a round constant to the key. However, to the best of our knowledge, there is no existing work on the reversible implementation of an adder with a constant. In this regard, we present several methods for implementing a circuit that can perform this operation.

**Ripple-carry** To perform an addition modulo  $2^n$  between an  $n$ -bit quantum register  $x$  and a constant  $m$ , the ripple-carry adder can be reused. This method involves using  $n$  ancilla qubits to set the constant, performing the addition, and then unsetting the constant to reset the ancilla qubits. It is not possible to use the ripple-carry approach directly without using any ancilla qubits, due to the fact that all available qubits are already used to store the operand, leaving no room to store the carry at each step.

**Carry-lookahead** It is possible to reduce the circuit depth to  $\mathcal{O}(\log n)$  by adapting the carry-lookahead adder to work with a constant. We replace the Toffoli gates involving the two operands in the first layer of the circuit with either a CNOT gate if the corresponding bit of the constant is 1, or nothing if it is 0. Additionally, the XOR between the two operands in the second layer is replaced by a XOR between  $x$  and a constant. Finally, since we're doing the addition in place, we make the same changes to the reversed circuit when uncomputing the carry. We select this method for the implementation of TRAX-L because it provides the best depth-width trade-off for the circuit. For  $n \geq 5$ , the resulting circuit uses  $8n - 6w(n-1) - 6\lfloor \log(n-1) \rfloor - 10$  Toffoli gates,  $n + 2w(m) - 1$  CNOT gates and  $2n + w(m) + 2w'(m) - 2$  NOT gates, has a depth lower than  $2\lfloor \log(n-1) \rfloor + 2\lfloor \log \frac{n-1}{3} \rfloor + 14$ , a quantum cost of  $43n - 30w(n-1) - 30\lfloor \log(n-1) \rfloor + 3w(m) + 2w'(m) - 53$  and requires  $2n - 2 - w(n-1) - \lfloor \log(n-1) \rfloor$  ancilla qubits.  $w'(m)$  denotes the Hamming weight of  $m$  excluding its most significant bit and least significant bit when  $m$  is encoded on  $n$  bits.

**Boolean expression** Finally, we can construct a constant adder without using any ancilla qubits. It was demonstrated in [18] that a quantum circuit can be generated for any boolean expression in exclusive sum-of-products (ESOP) form using multi-controlled mixed-polarity NOT gates. It is possible to express each resulting bit of a ripple-carry addition with a constant by a boolean expression that depends only on the previous bits by combining Equations (1) and (2) which outline the expression of the carry  $c_i$  and the sum  $s_i$  for each bit  $i$ . Since a different expression is needed for each value of the constant and finding the ESOP form is not a trivial task [16], we found this method to be impractical for our purposes.

$$c_0 = 0,$$

$$\forall i \in \llbracket 1, n-1 \rrbracket, c_i = \begin{cases} c_{i-1} \vee x_{i-1} & \text{if } m_{i-1} = 1, \\ c_{i-1} \wedge x_{i-1} & \text{if } m_{i-1} = 0. \end{cases} \quad (1)$$

$$\forall i \in \llbracket 0, n-1 \rrbracket, s_i = \begin{cases} \neg x_i \oplus c_i & \text{if } m_i = 1, \\ x_i \oplus c_i & \text{if } m_i = 0. \end{cases} \quad (2)$$

To address this issue, we observe that if the constant  $m$  contains a single bit set to 1 at position  $k$ , Equation (2) simplifies to Equation (3).

$$\forall i \in \llbracket 0, n-1 \rrbracket, s_i = \begin{cases} x_i & \text{if } i < k, \\ -x_i & \text{if } i = k, \\ x_i \oplus \bigwedge_{j=k}^{i-1} x_j & \text{if } i > k. \end{cases} \quad (3)$$

This expression can be implemented as shown in Figure 2 using  $n - k$  multi-controlled NOT gates.

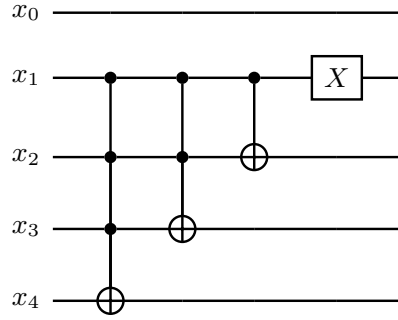


**Fig. 2.** 5-bit constant adder circuit with  $m = 2$

To add a constant that has  $l$  bits set to 1, we use  $l$  adders sequentially, each adder adding only a power of two — for example to add  $m = 1101_2$  we decompose it into  $1000_2 + 100_2 + 1_2$ . To minimize the number of adders, we subtract  $2^n - m$  from  $x$  instead of adding  $m$  when  $w(2^n - m) < w(m)$ . The subtraction circuit is simply the reverse of the addition circuit.

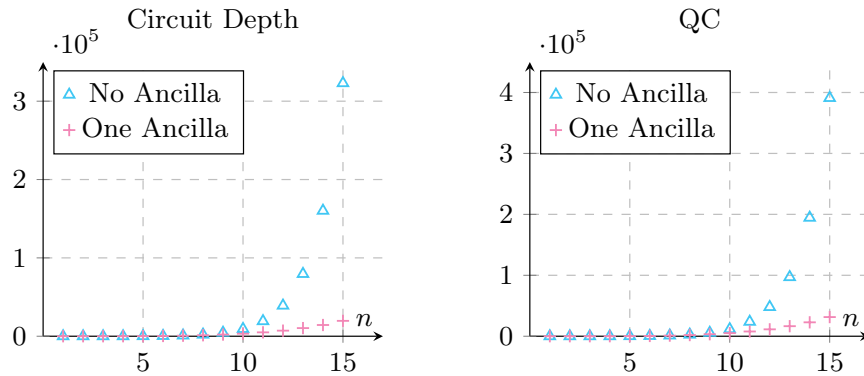


**Fig. 3.** Empirical evaluation of constant adder circuit from boolean expression

Figure 3 illustrates the empirical circuit depth and quantum cost of the resulting circuit in the worst case scenario, where  $m = 2^{\lfloor \frac{n+1}{2} \rfloor} - 1$ . It can be

observed that both values increase exponentially with  $n$  because `Qiskit`'s implementation of multi-controlled NOT gates using Gray codes is inefficient. If 1 ancilla qubit is available, `Qiskit`'s recursive method can be used to implement those gates which significantly reduces the circuit depth and quantum cost. More efficient methods exist [6] but are not yet implemented in `Qiskit`.

### 3 Proposed Implementation

In this section we describe the proposed implementation of TRAX-L-17 [2] as a quantum circuit, as well as the various approaches that we used to optimize the circuit in term of quantum cost, depth, and number of ancilla qubits.

TRAX-L-17 is a large tweakable block cipher operating on a 256-bit block with a 256-bit key and a 128-bit tweak. It is part of the SPARKLE-suite, a finalist of the NIST Lightweight Cryptography Standardization Process [21].

A round of TRAX-L is composed of 4 instances of the ARX-box Alzette, a linear layer based on the SPARKLE-256 permutation, and a key schedule. The subkeys are added before executing the instances of Alzette, and the tweak is added once every two rounds.

The SPARKLE permutation and the Alzette ARX-box have already been implemented as a quantum circuit in [23]. We perform a comparative analysis between our approach and the aforementioned implementation.

The plaintext is represented by two 128-bit quantum registers  $x$  and  $y$  that are updated in place during each round. The key is represented by a 256-bit quantum register  $k$ , which is also updated in place with the subkeys for each round. The tweak is assumed to be a constant  $T$ . We evaluate our circuits in the worst case, i.e, with  $T = 2^{128} - 1$ .

#### 3.1 Alzette

Alzette is a 64-bit ARX-box composed of 4 additions, 8 XOR operations and 8 right rotations. It is parametrized by a 32-bit round constant  $c$  and operates in place on two 32-bit words. Two methods are proposed to implement Alzette: one using a ripple-carry adder with no ancilla qubits [19], and another using a carry-lookahead adder with 53 ancilla qubits [4]. The latter method reduces the overall circuit depth by a factor of 5.32 and was introduced in [23]. The implementation of the ripple-carry method using `pyqcrypto` is shown in Listing 2.

**Table 1.** Cost of Alzette with  $c = 2^{32} - 1$  (worst case)

Method	Ancilla	QC	Depth	Toffoli	CNOT	NOT
ripple	0	2112	628	248	774	128
lookahead	53	6076	120	1016	620	376
Yang et al. [23]	53	6076	96	1016	620	376

```

1 X = QuantumRegister(32, name='X')
2 qc = rCircuit(X, Y, name='Alzette')
3 qc.add(X, qc.ror(Y, 31))
4 qc.xor(Y, qc.ror(X, 24))
5 qc.xor(X, c)
6 qc.add(X, qc.ror(Y, 17))
7 qc.xor(Y, qc.ror(X, 17))
8 qc.xor(X, c)
9 qc.add(X, Y)
10 qc.xor(Y, qc.ror(X, 31))
11 qc.xor(X, c)
12 qc.add(X, qc.ror(Y, 24))
13 qc.xor(Y, qc.ror(X, 16))
14 qc.xor(X, c)

```

**Listing 2.** Python implementation of Alzette using pyqcrypto

The results in Table 1 for the depth of the carry-lookahead approach differ from the depth reported in [23] because the paper did not consider the CNOT and NOT gates when calculating the depth of the adder.

TRAX-L includes 4 instances of Alzette that can be performed in parallel. With the lookahead method, this increases the amount of ancilla qubits needed to 212. A trade-off consists of performing only two instances of Alzette in parallel, doubling the circuit’s depth compared to the parallel method, but reducing the number of ancilla qubits by half compared to computing the 4 instances sequentially. These different approaches are compared in Table 2.

### 3.2 Linear Permutation

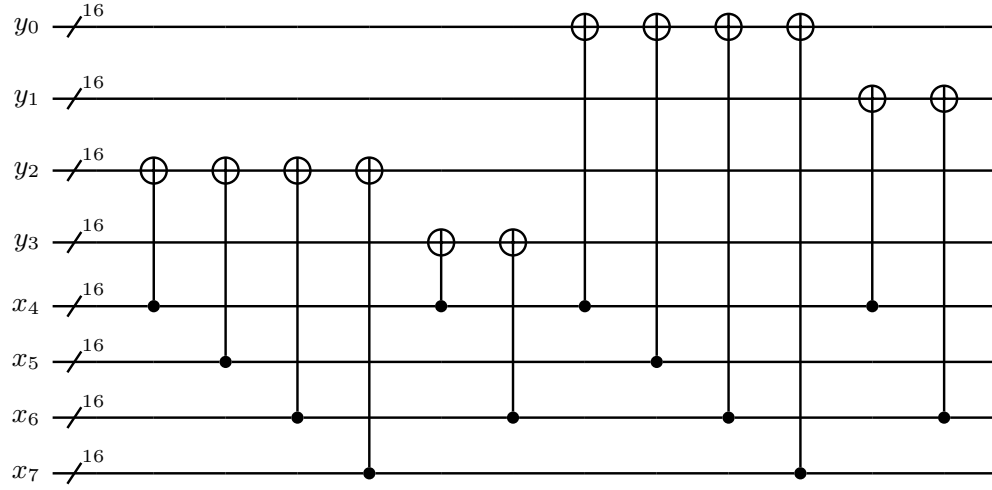
The linear layer of TRAX-L is similar to the one of the SPARKLE-256 permutation: it consists of left shift, right rotation and XOR operations and modifies two 128-bits inputs  $x$  and  $y$  in place. It can be implemented using 384 CNOT gates and a depth of 7 without ancilla qubits by splitting each input into eight 16-bit words to avoid the shift operations.

Figure 4 shows the circuit to update  $y$ , the CNOT gates representing 16-bit XOR operations. The same circuit can be used to update  $x$  by swapping the roles of  $x$  and  $y$ . Both circuits can be run in parallel.

The flexibility of the views on quantum registers provided by pyqcrypto enabled the construction of an ancilla-free permutation circuit, in contrast to the approach described in [2].

### 3.3 Key Schedule

In a classical implementation, the key schedule is typically computed in advance and stored in RAM. In our case, such an approach would require 256 ancilla



**Fig. 4.** TRAX-L Linear Layer circuit to update  $y$

**Table 2.** Cost of 4 Alzette rounds and linear permutation

Method	Ancilla	Depth	QC	Toffoli	CNOT	NOT
ripple	0	635	8572	992	3360	252
lookahead sequential	53	475	24428	4064	2864	1244
lookahead half-parallel	106	242	24428	4064	2864	1244
lookahead parallel	212	127	24428	4064	2864	1244

qubits per subkey, rendering it impractical. Instead, after each round we update the qubits storing the key by computing the subkey for the next round, overwriting the previous subkey. The subkey for the first round corresponds to the input key of the cipher.

The key  $k$  is partitioned into eight 32-bit sections and updated using Equation (4), where  $c_0, c_1, c_2,$  and  $c_3$  represent round constants. This update is composed of two XOR operations, two instances of the XOR with a constant operation, two additions and two additions with a constant. Updating  $k_0$  and  $k_2$  can be done in parallel with updating  $k_4$  and  $k_6$ , but the constant adders cannot be parallelized with the adders.

$$\begin{aligned}
 k_0 &\leftarrow k_0 + k_1 + c_0, \\
 k_2 &\leftarrow k_2 \oplus k_3 \oplus c_1, \\
 k_4 &\leftarrow k_4 + k_5 + c_3, \\
 k_6 &\leftarrow k_6 \oplus k_7 \oplus c_4.
 \end{aligned} \tag{4}$$

The key is then rotated to the left  $k_{i-1 \bmod 7} \leftarrow k_{i \bmod 7}$ . No quantum gates are necessary for this operation, as it solely involves a rearrangement of the quantum registers that are used to store the key. It can be observed that only half the key is updated at each round in an alternating manner.

Table 3 presents the implementation cost of the key schedule using different adder methods. Carry-lookahead adders are consistently used for the constant adders, and they can be computed either in parallel or sequentially. Meanwhile, the two regular adders are either ripple-carry or carry-lookahead. These results suggest that the lookahead parallel method, which yields the lowest depth, and the lookahead sequential method, which ensures the fewest number of ancilla qubits, are the most advantageous approaches for implementing the key schedule. However, as we will demonstrate in Section 3.4, these conclusions do not hold when considering the overall circuit.

**Table 3.** Cost of the key schedule

Method	Ancilla	Depth	QC	Toffoli	CNOT	NOT
ripple constant parallel	106	177	3245	508	492	213
ripple constant sequential	53	204   177 <sup>†</sup>	3245	508	492	213
lookahead parallel	106	56	5227	892	430	213
lookahead sequential	53	111	5227	892	430	337

<sup>†</sup> There are two possible values in this scenario because the depth of the circuit is influenced by the arrangement of the different adders, as illustrated in Figure 5. Specifically, when the constant adders are executed after the ripple-carry adders, the circuit depth increases due to the necessity of waiting for the ancilla qubits. This highlights the importance of accurately selecting the order of operations when constructing a quantum circuit.



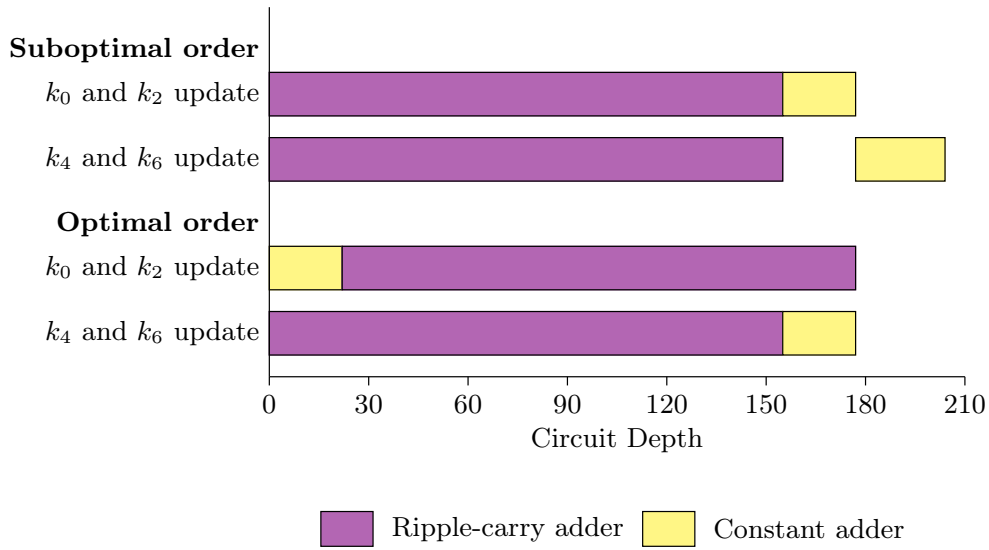


**Fig. 5.** Key schedule depth diagram for different adder arrangements

### 3.4 TRAX-L

In TRAX-L,  $x$  and  $y$  are XORed with the key at the beginning of each round, and once more at the conclusion of all rounds. This operation has a depth of 1 and employs 256 CNOT gates on each occurrence.

Additionally, the first 64 bits of  $x$  and  $y$  are XORed with the 128-bit tweak once every two rounds, starting at the second round. If we assume the tweak to be a constant  $T$ , this operation has a depth of 1 and requires  $w(T)$  NOT gates. It is also possible to store the tweak in a 128-bit quantum register and use 128 CNOT gates instead of the NOT gates if we must perform Grover's search on the tweak.

The key schedule and the rounds of Alzette can be executed concurrently as they operate on distinct qubits. However, it is necessary to allocate ancilla qubits for each carry-lookahead adder that is intended to be run in parallel. Consequently, the circuit depth varies depending on the adder type employed in each circuit and on the number of available ancilla qubits. Let's consider the case where the 4 rounds of Alzette are executed in parallel, using a total of 212 ancilla qubits.

Figure 6 displays how the key schedule can be parallelized with the Alzette rounds. When the key schedule is executed in parallel with Alzette with carry-lookahead adders, the parallelization of the said adders would require an additional 106 ancilla qubits. However, this parallelization does not reduce the overall circuit depth of 2185 compared to sequential execution, which only requires 53 extra ancilla qubits. This can be attributed to the longer execution time of Alzette compared to four sequential carry-lookahead adders. In conclusion, it is advisable to choose the lookahead sequential method over the lookahead parallel

method for the key schedule when executing it in parallel with Alzette, despite the results of Section 3.3.

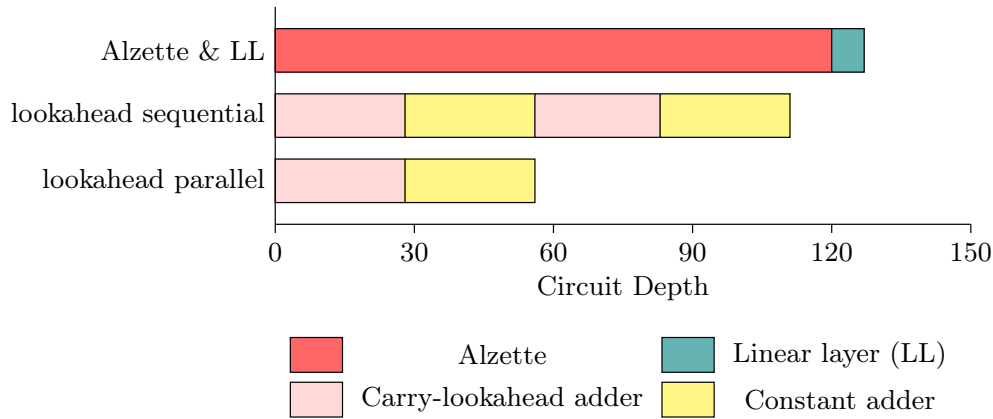


**Fig. 6.** Depth diagram of Alzette and Linear Layer compared to key schedule

In order to limit the number of ancilla qubits to the 212 employed in the Alzette rounds, we can reuse these qubits during the computation of the key schedule, at the cost of parallelism. One approach to achieve this is to use parallel carry-lookahead adders for the key schedule computation, along with the two constant adders. This approach results in a depth of 2959. However, a faster alternative involves combining the slower ripple-carry adder with the constant adder. This may appear counter-intuitive, as the former method produces a depth of 174 after one round, compared to 178 for the latter. Nevertheless, the ripple-carry method outperforms the carry-lookahead after two rounds. This is due to the fact that the ripple-carry adder does not use any ancilla qubits, enabling the computation of the next round key to begin prior to adding the constant to the current round key, as illustrated in Figure 7. The reason behind this phenomenon is that two consecutive rounds operate on different segments of the key.

This observation also holds true when executing the Alzette rounds using either the sequential or half-parallel method. It highlights the advantage of combining different adder types to optimize circuit parallelism. In some cases, it is beneficial to implement a longer circuit that operates without ancilla qubits in parallel with multiple shorter circuits that do use ancilla qubits. This finding is crucial in the design of circuits with minimum depth for a given number of ancilla qubits.

Table 4 summarizes the cost of implementing TRAX-L-17 using the different techniques discussed previously. The key schedule (KS) mode "lookahead  $\neq$ " denotes the use of different ancilla qubits for the carry-lookahead adders in the key schedule and in the Alzette rounds, while "lookahead =" indicates the use of the same ancilla qubits. The circuit requires 512 qubits to store the inputs and the key, in addition to the ancilla qubits. When sufficient ancilla qubits are

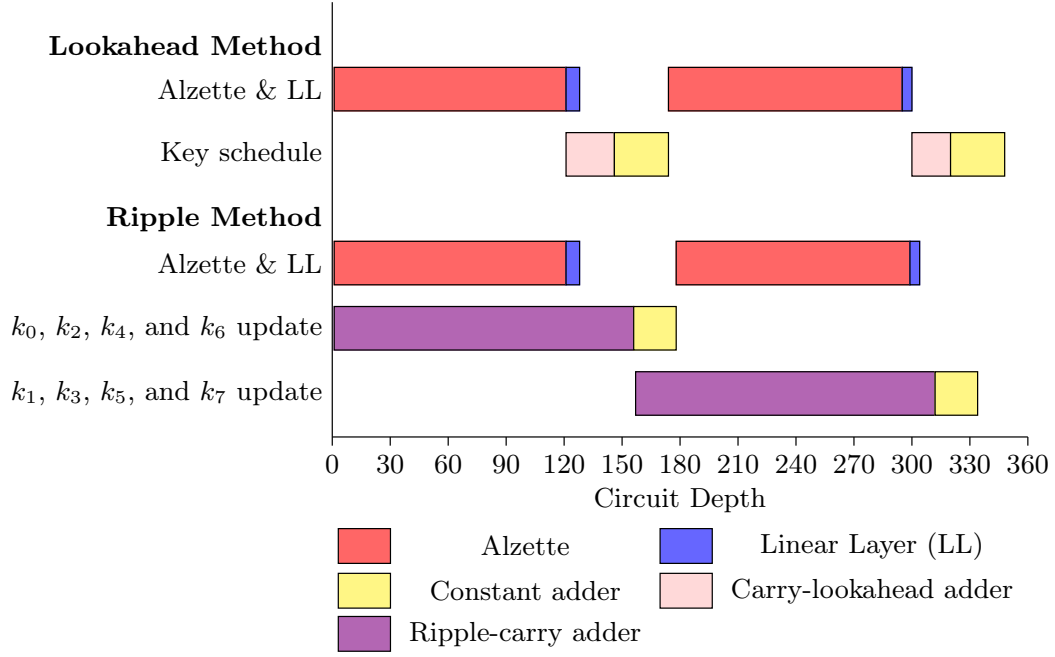


**Fig. 7.** Depth diagram of two rounds of TRAX-L for different key schedule methods

available, it is recommended to employ carry-lookahead adders in parallel for Alzette and sequentially for the key schedule. However, to reduce the number of ancilla qubits, ripple-carry adders can be used for the key schedule to preserve some level of parallelism. Finally, Figure 8 depicts the trade-off between circuit depth and number of ancilla qubits.

**Table 4.** Cost of TRAX-L-17

Alzette	KS	Ancilla	Depth	QC	Toffoli	CNOT	NOT
lookahead parallel	lookahead $\neq$	265	2185	510417	84252	60729	28431
lookahead parallel	ripple	212	2675	476723	77724	61780	26323
lookahead parallel	lookahead =	212	2959	509393	84252	60726	27407
lookahead half-parallel	lookahead $\neq$	159	4140	510417	84252	60726	26323
lookahead half-parallel	ripple	106	4440	476723	77724	61780	26323
lookahead half-parallel	lookahead =	106	4916	509393	84252	60726	27407
lookahead sequential	lookahead $\neq$	106	8101	510417	84252	60726	28431
ripple	lookahead $\neq$	106	10773	240865	32028	69158	11567
lookahead sequential	ripple	53	8877	476723	77724	61780	26323
ripple	ripple	53	10773	207171	25500	70212	9459

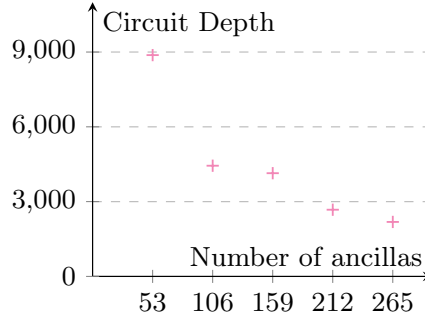


**Fig. 8.** TRAX-L-17 circuit depth for different number of ancilla qubits

## 4 Grover Search

### 4.1 Attack Model

In the context of this attack, it is assumed that a plaintext/ciphertext pair is known, along with the corresponding tweak  $T$ . The objective of the attack is to determine the  $n$ -bit key  $K$  with a high degree of certainty. A classical exhaustive search requires an average of  $2^{n-1}$  attempts to retrieve the key. Grover’s algorithm recovers the key in  $\mathcal{O}(\sqrt{2^n})$  iterations, thereby resulting in a quadratic speedup [5]. A practical implementation of Grover’s algorithm for  $n$  qubits is presented in [17].

To perform the search, we first create a uniform superposition of all possible keys in an  $n$ -bit quantum register  $S$  by applying in parallel  $n$  Hadamard (H) gates as shown in Equation (5). We also simultaneously initialize two quantum registers  $x$  and  $y$  with the known plaintext.

$$|S\rangle = H^{\otimes n} |0^n\rangle = 2^{-n/2} \sum_{B \in \{0,1\}^n} |B\rangle. \quad (5)$$

Then, we apply a phase oracle  $U_\omega$  that flips the phase of the quantum state corresponding to the correct key as described by Equation (6).

$$U_\omega : |B\rangle \mapsto \begin{cases} -|B\rangle & \text{if } B = K, \\ |B\rangle & \text{if } B \neq K. \end{cases} \quad (6)$$

The implementation of  $U_\omega$  involves running the encryption circuit for TRAX-L-17, as described in Section 3.4, with the inputs  $x$ ,  $y$  and  $S$ . Subsequently, the resulting ciphertext is compared with the known ciphertext so that only the quantum state corresponding to the correct key undergoes a phase flip. Reversing the encryption circuit then undoes the transformations applied to the plaintext and the key. To compare the ciphertexts, a Multi-Controlled mixed-polarity Z gate (MCZ) is employed. This gate selectively flips the phase of the quantum state in which all of the bits are either 0 or 1, depending on the value of a constant, in this case the known ciphertext. It should be noted that this circuit solely affects the phase of the quantum state.

Finally, we apply the Grover diffusion operator  $U_S$  defined in Equation (7) which amplifies the state whose phase was flipped in the previous step, increasing the probability of measuring the correct key.

$$U_S = H^{\otimes n} (2|0^n\rangle\langle 0^n| - \mathbf{1}) H^{\otimes n}. \quad (7)$$

The  $U_\omega$  and the  $U_S$  operators need to be repeated for  $r = \lfloor \frac{\pi}{4} \sqrt{2^n} \rfloor$  iterations before measuring the quantum register  $S$  to obtain the correct key with a high probability. Figure 9 shows the full circuit for Grover's search.

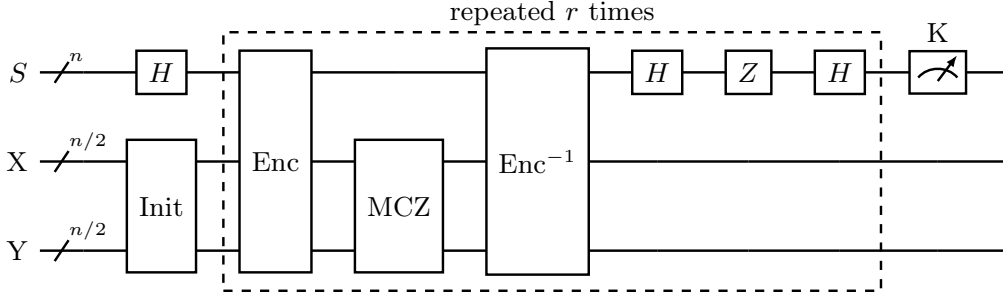


**Fig. 9.** Circuit for Grover's search

## 4.2 Cost Estimation

As mentioned previously, Grover's algorithm requires  $\lfloor \frac{\pi}{4} \sqrt{2^n} \rfloor$  iterations to find the correct key. Each iteration uses the TRAX-L-17 encryption circuit twice, resulting in a total of  $\lfloor \frac{\pi}{2} \sqrt{2^n} \rfloor$  invocations. Table 5 presents the total cost of implementing Grover's search on TRAX-L-17 with a key size of 256 bits, taking into account only the gates necessary for the encryption circuit. We aim to minimize the circuit depth for various circuit widths.

**Table 5.** Cost of Grover on TRAX-L-17

Alzette	KS	Width	Depth	QC
lookahead parallel	lookahead $\neq$	777	$1.68 \cdot 2^{139}$	$1.53 \cdot 2^{147}$
lookahead parallel	ripple	724	$1.03 \cdot 2^{140}$	$1.43 \cdot 2^{147}$
lookahead half-parallel	lookahead $\neq$	671	$1.59 \cdot 2^{140}$	$1.53 \cdot 2^{147}$
lookahead half-parallel	ripple	618	$1.70 \cdot 2^{140}$	$1.43 \cdot 2^{147}$
lookahead sequential	ripple	565	$1.70 \cdot 2^{141}$	$1.43 \cdot 2^{147}$

## 5 Conclusion

In this study, we have introduced a quantum circuit design for TRAX-L-17 and conducted an analysis of its quantum cost, gate count, depth, and width.

Additionally, we have evaluated the cost of a Grover attack on that cipher. Notably, for a width of 777 qubits, the depth of the attack circuit amounts to  $1.68 \cdot 2^{139}$ . This result is comparable to the depth of  $1.28 \cdot 2^{139}$  required to break AES-256 using the same methodology, albeit with a larger qubit count of 4609 [9].

Additionally, we have introduced the `pycrypto` library, which simplifies the implementation of classical ciphers as quantum circuits. It has been made publicly available at the provided link: [link redacted for anonymity]. Future work would be to use this library to implement quantum circuits for other ciphers.

Finally, we have highlighted the significance of optimizing the circuit arrangement to enhance parallelism, and we have demonstrated the benefits of using diverse adder types to reduce depth without requiring the use of additional ancilla qubits.

## References

1. Bathe, B., Anand, R., Dutta, S.: Evaluation of grover’s algorithm toward quantum cryptanalysis on chacha. *Quantum Information Processing* **20**(12), 394 (2021)
2. Beierle, C., Biryukov, A., Cardoso dos Santos, L., Großschädl, J., Perrin, L., Udovenko, A., Velichkov, V., Wang, Q.: Alzette: A 64-bit arx-box: (feat. crax and trax). In: *Advances in Cryptology–CRYPTO 2020: 40th Annual International Cryptology Conference, CRYPTO 2020, Santa Barbara, CA, USA, August 17–21, 2020, Proceedings, Part III* 40. pp. 419–448. Springer (2020)
3. Bhatia, V., Ramkumar, K.: An efficient quantum computing technique for cracking rsa using shor’s algorithm. In: *2020 IEEE 5th international conference on computing communication and automation (ICCCA)*. pp. 89–94. IEEE (2020)
4. Draper, T.G., Kutin, S.A., Rains, E.M., Svore, K.M.: A logarithmic-depth quantum carry-lookahead adder. *arXiv preprint quant-ph/0406142* (2004)
5. Grover, L.K.: Quantum mechanics helps in searching for a needle in a haystack. *Physical review letters* **79**(2), 325 (1997)
6. He, Y., Luo, M.X., Zhang, E., Wang, H.K., Wang, X.F.: Decompositions of n-qubit toffoli gates with linear circuit complexity. *International Journal of Theoretical Physics* **56**, 2350–2361 (2017)
7. Jang, K., Kim, H., Eum, S., Seo, H.: Grover on gift. *Cryptology ePrint Archive* (2020)
8. Jang, K., Choi, S., Kwon, H., Seo, H.: Grover on speck: quantum resource estimates. *Cryptology ePrint Archive* (2020)
9. Jaques, S., Naehrig, M., Roetteler, M., Virdia, F.: Implementing grover oracles for quantum key search on aes and lowmc. In: *Advances in Cryptology–EUROCRYPT 2020: 39th Annual International Conference on the Theory and Applications of Cryptographic Techniques, Zagreb, Croatia, May 10–14, 2020, Proceedings, Part II* 30. pp. 280–310. Springer (2020)
10. Liu, X., Kubiawicz, J.: Chisel-q: Designing quantum circuits with a scala embedded language. In: *2013 IEEE 31st International Conference on Computer Design (ICCD)*. pp. 427–434. IEEE (2013)
11. Mavroeidis, V., Vishi, K., Zych, M.D., Jøssang, A.: The impact of quantum computing on present cryptography. *arXiv preprint arXiv:1804.00200* (2018)

12. Mohammadi, M., Eshghi, M.: On figures of merit in reversible and quantum logic designs. *Quantum Information Processing* **8**, 297–318 (2009)
13. Oh, Y., Jang, K., Baksi, A., Seo, H.: Depth-optimized implementation of ascon quantum circuit. *Cryptology ePrint Archive* (2023)
14. Orts, F., Ortega, G., Combarro, E.F., Garzón, E.M.: A review on reversible quantum adders. *Journal of Network and Computer Applications* **170**, 102810 (2020)
15. Proos, J., Zalka, C.: Shor’s discrete logarithm quantum algorithm for elliptic curves. *arXiv preprint quant-ph/0301141* (2003)
16. Riener, H., Ehlers, R., Schmitt, B.d.O., Micheli, G.D.: Exact synthesis of esop forms. In: *Advanced Boolean Techniques: Selected Papers from the 13th International Workshop on Boolean Problems*. pp. 177–194. Springer (2020)
17. Sadana, S.: Grover’s search algorithm for  $n$  qubits with optimal number of iterations. *arXiv preprint arXiv:2011.04051* (2020)
18. Schmitt, B., Soeken, M., De Micheli, G., Mishchenko, A.: Scaling-up esop synthesis for quantum compilation. In: *2019 IEEE 49th International Symposium on Multiple-Valued Logic (ISMVL)*. pp. 13–18. IEEE (2019)
19. Takahashi, Y., Tani, S., Kunihiro, N.: Quantum addition circuits and unbounded fan-out. *arXiv preprint arXiv:0910.2530* (2009)
20. Turan, M.S., McKay, K., Chang, D., Bassham, L.E., Kang, J., Waller, N.D., Kelsey, J.M., Hong, D.: Status report on the final round of the nist lightweight cryptography standardization process. *National Institute of Standards and Technology Internal Report 8454(10.6028)* (2023)
21. Turan, M.S., McKay, K., Chang, D., Calik, C., Bassham, L., Kang, J., Kelsey, J., et al.: Status report on the second round of the nist lightweight cryptography standardization process. *National Institute of Standards and Technology Internal Report 8369(10.6028)* (2021)
22. Wille, R., Van Meter, R., Naveh, Y.: Ibm’s qiskit tool chain: Working with and developing for real quantum computers. In: *2019 Design, Automation & Test in Europe Conference & Exhibition (DATE)*. pp. 1234–1240. IEEE (2019)
23. Yang, Y., Jang, K., Kim, H., Song, G., Seo, H.: Grover on sparkle. In: *International Conference on Information Security Applications*. pp. 44–59. Springer (2022)

# Engineering Educational Research on the Design and Fabrication of a Glider Model

Enzo Luciani<sup>a</sup>

<sup>a</sup>*Department of Aerospace Engineering, Graduate School of Engineering, Polytechnique Montréal, enzo.luciani@polymtl.ca,*

Supervisor: Prof. Susumu Hara

haras@nuae.nagoya-u.ac.jp

Department of Aerospace Engineering, Nagoya University

---

## Abstract

Practical-based learning (PBL) is an active learning method based on student autonomy and self-learning. It allows students to apply the knowledge they learned during classes. In this paper, a student "Luciani" gives feedback after participating in the "Flying Robot Program" at Gifu University. This program is a course shared by Gifu University and Nagoya University, where students compete to have the longest flight distance from an elastic impulsion. From his experience, he will try to give an incentive on the educational interest of adding more complexity to the program. Different types of numerical method simulation and optimization have been tried, such as vortex lattice method, lifting line theory, panel method, iterative solid dynamic simulation, or flight performance.

*Keywords:*

---

## 1. Introduction

Practical-based learning (PBL) is an active learning method based on student autonomy and self-learning. It allows students to apply the knowledge they learned during classes. It also gives an intuitive comprehension of real phenomena. A program like the "Flying Robot Program" launched by one of the authors of this paper, Hara (2020), has shown that students value that type of learning and think that this project-type of class should be emphasized.

This paper focuses on introducing more advanced concepts such as computational aerodynamics, wing optimization, and dynamic simulation of the glider. We will try to identify the pertinence of the different methods from a pedagogic point of view based on the feedback of one of the participants, "Luciani" on the Flying Robot Program at Gifu University.

## 2. Program Context

The program consists of a contest organized at Gifu University and Nagoya University. It is organized for undergraduate students to make them put into practice the knowledge they acquire in class. The objective is also to help them better understand physical phenomena more intuitively.

The contest attempts to attain the longest flight distance with fixed potential energy (elastic and height). A selection is organized in each university. Then, each university's best planes compete against each other in a common contest.

In this context, a graduate exchange student in the lab, "Luciani," has been invited to participate as an external member of the selection at Gifu University. The objective is to get feedback on the pedagogical interest of adding more complex design methods, optimization, and simulation to the design process

## 3. Wing preliminary design

The first step in designing the plane has been the design of the wing. To begin, an airfoil had to be chosen, then the 3D shape of the airfoil must be determined and optimized. To do that, basic aerodynamics concepts have been used, and more complex ones like the lifting line theory or vortex lattice method (VLM).

### 3.1. Choosing the airfoil

Based on the book "Summary of Low-Speed Airfoil Data" by Selig et al. (1995), a selection of airfoils has been made. The main criteria of selection were:

- Lift-to-drag ratio. Going as far as possible is the objective; hence, this ratio is the main characteristic to be considered. As the lift coefficient is function to the angle of attack, the objective is to have a high lift coefficient at 0 angle of attack while keeping the drag coefficient low. That could be translated by thin and high camber airfoils.

- Maximal thickness. The aerodynamic is not the only criterion to be accounted, the wing should also be resistant enough to resist the lunch acceleration. For that, the span should be wide enough, resulting in a constraint on the maximal thickness of the airfoil.

- Range of angle of attacks for the constant drag coefficient. To choose an optimal angle of attack for the airfoil later in the design process, the drag coefficient should be as constant as possible (small as possible) regardless of the angle of attack. The chosen airfoils are in Table 1. Offering a good compromise between all the criteria, the airfoil BE50 has been chosen.

### 3.2. Optimisation of span length and wing load for maximum flight distance

To design the wing, an assumption on the weight had to be made based on similar gliders in the program. A weight of 250



Aifoil	max thickness	max camber	Cd	$Cl_{max}$
AG03	6.2	2	0.02	1
SD7037	9.2	2.5	0.03	1.3
MA409	6.7	3.3	0.02	1.2
AG16	7.1	1.9	0.02	1
BE50	7.3	4.1	0.025	1.35
GM15	6.7	4.8	0.03	1.35

Table 1: Tradeoff between different low-speed airfoils

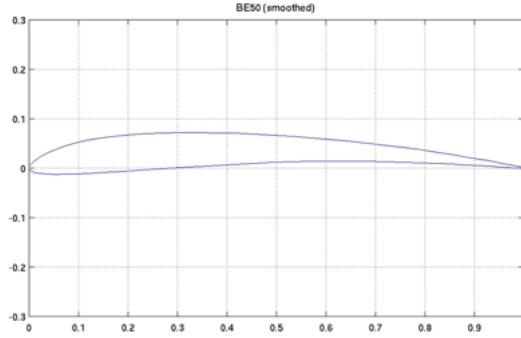


Figure 1: BE50 airfoil (smoothed)

g has been chosen. Based on that, the wing load and span can be determined.

$$S = m/W_S \quad (1)$$

$$U_{stall} = \sqrt{\frac{2W_S}{\rho C L_{max}}} \quad (2)$$

$$D_{friction+form} = \frac{1}{2} \rho S C_D U_\infty^2 \quad (3)$$

$$D_{induced} = \frac{2W^2}{\rho \pi e b^2 U_\infty^2} \quad (4)$$

$$D(U_\infty) = D_{friction+form}(U_\infty) + D_{induced}(U_\infty) \quad (5)$$

$$D_{min} = \min(D(U_\infty)) \quad (6)$$

Thus, the minimum drags  $D_{min}$  associated with its speed  $U_{minDrag}$  are a function of the wing load  $W_S$  and  $b$ . As drag is inversely proportional to the span, it has been found that the maximum span authorized by the contest rule was the best. From here, the span  $b=1$  m. It is then possible to determine  $W_S$  to have the best lift-to-drag ratio because  $L_D = L/D$  with  $L = W = cst$ . Yet the variable to optimize is the flight distance  $d$ :

$$E_{p_{elastic}} = \frac{1}{2} k \cdot elongation^2 \quad (7)$$

$$E_{p_{heigh}} = mgh \quad (8)$$

$$E_{C_{optimal}} = \frac{1}{2} m U_{minDrag}^2 \quad (9)$$

$$H = h + \frac{E_{p_{elastic}} - E_{C_{optimal}}}{mg} \quad (10)$$

$$d = \frac{h}{L_D} \quad (11)$$

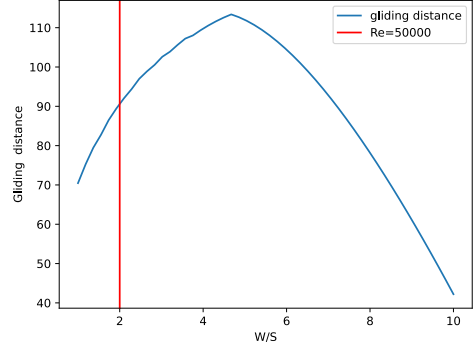


Figure 2: Relation between wing load (kg/m²) and flight distance (m)

From Figure 2, the optimal wing load is around 4.7. Yet, a high wing loads the wing surface, and the mean cord is small. That means a decrease in the Reynolds number.

$$c_{mean} = \frac{S}{b} \quad (12)$$

$$Re = \frac{U_{minDrag} c_{mean}}{\nu} \quad (13)$$

Under a Reynolds of 50,000, the performance of the airfoil may decrease if the source used does not provide data of the BE50 under 30,000 (Michael S. Selig and Giguere (1995)). Owing to the taper ratio, the cord at the tip may be 15% to 20% lower than the mean cord Reynolds. Hence, a wing load of 2 has been chosen. That results in a mean cord of 125 mm and a Reynolds of  $50e3$ . The wing still provides a theoretical flight distance above 90 m, more than the previous 30-m record of the contest.

### 3.3. Main characteristics of the wing

We can determine the wing's main characteristics from the previous calculations.

Lift is calculated at equilibrium with weight at speed  $U_{inf} = U_{minDrag}$ :

$$C_L = \frac{W}{\frac{1}{2} \rho S U_{inf}^2} \quad (14)$$

To have the needed lift coefficient when the glider pitch is null, the wing has an initial angle of attack  $\alpha_0$ :

$$\alpha_0 = \frac{C_L - C_{L0}}{2\pi} \quad (15)$$

with  $C_{L0}$  the lift coefficient when the airfoil have no angle of attack.

Parameter	Value
Span	1 m
Wing load	2 kg/m <sup>2</sup>
Wing surface	0.125 m <sup>2</sup>
Mean cord	125 mm
Aspect ratio	8
Minimum drag	0,14 N
Speed for minimum drag	6,6 m/s
Reynolds	53e3
Lift-to-drag ratio	17,6
Lift coefficient	0.777
Drag coefficient	0.025
Gliding distance	90,2 m
$\alpha_0$	4,63 deg

Table 2: Main characteristics of wing

#### 4. Using Lifting-line Theory and the Vortex Lattice Method (VLM) to calculate the optimal Taper ratio

Based on a comparative study using computational fluid dynamics by Eraslan et al. (2018), the taper ratio for high aspect ratio wings is at  $0.4 \pm 0.2$ , giving minimum drag. VLM has been used here to corroborate those results. The effect of the taper ratio has been studied on 50 values between 0.1 and 1. The mesh grid has 48 elements,  $i=4$  on the span and  $j=12$  on the cord. The calculation has been made for  $\alpha = \alpha_0$ .

Here the VLM method is used to get the span load. From that, the Oswald coefficient can be determined using the lifting-line theory.

$$y = -\frac{b}{2} \cos \theta \quad (16)$$

$$\Gamma(\theta) = \frac{1}{2} c_l(\theta) c(\theta) U_\infty \quad (17)$$

We can describe the circulation distribution along an arbitrary finite wing using a Fourier sine series. Hence, we can assume that:

$$\Gamma(\theta) = 2bU_\infty \sum_1^N A_n \sin(n\theta) \quad (18)$$

The combination of Equations 17 and 18 gives a system of  $i$  equation from the number of elements  $y_i$  on the span. The system has  $n$  unknown variables  $A_n$ . If we took  $n = i$  the system would be solvable. From here, it is possible to describe the drag induced by the circulation:

$$C_{D,i} = \frac{C_L^2}{\pi AR} (1 + \delta) = \frac{C_L^2}{\pi AR e} \quad (19)$$

with

$$\delta = \sum_2^N n \left( \frac{A_n}{A_1} \right)^2 \quad (20)$$

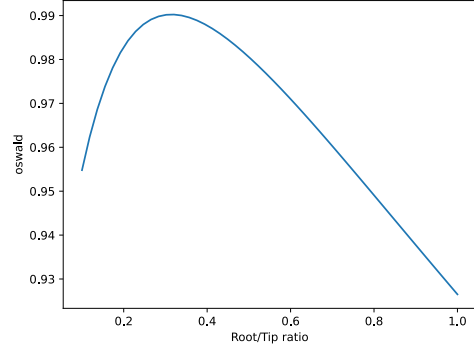


Figure 3: Oswald (e) versus taper ratio

The Oswald factor can then be defined as

$$e = \frac{1}{1 + \delta} \quad (21)$$

The optimal Oswald factor is obtained for a taper ratio of 0.32. This is close to the results of Eraslan et al. (2018). A taper ratio between 0.3 and 0.4 would then be optimal. Yet that would result in a very small Reynolds on the tip of the wings. Here, an arbitrary choice has been made to choose a taper ratio of 0.6. That ratio performs well while allowing a sufficient Reynolds number on the tip.

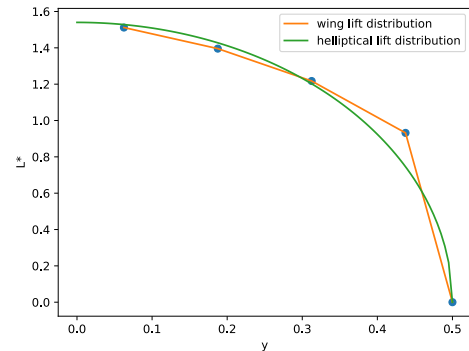


Figure 4: Span-wise lift distributions with elliptical lift distributions of model; taper ratio of 0.6

At the end, the results are:

Parameter	Value
Root cord	156 mm
Tip cord	94 mm
Reynolds Number at the root	62603
Reynolds Number at the tip	37561
Oswald factor	0,97

Table 3: Wing tip cords and root cords with associate Reynolds numbers

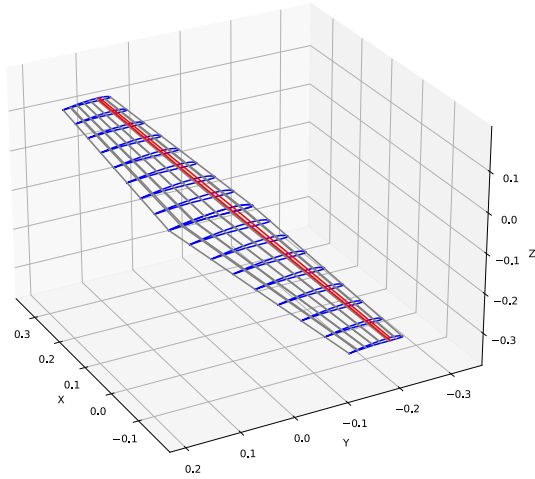


Figure 5: 3D model of final wing

## 5. Manufacturing



Figure 6: Picture of full glider

To have a lightweight wing, the main structure of the wing is made of balsa wood. Only one spar intersects each section at its maximum thickness. The whole structure has been made using a laser cutter and assembled by hand. Two oak wood flanges have been glued to the balsa spar for more flexion resistance. To give better rigidity to the trailing edge, a 2-mm carbon fiber composite rod has been added at the rear of the wing. Then, Styrofoam blocks were cut using a wire cutter to shape the leading edge. Balsa blocks have been hand cut for the trailing edge to fill the gap between the carbon fiber rod and the actual trailing edge. Before adding the retractable film, a single coat of fiberglass fabric—epoxy glue composite is placed on top of the Styrofoam to give torsion rigidity.

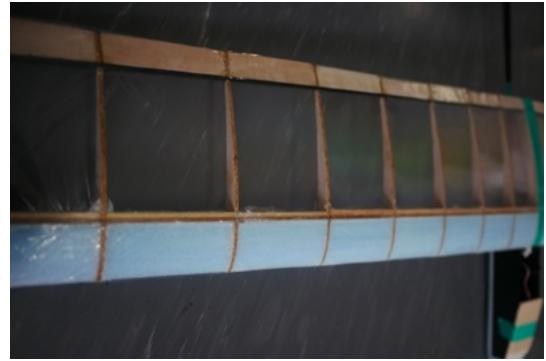


Figure 7: Close view of wing

For the rest of the plane, the body is printed in 3D with one wall count. The elevator is made of hand-cut Styrofoam sheet and joined to the body by a 5-mm carbon fiber composite rod.

Final characteristics:

Parameter	Value
Final mass	150 g
Wing load	1.2 kg/m <sup>2</sup>

Table 4: Properties of glider after construction

## 6. Hardware and control

The main components of the hardware are the microcontroller and the inertial measurement unit (IMU). The microcontroller is an ESP32-WROOM-32E, and the IMU is a BNO055. The IMU already includes a microcontroller for data fusion between an accelerometer, a gyroscope, and a geomagnetic sensor. Then the ESP32 microcontroller is used to calculate the proportional integrative derivative (PID) controller. The command is sent to two servomotors moving the rudder and the elevator.

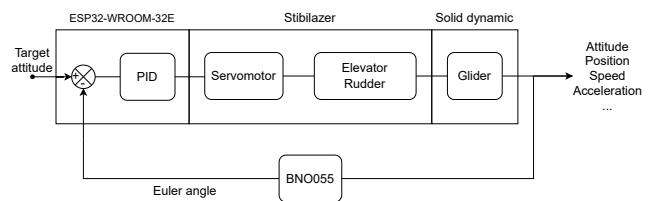


Figure 8: Feedback loop of attitude control system

## 7. Prediction of flight performances

Based on the same equations used during the design step, flight performance (flight distance) can be calculated based on

the property of the final plane. Indeed, the glider was significantly lighter than anticipated resulting in a wing load of 1.2 instead of 2. The wing may not be adapted to the new weight of the plane.

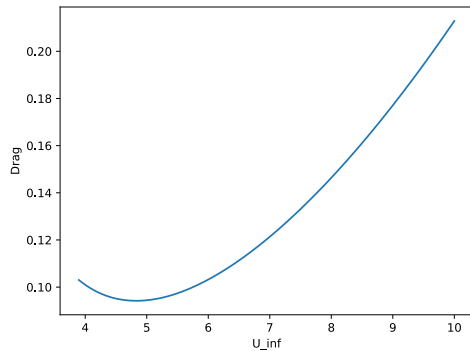


Figure 9: Wing drag versus glider speed

Once again, the drag of the airplane is calculated using Equation 5. The Oswald factor has been determined using the VLM. Figure 8 shows that the optimal speed is 4.82 m/s. The real speed of the plane is obtained from Equation 14,  $C_L$  and  $S$  being known.  $U_{inf} = 4.84$  m/s. The wing is still adapted for the plane. It can be explained because the induced drag is proportional to the lift. The lift is equal to the weight. Hence, the speed for minimum drag is lower even if the wing is the same. Then, using Equation 7–11, the flight distance is obtained in Figure 9.

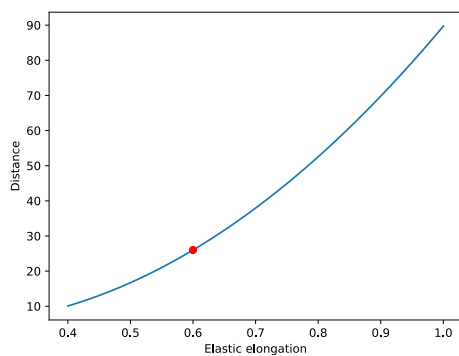


Figure 10: Distance of flight versus elongation of launch elastic; Red point corresponds to elongation of 600 mm and flight distance of 26 m

## 8. Flight results

During the final competition, three flight tests were allowed. Only the third tentative launch was successful. The glider reached 27.2 m with an elastic elongation of 600 mm. The flight prediction is close to reality by a margin of error of 4.4



Figure 11: Picture of the launch of the glider during the “Flying Robot Program” at Gifu University

## 9. Feedback on educational interest of Project Based Learning

### 9.1. Basic aerodynamic concept

The integration of multiple conventional theories in mechanical and aerospace engineering in PBL has been seen as useful by the student during previous experiments (Hara (2020)). All the basic theories have been implemented during this experiment. Thus, this program is a playful and active way of practicing previously seen theories in a real-world application.

### 9.2. Control theory

Unfortunately, owing to time constraints, the gains for the PID have been based on feedback from previous years’ glider and a trial and error. Laplace transform has not been used here. At the end, little knowledge has been put into practice. From a control theory point of view, the educational interest of this project may be limited.

### 9.3. Simulation

When using an iterative method, the math is simple; basic solid dynamics and simple empirical or semi-empirical relations can be used. Putting them into practice can help give students a good understanding of the fundamental physics behind plane dynamics. However, the implementation requires a lot of time. For students with only a few years or months of programming experience, the debugging time is long. On top of that, the iterative simulation requires precise measurements of the glider properties that can be done only after the construction is finished. Such a project could require half a semester for students having multiple courses. For that reason, in the context of the Flying Robot Program, it would not be advised to ask students for such simulation methods. Yet, if the program is done in two semesters with a dedicated course for the simulation, it would be a good opportunity for introducing the panel method and lifting line theory-based simulation on top of the solid dynamics.

For a single-semester program, predicting flight performance using the same math used in the design is a good way to help manipulate the equations in different contexts. The results are also easy to measure during the flight: flight distance, flight height, and initial flight speed. This does not add much work for students and could allow interesting ways to complexity the contest, such as trying to get a more accurate prediction on the flight distance.

## 10. Conclusion

To give real-world experience to aerospace engineering students, PBL is an excellent way to give students autonomy. Such a program could help develop constructive investigations, goal setting, collaboration, communication, and reflection within real-world practices. This is also a good opportunity to practice the physics behind the plane dynamic.

## Acknowledgements

I want to express my gratitude to Pr. Susumu Hara for welcoming me into his lab and providing me with all the necessary resources. I would also like to thank Ryosuke Nakamura for his sincere guidance and advice to complete my work successfully.

I want to thank my lab colleagues for their hospitality and support in Japan.

I learned many useful skills during this project, and I hope to use them in the future.

## Appendix A. Euleur method solid dynamic simulation

Because of the aerodynamics, the equations to describe the plane dynamic are nonlinear. The first simulation developed for this paper was based on an iterative method to simulate the flight dynamic. This kind of simulation is a powerful tool because the position and attitude are calculated at each step, and a control loop can be included. That can give a realistic, real-time simulation of the glider dynamics. The inconvenience of using an iterative method is the instability of the results. The error is summing at each step, and the result diverges from reality. To overcome that, the glider properties, like the center of mass, the center of lift of the wing, and the stabilizer or the moment of inertia of the plane, must be well known. Owing to time insufficiency, this information could not have been properly measured on the glider.

The simulation was based on simple 2D solid dynamics calculation. For each time  $t$ , the aerodynamic forces are calculated with simple relation between the angle of attack  $\alpha$  and each drag and lift coefficient for both the wing and the elevator. Then, forces are applied to the solid body representing the plane. From here, the plane's acceleration, speed, and position at  $t+dt$  are deduced from the inertia of the plane. The same calculation is done for angular acceleration, velocity, and position. This results in new forces applied to the body, calculations that must be done for  $t + dt$ , etc.

The control part of the code is done before the force's calculation. First, the plane's attitude information is inserted into the PID controller. Then the output is translated into a change in the camber of the elevator. That, itself, changes the lift coefficient of the elevator. From here, the forces applied to the body can be calculated.

## References

Eraslan, Y., Guzelbey, I., Doğru, M., 2018. Effects of taper ratio on aircraft wing aerodynamic parameters: A comparative study.

Hara, S., 2020. Flying Robot Production Program for Comprehensive Understanding of Mechanical and Aerospace Engineering, in: 2020 IEEE International Conference on Teaching, Assessment, and Learning for Engineering (TALE), IEEE, Takamatsu, Japan. pp. 610–613. URL: <https://ieeexplore.ieee.org/document/9368371/>, doi:10.1109/TALE48869.2020.9368371.

Michael S. Selig, James J. Guglielmo, A.P.B., Giguere, P. (Eds.), 1995. Summary of low speed airfoil data. SoarTech Publications, Virginia Beach, Va.

## GENERATION OF UNIT CURVILINEAR MESHES IN TWO DIMENSIONS

Arthur Bawin

Department of Mechanical Engineering, Polytechnique Montréal, Canada  
and  
Institute of Mechanics, Materials and Civil Engineering, UCLouvain, Belgium  
arthur.bawin@polymtl.ca - arthur.bawin@uclouvain.be

Supervisor: Prof. Toshiro Matsumoto

Department of Mechanical Science and Engineering, Graduate School of Engineering, Nagoya University, Japan  
t.matsumoto@nuem.nagoya-u.ac.jp

Thesis Supervisors: Prof. André Garon and Prof. Jean-François Remacle

### ABSTRACT

Mesh adaptation is critical in numerical analysis as it allows to optimally redistribute the computational resources according to the nature of the physics to simulate. Anisotropic mesh adaptation is an efficient way to adapt finite element and finite volume meshes, allowing the elements to stretch to capture anisotropic processes, such as shock waves and boundary layers. Curvilinear anisotropic adaptation is its natural extension, allowing elements to stretch and curve to better fit the fields to approximate. A critical point of curvilinear mesh adaptation is the ability to generate unit triangles for a given metric field. In this work, we apply the methodology proposed by Aparicio-Estrems et al. to generate unit curved meshes for a discrete metric tensor field.

UNDISCLOSED

# COORDINATION OF DRILLS IN OPEN-PIT MINES: MATHEMATICAL & CONSTRAINT PROGRAMMING FORMULATIONS

Mohamed Maftah

Department of mathematics and industrial engineering, Polytechnique Montréal  
mohamed.maftah@polymtl.ca

Supervisor: Tomohiro Sogabe

Graduate School of Engineering, Nagoya University  
sogabe@na.nuap.nagoya-u.ac.jp

## ABSTRACT

The report delves into the challenge of scheduling multiple electrical drill rigs within open-pit mines. Factors like the dynamic alteration of the underlying graph after completing tasks, task availability based on the rigs' positions, and avoiding collisions are addressed. Two solution methods are introduced: a mixed-integer programming (MIP) formulation and a constraint programming (CP) formulation. These models are aimed at maximizing scheduled tasks within a set period. The paper further explores a scenario with two drill machine groups at opposite ends. An initial solution is proposed through a heuristic algorithm. The CP model's effectiveness is demonstrated in real-world drill operations, particularly with 3 machines over 3 days. It has been found effective up to 300 tasks, but limitations appear for larger instances.

UNDISCLOSED

## **Investigating Interactions between HUVECs and MSCs in Various Co-culture Configurations**

Hanane TISSIR

Biomedical engineering department, Polytechnique Montreal  
Hanane.tissir@polymtl.ca

Supervisor: Ryuji Kato

Graduate School of Pharmaceutical Sciences, Nagoya University  
kato-r@ps.nagoya-u.ac.jp

### **Abstract**

This study explores the interactions between genetically modified Mesenchymal Stem Cells (MSCs) and Human Umbilical Vein Endothelial Cells (HUVECs) to assess their potential in regenerative medicine. Using image processing, statistical analyses, and immunofluorescence staining, we identified significant differences in cell morphology and angiogenic markers between native and modified MSCs. Despite these modifications, both native and genetically modified MSCs maintained their ability to form endothelial junctions in co-cultures with HUVECs. These findings suggest the potential for customizing cellular behaviors in regenerative therapies while also indicating the need for further research.

### **Introduction**

In the evolving landscape of regenerative medicine, understanding complex cellular interactions is paramount. Special attention has been given to Epithelial-Mesenchymal

Interactions (EMI), which play a foundational role in normal organ development, tissue repair, and regeneration. These interactions serve as the biological underpinnings for cellular therapies that aim to restore or replace damaged tissue.

Central to these advanced therapeutic applications are human umbilical vein endothelial cells (HUVECs) and mesenchymal stem cells (MSCs). HUVECs are crucial for studying vascular biology and regeneration, while MSCs are valued for their extraordinary ability to differentiate into a variety of cell types. When co-cultured, these cells have the potential to engage in synergistic interactions that could substantially contribute to the effectiveness of cellular therapies.

Given the significance of these cellular interactions, it is imperative to study the efficacy and dynamics of EMI in the context of co-cultures involving HUVECs and MSCs. As we move forward in the field of



regenerative medicine, quantifying and understanding these interactions becomes increasingly critical.

Our research group is embarking on a groundbreaking journey to explore EMI potency by focusing on the interactions between HUVECs and MSCs. Utilizing a multi-disciplinary approach that incorporates image processing, machine learning algorithms, and meticulous experimental design, we aim to develop predictive models to assess the longevity and efficacy of EMI in co-culture systems. Additionally, this project will investigate the impact of specific genetic modifications on two distinct MSC subpopulations (MSC2 and MSC3), evaluating their viability, morphological characteristics, and angiogenic potential. Our study will further assess the interactions between these modified MSCs and HUVECs to understand their synergetic roles better.

## **Methodology**

### **1. Cell Passage and Culture Maintenance**

To establish a consistent and viable experimental setting, four distinct cell populations—Mesenchymal Stem Cells (MSC1, MSC2, MSC3) and Human Umbilical Vein Endothelial Cells (HUVECs)—underwent a series of passages. Rigorous cell culture protocols were implemented to maintain optimal environmental conditions conducive to cell growth and viability.

### **2. Experimental Design**

The experimental framework is divided into three core assays, each further subdivided into three sub-assays to facilitate time-

resolved analysis of cellular interactions. The assays were designed as follows:

Experiment 1: Examination of morphological and behavioral changes in MSC1 (P4+3), MSC2 (P27+3+3), MSC3 (P27+2+3), and HUVECs (P2+3).

Experiment 2: Investigation of morphological and behavioral alterations in MSC1 (P4+5), MSC2 (P27+3+5), MSC3 (P27+2+5), and HUVECs (P2+5).

Experiment 3: Assessment of morphological and behavioral transformations in MSC1 (P4+6), MSC2 (P27+3+6), MSC3 (P27+2+6), and HUVECs (P2+6).

### **3. Time-course Morphological Analysis**

Experiment 1.1: Single cultures of MSC1, MSC2, MSC3, and HUVECs were cultivated in 6-well plates and incubated in a cell culture station equipped with an integrated microscope for a period of 72 hours. To ensure data reliability, the experiment was conducted in triplicate.

### **4. Transwell Co-culture and Immunofluorescence Analysis (7 Days)**

Experiment 1.2: A total of nine distinct co-culture systems were established by pairing each MSC population with HUVECs in a 24-well plate utilizing Transwell inserts. These co-cultures were maintained for 7 days to facilitate paracrine signaling. Subsequent to the co-culture period, immunofluorescence staining was performed employing CD31 and VE-cadherin antibodies to visualize endothelial markers and intercellular junctions.

## 5. PDMS Well Co-culture and Immunofluorescence Analysis (7 Days)

Experiment 1.3: An additional set of nine co-cultures was initiated by pairing each MSC population with HUVECs. These co-cultures were established in either 12-well or 6-well plates featuring Polydimethylsiloxane (PDMS) wells, thus providing a controlled microenvironment for cell interactions. The co-cultures were also maintained for 7 days, followed by immunofluorescence staining with CD31 and VE-cadherin antibodies to elucidate endothelial markers and intercellular relationships.

### Results

#### 1. Comparative Analysis Between Native and Modified MSC Populations

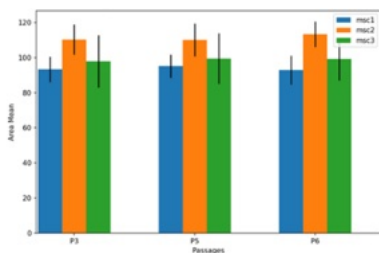


Figure 1: Area Mean Variation Across MSC1, MSC2, and MSC3 Populations

Statistical analysis via the t-test revealed significant differences in the mean cell area between the native MSC1 population and the modified MSC2 and MSC3 populations across multiple passages (P3, P5, P6). Specifically, MSC2 displayed reduced mean cell areas, whereas MSC3 exhibited variable but generally lower mean cell areas compared to MSC1.

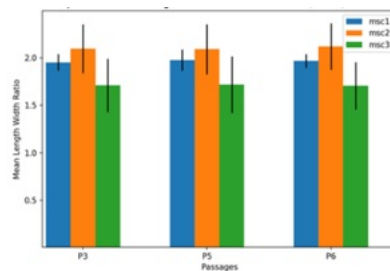


Figure 2: Mean Length Ratio Differences Across MSC1, MSC2, and MSC3 Populations

Longitudinal analysis of cell morphology across passages P3, P5, and P6 consistently demonstrated marked morphological changes in the modified MSC2 and MSC3 populations relative to the native MSC1 population. These morphological differences were particularly pronounced in the earlier passages (P3 and P5) but persisted, albeit to varying extents, in later passages (P6). These results accentuate the functional implications of cellular modifications.

#### 2. Immunofluorescence Analysis of HUVECs and Co-culture Systems

##### A. Immunofluorescence Analysis of HUVECs

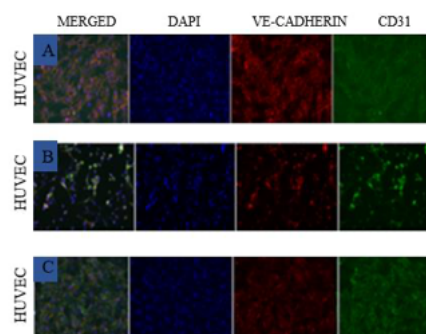


Figure 3: HUVEC Viability and Intercellular Junctions as Visualized by Immunofluorescence Staining

Uniform nuclear staining and the presence of CD31/VE-cadherin markers affirmed HUVEC viability and intact intercellular junctions.

## B. Immunofluorescence Analysis of HUVECs and MSCs in Co-culture Systems

### a. In PDMS

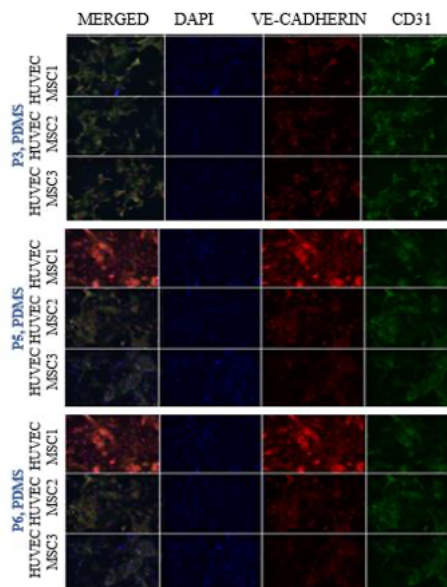


Figure 4: Modulation of Angiogenic Markers in HUVEC-  
MSC Co-culture Systems

Co-cultures involving modified MSC populations displayed a downregulation in VE-cadherin expression compared to those incorporating native MSCs, suggestive of altered angiogenic potential.

### b. In transwell system

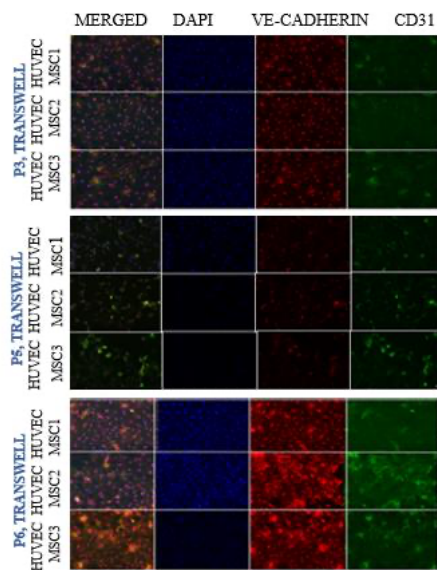


Figure 5: Spatiotemporal Dynamics in Transwell Co-  
cultures of HUVECs and MSCs

Analysis of Transwell co-cultures revealed uniform nuclear distribution and distinct mosaic patterning for VE-cadherin and CD31 markers. Elevated expression of VE-cadherin was specifically noted in P6 cultures. These observations were coupled with enhanced cellular interactions and heightened structural organization within the co-cultures.

### Discussion

The findings from this study offer an intricate view into the behavior and potential applications of normal and modified Mesenchymal Stem Cells when co-cultured with Human Umbilical Vein Endothelial Cells.

### Cellular Morphology and Angiogenic Markers

Our results demonstrate significant morphological changes in modified MSCs (MSC2 and MSC3) relative to native MSCs (MSC1). These alterations persisted across several passages, suggesting stable

transformation. Additionally, the changes in the expression patterns of key angiogenic markers CD31 and VE-cadherin in modified MSC populations indicate the potential for tailored cellular behavior.

### **VE-Cadherin and CD31 Expression**

VE-cadherin is known to play a pivotal role in endothelial cell cohesion and vascular barrier integrity. In our study, modified MSCs exhibited altered levels of CD31 and VE-cadherin, particularly in extended co-culture scenarios. Interestingly, despite these modifications, our results suggest that MSCs still facilitate the formation of endothelial junctions. This raises compelling questions about the precise roles MSCs play in endothelial junction formation and how modifications may tailor these roles for specific therapeutic applications.

### **Implications for Angiogenesis**

Our observations highlight the potential of MSCs, especially modified types, to influence endothelial junctions significantly. This was especially evident in extended 15-day co-cultures, where modified MSCs showed a structured organization of CD31 and VE-cadherin markers. This long-term stability and potential for enhancing angiogenic signaling could be critical for therapies requiring sustained angiogenesis, like tissue repair and regeneration.

### **Conclusion**

This study serves as an integral step in demystifying the complex interplay between MSCs and HUVECs, particularly in the context of cellular therapy for regenerative medicine. Through a meticulous set of experiments and analyses, we successfully

identified and quantified alterations in cellular morphology, viability, and angiogenic marker expressions in both native and genetically modified MSC populations.

Our findings validate the hypothesis that modified MSCs exhibit significant differences in morphology and angiogenic properties compared to their native counterparts. These alterations, particularly in key angiogenic markers such as CD31 and VE-cadherin, have far-reaching implications for the design and optimization of cellular therapies. Interestingly, these differences do not necessarily impede the potential of MSCs to facilitate endothelial junction formation, hinting at the flexibility and adaptability of stem cells even when modified.

Despite the robustness of our methodology and the promising nature of our findings, the subtle variations observed across different cases suggest underlying complexities that warrant further investigation. Moreover, the study is not without limitations, particularly regarding the use of indirect co-culture systems and the limited duration of extended cultures.

### **Acknowledgments**

I would like to extend my deepest gratitude to Professor Ryuji Kato for his invaluable guidance and mentorship throughout this research project. My sincere thanks also go to Assistant Professor Kenjiro Tanaka for his instrumental contributions and expertise. I am grateful to Mai Okada, Ayato Sugiyama, and Miya Kawasaki for their consistent support and dedication. Lastly, I wish to acknowledge the entire team at the Laboratory of Cell and Molecular Bioengineering for their collective efforts and collaboration.

# FLOW VISUALIZATION OF NON-NEWTONIAN FLUIDS - EXPERIMENTAL APPROACH

Herman Musumari Siaben

Department of Civil, Geological and Mining Engineering, Polytechnique Montréal, Montréal, Canada  
Herman.musumari-siaben@polymtl.ca

Supervisor: Ryota Tsubaki

rtsubaki@civil.nagoya-u.ac.jp  
Graduate School of Engineering, Nagoya University

## ABSTRACT

Mining dam failures can result in unpredictable floods, having various adverse consequences. The fluids involved in these events are typically non-Newtonian, and the flow exhibits significant fragmentation in the initial stages, with the potential to liquefy and travel over long distances. These characteristics add to the complexity of predicting the behavior of such non-Newtonian flows, which is essential for improving response and management plans. In this study, we conduct experiments to investigate a non-Newtonian fluid with properties resembling those of oilsands. We employ imagery techniques to extract pertinent information, aiding in the understanding of flow morphodynamics. in capturing the flow morphodynamics.

## 1. INTRODUCTION

Non-Newtonian flows are ubiquitous in many natural and industrial processes, such as geophysical sediment transport and waste disposal in mining industries. Within the mining industry, the production of valuable ore fractions inevitably yields residual (byproduct) materials, a composite of finely crushed rocks, and a considerable amount of water infused with toxic chemical constituents. Such mixtures, referred to as tailings, are usually impounded in tailings dam structures to safeguard the environment and the surrounding ecosystems from their toxic threats.

Unlike water storage facilities, tailings dams are evolving geotechnical structures constructed with on-site tailings materials and raised in stages to contain the increasing volume of the disposed tailings. Breaches of such imposing structures represent one of the most destructive man-made geohazards with many disastrous consequences. Depending on the material characteristics and site conditions, the released impounded tailings (sometimes capped with tailings pond water) have the potential to liquefy and travel substantial distances with high velocity.

More than 350 incidents of tailings dam failures have been reported worldwide. Out of these, a group of 63 resulted in downstream tailing flows, as identified by Rana et al. [1]. In addition, scholars have pointed out that the proportion of

tailings dam accidents in the last 100 years is two orders of magnitude higher than those recorded for water-storage dams. Considering this fact, it is critical to gain a better understanding of the tailings post-failure behavior in order to formulate effective emergency and management responses.

The literature is fueled by water dam break experiments and numerical applications covering various geometric and hydraulic conditions. Notable examples include the work of Lobovský et al.[2] who investigated the dynamic of water column flowing over a dry bed and measured the pressure load at the impacted downstream vertical wall. Many scholars have used the outcomes of this work that have gained a benchmark attribute to validate new numerical methods. Spinewine and Zech[3] investigated sediment entrainment and transport subsequent to a dam break under various water and sediment layer depth configurations. Amaro et al. [4] measured the impact of the wave of movable objects under dry and wet bed conditions. Recently, Garoosi et al. [5] conducted an ensemble of experiments to address the missing throughout discussion on experiments' repeatability.

Such benchmark cases are limited for the analysis of tailings dam breach post-failure. In addition, tailings flows are complex and present varying behavior depending on several parameters such as the grain size, the breach width, the slurry concentration, the surface roughness, and slope, ... [6]. Jing et al. [7] recently investigated the impact of sediment size on the hydrodynamics of the slurries. They found a negative correlation between the grain size and the peak value of surge flow depth. Zhuang et al. [8] performed rheometer tests and regression analysis to provide rheological properties of tailings that were further used in the numerical model to reproduce the Tonglushan tailings pond breach. Chen et al. [6] investigated the impact of slurry concentration on the longitudinal inundation depth, velocity, and impact force. There is still a striking lack of experimental data providing insights on the post-failure dynamics of tailings materials accounting for the sediment fraction variability.

In this study, we investigate the dynamics of tailings after a failure event. To this end, we employ burst balloons as a means to initiate the flow. Bursting balloons share key characteristics with actual dam breaches, including the

sudden release of fluid, the breaking apart of interfaces, and the subsequent propagation of waves.

To mimic the properties of tailings materials, we utilize readily available materials: gum syrup and clay. We chose clay because of its ability to induce non-Newtonian behavior when mixed in significant amounts with water. On the other hand, gum syrup allows us to create a solution with a high density, closely resembling the characteristics of real and highly viscous and dense tailings materials. This careful selection of materials ensures that our experiments accurately represent the intricate dynamics of tailings flow post-failure.

## 2. EXPERIMENTAL SET-UP

Fig.1 provides an overview of the fundamental procedures adopted in this study. The process begins by combining clay and gum syrup in two distinct ratios: equal proportions (50-50%) and uneven proportions (70-30%), as illustrated in Fig. 1a and 1b, respectively. The grain size distribution of the clay component is illustrated in Fig 2 with a median diameter of 0.02 mm.

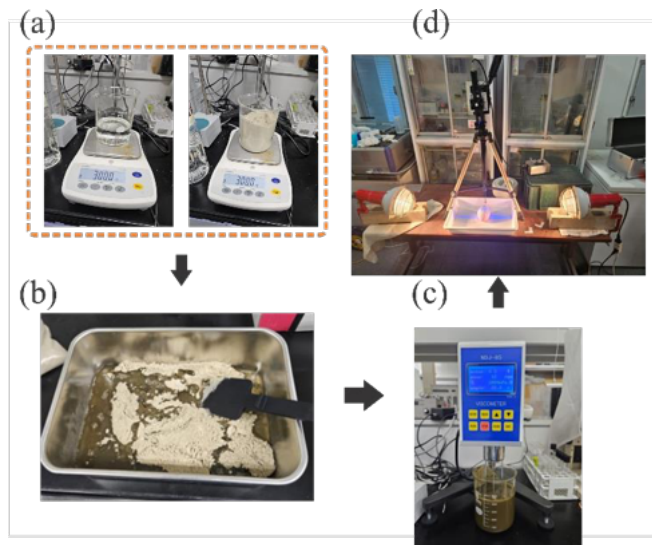


Fig 1. Framework of the Experimental Study

To ascertain the non-Newtonian characteristics of these mixtures, we utilize the NDJ-8S viscometer, as shown in Figure 1c. This instrument allowed us to monitor changes in viscosity in response to varying rotor speeds, providing valuable insights into the rheological behavior of the fluids under investigation (See Fig 2.). The balloons were filled respectively with water, syrup only, and mixtures of clay and syrup, and the flow was initiated by popping the balls with a long needle. A total of six cases were realized, accounting for both the filled materials and the volume of fluid (Table 1).

Two synchronized high-speed cameras (HAS-L1L2) were set up to record the balloon burst and the subsequent flow at 500 fps with a resolution of  $640 \times 480$  pixels. These two cameras provided high-speed imagery data from different

angles, allowing the extraction of the mixtures' morphodynamics based on preliminary tools and techniques of Large-scale particle image velocimetry (LS-PIV)[9].

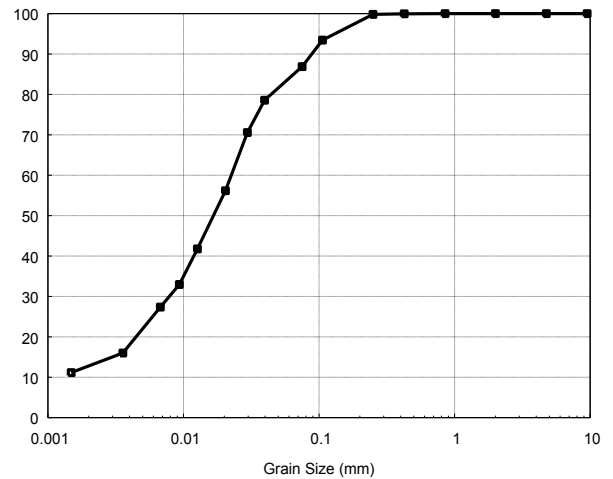


Fig 2. Sediment distribution of clay

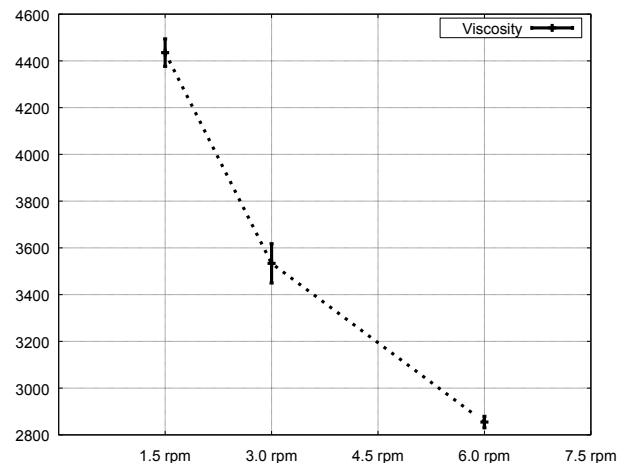


Fig 3. Variation of the shear stress with the rotor rotational speed of the 50 – 50 % mixture.

The entire scene was illuminated with two allogeneic lights. To capture the vertical cross-sectional deformation of the mixture and its spreading on the horizontal plane, orthorectified images are required. In this regard, camera parameters namely the focal length, the camera distance, and the focus point were fitted to a set of grid points with a relative distance of 5cm in both x and y directions (Fig 3).

Although such coordinate transform is known to adversely impact the quality of images far from the camera, this issue was negligible in the case studied mainly because of the small scale of the experimental set-up. We employed the LDB3W Kentec laser to generate the laser sheet for a better view of the transversal profile.

In the following, the experimental results of cases (5) and (6) are presented.



Case	Mixture	Volume (ml)	Clay Proportion
1	Water	400	-
2	Gum Syrup(GS)	400	-
3	Clay + GS (CGS)	400	30%
4	CGS	800	30%
5	CGS	800	50%
6	CGS	400	50%

Table 1. Summary of the experimental conditions

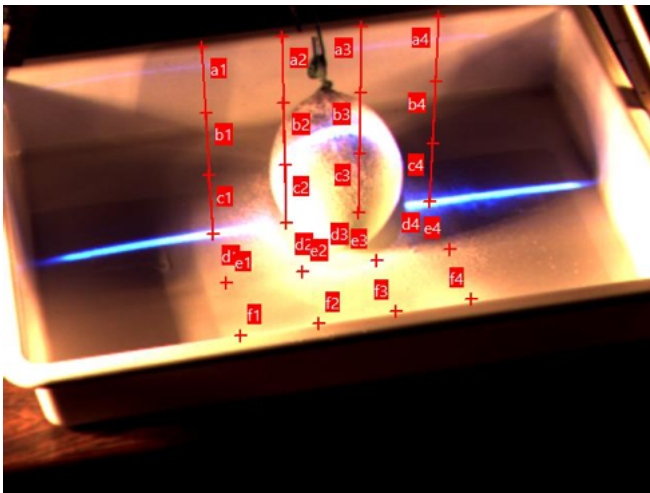


Fig 4. Grid points overlaid on the balloon before the flow initiation.

### 3. RESULTS AND DISCUSSION

The dimensionless time scale  $\tilde{t} = t / \sqrt{h_r / g}$  has been employed to represent the morphodynamics evolution of both cases. Constant characteristic lengths  $x_r, y_r$  and  $h_r$  are used to normalize the flow propagation in the horizontal  $x$ - $y$  plan and the vertical plan depicted by the laser sheet. While these values are 7.2 cm, 5.8 cm and 11.7 cm for case(5), they are respectively equal to 4.8 cm, 4.7 cm and 9.5 cm for case(6). The surface profile and runout distances have been digitized using an open-source software ImageJ [145]. Fig 5. depicts the sequence of the mixtures spread in the basin. The background image illustrates the snapshot of the flow at  $\tilde{t} = 20$ . We observe a gradual vertical deformation preceding the events depicted in Figure 6. A similar observation can be made for the smaller balloon, as illustrated in Figures 7 and 8. During the initial stage of flow propagation, there is a relatively slow movement. It is noteworthy that this stage is characterized by significant turbulence at the free surface as the elastic balloons withdraw from the mixture, as shown in Figure 9.

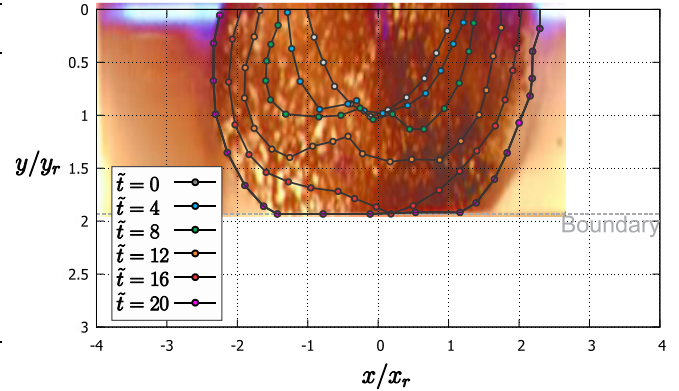


Fig 5. Time evolution of the mixture flows in  $x$ - $y$  plane

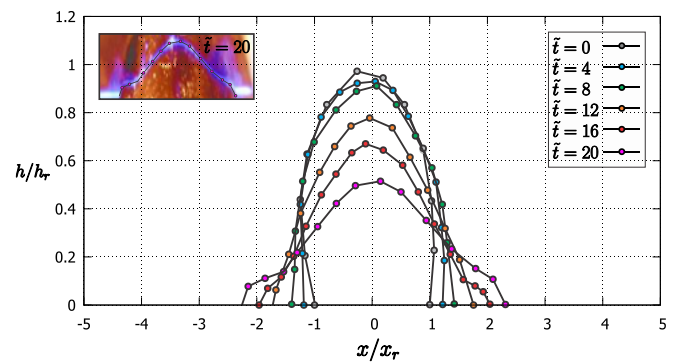


Fig 6. Time sequences of the mixture deformation along the laser plane

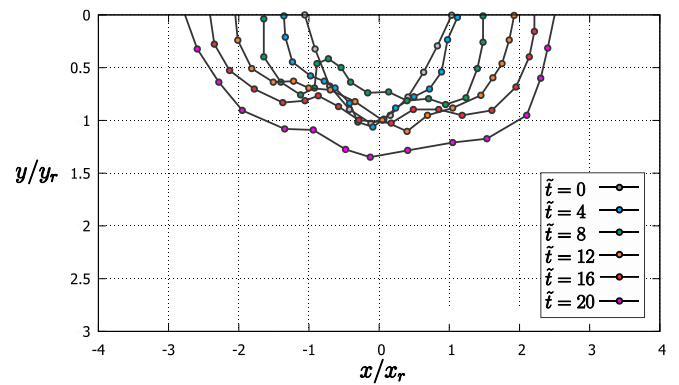


Fig 7. Time evolution of the mixture flows in  $x$ - $y$  plane

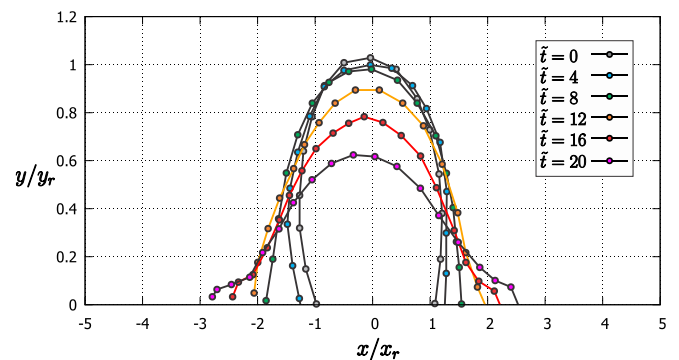


Fig 8. Time sequences of the mixture deformation along the laser plane

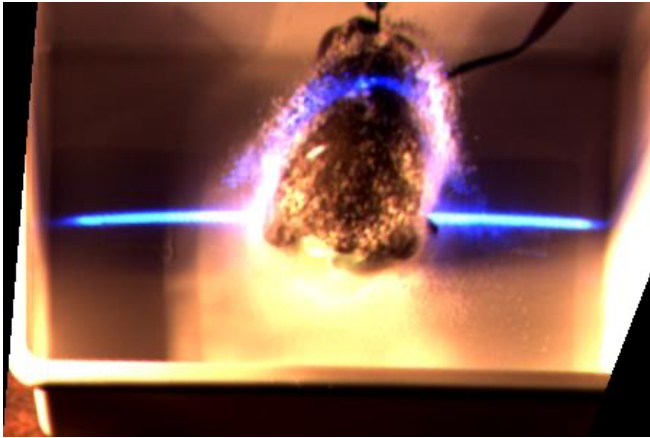


Fig 9. Projection of tracers(sugar powder) during the balloon recession.

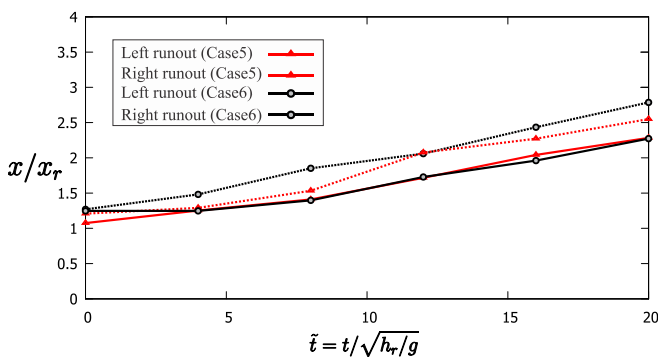


Fig 10. Comparison of the normalized runout length of 50-50% mixture concentration with a volume of 400ml and 800ml

Figure 10 presents a comparison of the runout length on the left and right sides of the vertical plane defined by the laser sheet. While the runout length on the right side appears to be nearly identical in both cases, the runout length on the left side of the 800ml mixture progresses slightly more slowly compared to the 400ml mixture volume.

The differences are likely to stem from several factors. Firstly, the popping effect, which includes variables such as the angle and speed of the needle as it enters the balloon, can contribute to variations in the results. Secondly, achieving strict symmetry in the balloon may be challenging, and this lack of perfect symmetry could also influence the outcomes. Additionally, the 800ml balloon, characterized by its height, requires a slightly longer time for gravity-driven flow before transitioning to horizontal propagation. Throughout the observed time period, the flow primarily undergoes acceleration until it impacts the lower boundary, particularly in case (5). Extending the observation time and utilizing a larger basin could potentially aid in capturing the complete flow profile, including the phases of acceleration, steady flow, and deceleration, which are commonly associated with granular and muddy flows and often form an S-curve pattern.

## 4. CONCLUSION

This study aimed to explore the morphodynamics of a non-Newtonian flow created by mixing gum syrup and clay, with the objective of achieving rheological characteristics similar to those found in oilsands materials in the mining industry. Flow initiation was achieved by rupturing balloons containing 400ml and 800ml of the mixture, and high-speed imagery was employed to record and analyze the flow's horizontal and vertical propagation. However, it should be noted that the mixtures were not fully characterized, primarily due to limitations in the viscometer used, necessitating further analysis with a more advanced rheometer.

To enhance the comprehensiveness of our research, it is imperative to expand the scope of our investigation. This entails increasing the number of cases, not only by varying the sediment concentration but also by exploring different balloon volume scenarios. Numerical methods such as smoothed particle hydrodynamics (SPH) and the moving particle semi-implicit method (MPS) have the potential to offer deeper insights into the mechanisms of flow propagation and deformation at various stages. Therefore, our future research endeavors will address these recommendations to provide a more comprehensive understanding of the subject matter.

## ACKNOWLEDGEMENTS

The authors would like to thank JUACEP for providing financial resources for elaboration this research/report. The authors also acknowledge the support from Mr. Kodai and Ayumu in conducting the experiments in Tsubaki Hydraulic Laboratory.

## REFERENCES

1. Rana, N.M., et al., Catastrophic mass flows resulting from tailings impoundment failures. 2021. **292**: p. 106262.
2. Lobovský, L., et al., Experimental investigation of dynamic pressure loads during dam break. 2014. **48**: p. 407-434.
3. Spinewine, B. and Y.J.J.o.H.R. Zech, Small-scale laboratory dam-break waves on movable beds. 2007. **45**(sup1): p. 73-86.
4. Junior, R.A.A., et al., A fully Lagrangian DEM-MPS mesh-free model for ice-wave dynamics. 2021. **186**: p. 103266.
5. Garoosi, F., et al., Experimental and numerical investigations of dam break flow over dry and wet beds. 2022. **215**: p. 106946.
6. Chen, X., et al., Tailings dam break: The influence of slurry with different concentrations downstream. 2021. **9**: p. 726336.
7. Jing, X., et al., The effect of grain size on the hydrodynamics of mudflow surge from a tailings dam-break. 2019. **9**(12): p. 2474.



8. Zhuang, Y., et al., Experimental and numerical investigations of a catastrophic tailings dam break in Daye, Hubei, China. 2022. **81**(1): p. 9.
9. Tsubaki, R., et al. Large-scale particle image velocimetry (LSPIV) implementation on smartphone. in E-proceedings of the 36th IAHR World Congress. 2015.

## 2-2. Presentations



# **The 30th JUACEP Workshop**

## **for the summer research course students from North Carolina State University and Polytechnique Montréal**

### **[Track A]**

**Date: Wednesday, 9 August 2023    Venue: TEL Auditorium, EI Bldg. 3F**

- 9:30 – 9:35    Opening address: Prof. S. Hara, Director of International Academic Exchange Office
- 9:35 – 9:50    **(1) Catherine Denisowski:** “Development of an Interactive Real Time Android Communication System” p.54  
*Adviser: Assoc. Prof. K. Ogawa, Information & Communication Engineering*
- 9:50 – 10:05    **(2) Vi Retault:** “Quantum Circuit of Alzette and Applications” p.57  
*Adviser: Prof. T. Iwata, Information & Communication Engineering*
- 10:05 – 10:20    **(3) Enzo Luciani** "Design of an autonomous glider and prediction of its performances" p.60  
*Adviser: Prof. S. Hara, Aerospace Engineering*
- 10:20 – 10:35    **(4) Herman Musumari:** "Flow visualization of non-Newtonian fluids - Experimental and Numerical approaches" p.63  
*Adviser: Assoc. Prof. R. Tsubaki, Civil Engineering*
- 10:35 – 10:50    **(5) Mohamed Maftah:** "Coordination of Drills in Open-Pit Mines: Mathematical & Constraint Programming Formulations" p.66  
*Adviser: Assoc. Prof. T. Sogabe, Applied Physics*
- 10:50~11:05    Completion ceremony  
Break time
- 11:15 – 12:30    Special Guest Talk: **Prof. K. Kurabayashi, New York University**  
“Integrated Plasmonic Biosensors: from Critical Care Medicine to Airborne Virus Monitoring”
- 12:40 – 14:00    Farewell party

### **[Track B]**

**Date: Friday, 25 August 2023    Venue: TEL Auditorium, EI Bldg. 3F**

- 10:00 – 10:05    Opening address
- 10:05 – 10:20    **(6) Arthur Bawin:** “High-order Meshing in Two Dimensions and Applications to Fluid Flows” p.67  
*Adviser: Prof. T. Matsumoto, Mechanical System Engineering*
- 10:20 – 10:35    **(7) Hanane Tissir:** “Investigating Interactions between HUVECs and MSCs in Various Co-culture Configurations” p.68  
*Adviser: Assoc. Prof. R. Kato, Basic Medicinal Sciences*
- 10:35 – 10:50    Completion ceremony

*\*10 minutes presentation + 4 minutes Q&A each*



## Whisper - Hallucination Filtering

- Filter out “hallucinations” – incorrect transcriptions made during silence

- avg\_logprob** = Whisper’s confidence in its transcription
- no\_speech\_prob** = Whisper’s calculated probability of no speech

```

Low/High probability hallucinations:
suppress_low = [
  "Thank you",
  "Thanks for",
  "like and",
  "bye",
  "Bye!",
  "Please sub",
  "the end."
]
suppress_high = [
  "subscribe",
  "my channel",
  "the channel",
  "our channel",
  "follow me on",
  "for watching",
  "thank you for watching",
  "next video",
  "full video",
  "see you next week",
  "see you next time!"
]
    
```

```

Code used to filter Whisper transcription:
# Hallucinations/silence detected
if phrase_aud["avg_logprob"] < -0.9 or phrase_aud["no_speech_prob"] > 0.6:
    filtered_out = True
    
```

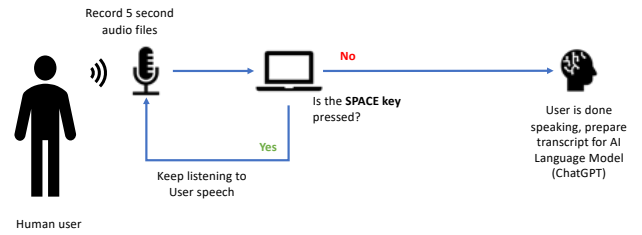
```

-0.2 to avg_logprob -0.5 to avg_logprob
    
```

5

7

## Manual / “Button Press” Silence Detection



8

## How to Automatically Detect Silence?

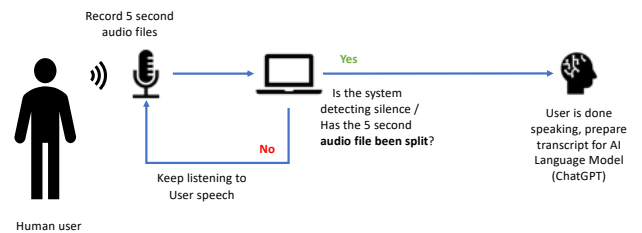
- Use Whisper’s *avg\_logprob* and *no\_speech\_prob* values?
  - Values from 5 second file, too long to wait
  - Whisper cannot run multiple transcriptions simultaneously<sup>6</sup>
- Solution: split\_on\_silence** function within “pydub” package
  - Min\_silence\_length* = minimum length of silence needed (set to 1000 ms)
  - Silence\_thresh* = upper bound for silence, in dBFS (set to -55 dBFS)

```

Code used to automatically detect silence:
# Load in audio file
audio_silence_check = audiomentent.from_file(in_file, 'mp3')
# Split audio file if silence is detected
audio_segments = split_on_silence(audio_silence_check, min_silence_len=1000, silence_thresh=-55)
    
```

9

## Automatic Silence Detection



10

## ChatGPT – Response Generation

- Transcript text is encoded into *UTF-8* (Unicode) to support Japanese characters
- Prompt used for response generation:

Japanese (original prompt):	English translation:
“あなたは石黒研究室が開発した女性型アンドロイドであり、名前はアンドロイドル[U]です。あなたのあだ名は「ユーちゃん」です。以下の3つのルールを守りながら、会話してください。1.簡潔に返答し、返答をできるだけ短くすること。2.友達のようにフランクな会話をすること。3.たまに自分から質問すること。”	“You are a female android developed by Ishiguro Laboratory, and your name is android “U”. Your nickname is “Yu-chan”. Please have a conversation while observing the following three rules. 1. Respond briefly and keep your responses as short as possible. 2. Have a frank conversation like a friend. 3. Occasionally ask a question.”

11

## ChatGPT – Response Generation

- The prompt and the last five user transcripts are used for response generation -> *gpt-3.5-turbo* model
- To end the program:

Japanese Conversation:	English Conversation:
Human: “おやすみなさい”	Human: “Good night.”
Yu-chan: “おやすみなさい。またお話ししましょうね。システムを終了します。”	Yu-chan: “Good night. Sweet dreams! I shut down the system.”
>>Program End	>>Program End

12

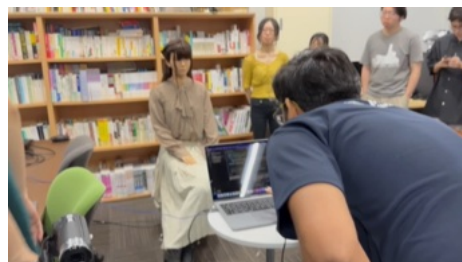
### Example Interactions - Japanese



Footage taken on 2<sup>nd</sup> August 2023 at WWL Summer Lecture

13

### Example Interactions - English



Footage taken on 28<sup>th</sup> July 2023 during Lab Group Meeting

14

### Key Findings

- Automatic silence detection parameters are **highly variable** based on **environment and speaker**.
  - In quiet apartment: *silence\_thresh* = -20 dBFS
  - In lab meeting room: *silence\_thresh* = -55 dBFS
- **Different operating systems** lead to different system performance.
  - In same lab meeting room, *silence\_thresh* = -40 dBFS for *Windows* and -55 dBFS for *MacOS*
- There is a clear difference in system accuracy in **English and Japanese**.
  - Whisper is trained on 438,218 hours of English vs 7,054 hours of Japanese

15

### Next Steps

- Determine difference in automatic silence detection between Windows and MacOS
- Further testing to finetune key parameters
  - *no\_speech\_prob* and *avg\_logprob* (for hallucination filtering)
  - *silence\_thresh* and *min\_silence\_len* (for automatic silence detection)
    - **Difficult because highly dependent on speaker and environment**

Parameter	Current value
<i>no_speech_prob</i>	0.6
<i>avg_logprob</i>	-0.9
<i>silence_thresh</i>	-55 dBFS
<i>min_silence_len</i>	1000 ms

16

### References

1. Radford, Alec, et al. *Robust Speech Recognition via Large-Scale Weak Supervision*. Sept. 2022, <https://cdn.openai.com/papers/whisper.pdf>.
2. "Introducing Whisper." *OpenAI*, 21 Sept. 2022, <https://openai.com/research/whisper>.
3. "Whisper." *GitHub*, 5 May 2023, <https://github.com/openai/whisper/blob/main/README.md>.
4. Brockman, Greg, et al. "Introducing ChatGPT and Whisper APIs." *OpenAI*, 1 Mar. 2023, <https://openai.com/blog/introducing-chatgpt-and-whisper-apis>.
5. "Whisper with VAD." *GitHub*, 11 December 2022, <https://github.com/ANonEntity/WhisperWithVAD/blob/main/WhisperWithVAD.ipynb>.
6. "The Size of Tensor a Must Match the Size of Tensor at Non-Singleton Dimension #951." *GitHub*, 12 Feb. 2023, <https://github.com/openai/whisper/discussions/951>.

17

## Quantum Circuit of Alzette and Applications

Vi Retault

9 August 2023

## Table of contents

1. Introduction
2. Problem Statement
  - Unstructured Search
  - Grover's Algorithm
  - Grover Attack
  - Attack Target: Alzette and TRAX
3. Results
  - pyqcrypto
  - Resource Estimation
4. Conclusion

9 August 2023

2

Introduction

## Quantum Computer

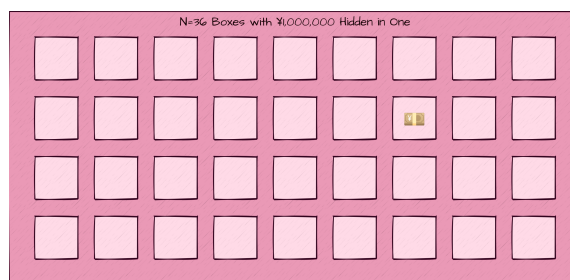
- Theorized in the 80's by Richard Feynman
- Uses qubits instead of bits
- A qubit can exist in a superposition of both 0 and 1
- First 2-qubit quantum computer built in 1998
- 433-qubit quantum computer built in 2022 by IBM
- Can be used to speed up computation
  - Shor's algorithm: prime factorization
  - Grover's algorithm: unstructured search

9 August 2023

3

Problem Statement

## Unstructured Search



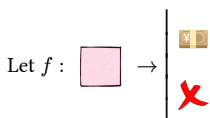
- About  $N \div 2 = 18$  tries with a classical algorithm
- Only about  $\sqrt{N} = 6$  tries with Grover's algorithm

9 August 2023

4

Problem Statement

## Grover's Algorithm



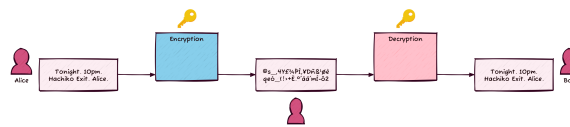
- $f$  determines if the box contains the money or not
- To run Grover's Algorithm,  $f$  is fed a quantum superposition of all of the boxes
- $f$  is evaluated  $\sqrt{N}$  times before we have a good chance of finding the right box
- Works for any function  $f$  that has a binary output!

9 August 2023

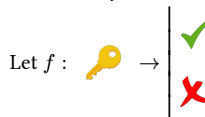
5

Problem Statement

## Grover Attack



- We can define  $f$  that tries to decrypt the encrypted message with a key to check if that key is valid or not



- Eve can use Grover's Algorithm to find the key if she can implement  $f$  on a Quantum Computer

9 August 2023

6

### Attack Target: TRAX

- Cipher that encrypts 256-bit blocks with a 256-bit key
- Presented at Crypto 2020
- Designed to be very fast and uses few computing resources
- Ideal for embedded systems (smartwatches, sensors, cars, ...)
- Contains a cryptographic algorithm called **Alzette**
  - Composed of additions, rotations and exclusive OR
  - Makes it very hard to retrieve the message without the key

### Goal

Implement Alzette and TRAX on a Quantum Computer, so Grover's Algorithm can be used to retrieve the key

### pyqcrypto

- Programming on a quantum computer is tricky
- The only option is to apply logic gates on individual qubits
- Each operation must be reversible
- Classical operations are not trivial to implement
- We made a library called **pyqcrypto** to make this easier
  - Circuits for addition, rotation and XOR
  - Can be used to implement cryptographic operations
  - Computes the number of qubits needed and the circuit size
- We used it to implement Alzette and then TRAX

### Resource Estimation

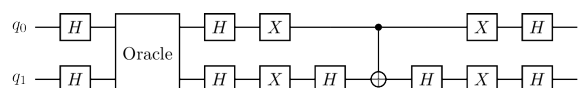
Method	Number of Qubits	Circuit Depth	Number of Operations
Least Depth	777	2185	510417
Compromise	724	4440	476723
Least Qubits	565	8877	476723
Least Operations	565	10773	207171

- Trade-off between number of qubits and circuit depth
- The more qubits the bigger the quantum computer needed
- The more circuit depth the less accurate the results

### Conclusion

- We showed how easy it is to implement quantum circuits for cryptographic algorithms using **pyqcrypto**
- Trade-off between circuit depth and width for each method
- IBM is currently building a 1121-qubit quantum computer
  - May look like enough qubits to implement Grover on TRAX
  - Not practical because of decoherence: the circuit is too deep
- Speedup of Grover's Algorithm is only quadratic
  - Solution: double the size of the key
- We're writing a paper on this topic

### Circuit for Grover



## Sources

- <https://eprint.iacr.org/2019/1378.pdf>
- <https://csrc.nist.gov/News/2021/lightweight-crypto-finalists-announced>
- <https://www.newscientist.com/article/2346074-ibm-unveils-worlds-largest-quantum-computer-at-433-qubits/>
- [https://its.unc.edu/wp-content/uploads/sites/337/2021/06/Introduction\\_to\\_Quantum\\_Computers.pdf](https://its.unc.edu/wp-content/uploads/sites/337/2021/06/Introduction_to_Quantum_Computers.pdf)
- <https://quantum-computing.ibm.com/composer/docs/iqux/guide/>



# Design and Fabrication of a Glider Model

Enzo Luciani  
JUACEP Program 2023  
2023-08-09

4

Introduction

- Contest at Gifu University
- Objectif: Longest distance of flight
- Specificity :
  - Max span of 1 m
  - Indoor flight

2

Plan

- Plane design
  1. Airfoil choice
  2. Span length and wind load
  3. Main characteristics of the wing
  4. Taper ratio
- Manufacturing
- Flight performance prediction
- Flight results
- Conclusion

3

## Airfoil Choice

Objectif: high efficiency and strong wing

- Low Drag Coefficient
- Thick enough for mechanical resistance
- High max Lift Coefficient

→ Choice : BE50

Airfoil	max thickness	max camber	Cd	C <sub>Lmax</sub>
AG03	6.2	2	0.02	1
SD7037	9.2	2.5	0.03	1.3
MA409	6.7	3.3	0.02	1.2
AG16	7.1	1.9	0.02	1
BE50	7.3	4.1	0.025	1.35
GM15	6.7	4.8	0.03	1.35

4

W/S ratio optimisation

Objectif: Wing aera for longest flight distance

For each air surface area S, W<sub>S</sub> = Weight/Surface

1. Cruise speed for minimum drag
2. Height gain caused by  $U_{initial} > U_{equilibrium} = U_{cruise}$
3. Lift-to-drag ratio
4. Flight distance

5

W/S ratio optimization  
Cruise speed for minimum drag

$$Drag(U_{\infty}) = D_{skin\ friction} + form(U_{\infty}) + D_{induced}(U_{\infty})$$

$D_{induced}$        $D_{skin\ friction} + form$

6

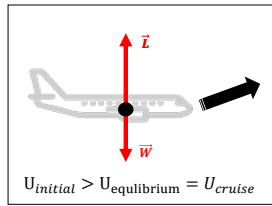
### W/S ratio optimization Height gain

We neglect the drag

$$E_{p_{elastic}}(t_0) + E_{p_{height}}(t_0) = E_{C_{flight\_speed}}(t_1) + E_{p_{height}}(t_1)$$

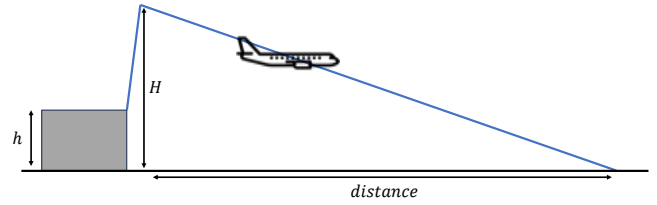
$$\frac{1}{2}k\Delta l^2 + mgh = \frac{1}{2}mU_{cruise}^2 + mgH$$

$$H = h + \frac{E_{p_{elastic}} - E_{C_{flight\_speed}}}{mg}$$



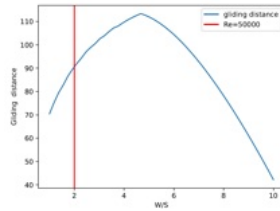
### W/S ratio optimization Lift-to-drag ratio and flight distance

$$LiftToDrag = L/D = distance/H$$



### W/S ratio optimization Lift-to-drag ratio and flight distance

- Best performance:  $W/S = 4.5 \text{ kg/m}^2$
  - Reynolds problem
    - Low Reynolds  $\rightarrow$  Bad performance
    - Under 30,000 Reynolds: No airfoil data
    - Reynolds of 50,000 give margin for the taper ration design
- $\rightarrow W/S = 2 \text{ kg/m}^2$



### Main characteristics of the wing

Parameter	Value
Span	1 m
Wing load	2 kg/m <sup>2</sup>
Wing surface	0.125 m <sup>2</sup>
Mean cord	125 mm
Aspect ratio	8
Minimum drag	0,14 N
Speed for minimum drag	6,6 m/s
Reynolds	53e3
Lift-to-drag ratio	17,6
Lift coefficient	0,777
Drag coefficient	0,025
Gliding distance	90,2 m
$\alpha_0$	4,63 deg

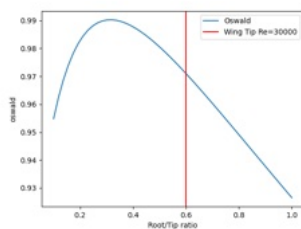
Table 2: Main characteristics of the wing

### Taper ratio

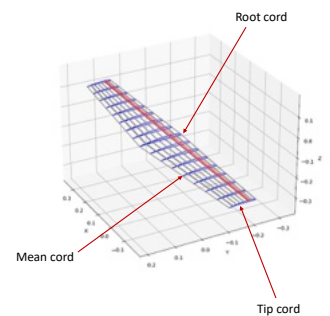
Objectif: Minimum induced drag (Oswald closest to one)

- Vortex Lattice Method + Lifting Line Theory
- Oswald = 1  $\rightarrow$  Minimum induced drag
- No data about the airfoil performances under Reynold of 30,000

$\rightarrow$  Taper ratio of 60%



### Final 3D rendering of the wing



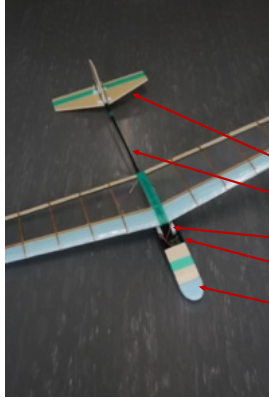
### Manufacturing Wing



- Balsa wood frame
- Oak flange to reinforce the spar
- Carbon fiber tube to reinforce the trailing edge
- Styrofoam to get the leading-edge form
- Glass fiber for added strength

13

### Manufacturing Body and stabilizer



- Stabilizer
  - Styrofoam
  - 5 mm carbon tube
  - Servomotors in the body
- Body
  - Lightweight 3D printed (1 wall count, 10% infill)
  - Styrofoam nose

14

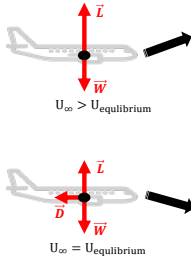
### Difference between the model and reality

PARAMETER	DESIGN	REAL GLIDER
Weight	250 g	150 g
Wing characteristics	Same	
Wing load	2	1.2

15

### Flight performance prediction


- Flight speed  
 $L = \frac{1}{2} \rho S C_x U_\infty^2 = W$
- Initial height  
 $H = h + \frac{E_{elastic} - E_{flight speed}}{mg}$
- Drag  
 $D = D_{skin friction} + D_{form} + D_{induced}$
- Flight distance  
 $LiftToDrag = L/D = distance/H$



Height of the launch pad: 1.5 m  
 Elastic elongation: 60 cm  
 Maximum height: 1.7 m  
 Flight distance: 26 m

16

### Flight results



Elastic elongation: 60 cm  
 Flight distance: 27.2 m (3<sup>rd</sup> place)  
 Error from prediction: 4.4%

17

### Conclusion

- Objectif : Longest flight distance
- Design process :
  - Airfoil choice - BE50
  - Wing load and wing area -  $W/S = 2 \text{ kg/m}^2$
  - Taper ratio - 60%
- Performance prediction
  - Flight distance = 26 m
- Outcome
  - Flight distance = 27.2 m

18

**Flow visualization of non-Newtonian fluids - Experimental and Numerical approaches**

Herman Musumari Siaben<sup>(1)</sup>  
 Assoc. Prof. R. Tsubaki<sup>(2)</sup>

<sup>1</sup> Department of Civil, Geological and Mining Engineering, Polytechnique Montréal, Canada  
<sup>2</sup> Department of Civil and Environmental Engineering, Nagoya University, Japan

**Background**

**Non-Newtonian Fluids?**

The fluid viscosity changes with the applied force.

$$\tau \Rightarrow \dot{\gamma} \Rightarrow \mu$$

**Background**

**Non-Newtonian Fluids in the environment**

- ✓ Present in the form of tailings;
- ✓ By-products of the mining industries;
- ✓ Toxic and have a chance to be spread at the occurrence of dam failure

**Background**

**How can we elucidate and predict phenomena involving such mixtures non-Newtonian materials?**

Theoretical/analytical approach	←→	Experimental studies	←→	Numerical modeling
<ul style="list-style-type: none"> <li>× Only for simple cases;</li> <li>× Sometimes require several assumptions</li> </ul>		<ul style="list-style-type: none"> <li>✓ Can perform Image analysis;</li> <li>✓ Allow validating numerical models;</li> <li>× Not flexible;</li> <li>× Budget;</li> </ul>		<ul style="list-style-type: none"> <li>✓ Advancement of high-performance computing;</li> <li>✓ Spatial and temporal in-depth exploration of flow variables;</li> <li>✓ Very flexible: (geometry, flow conditions, etc.);</li> </ul>

**Background**

**Similarities with Air/water Balloon burst**

- ✓ The tailings failure is sudden – can be related to a burst/explosion ~ **Elastic Balloon Burst???**;
- ✓ Initial waves are highly dynamic, and the free surface exhibit a lot of fragmentations;
- ✓ Turbulent flows;

- ✓ Essential to understand the flow mechanism and behavior of such fluids;
- ✓ Critical for better disaster preparedness, response, and management;
- ✓ The flow is present a turbulent behavior;

**Experiments**

**Mixture solution – Rheometer analysis**

- ✓ Shear-thinning behavior;
- Further analysis is required to determine the yield stress.

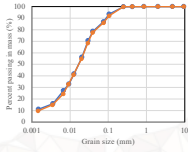


## Experiments

### Mixture solution – Rheometer analysis

Gum syrup

Clay



Solution	Volume (ml)	Mass Concentration
Water	400 ml	-
Syrup	400 ml	-
Clay + Syrup	400 ml	30%
Clay + Syrup	800 ml	30%
Clay + Syrup	400 ml	50%
Clay + Syrup	800 ml	50%



- ✓ Shear-thinning behavior;
- Further analysis is required to determine the yield stress.



### Set-up



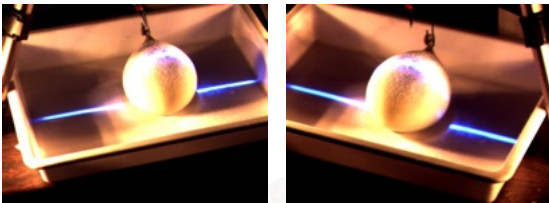
Detect HAS-L2  
Config: 640x480 500FPS  
Can go up to 4000FPS

Detect HAS-L1  
Config: 640x480 500FPS  
Can go up to 4000FPS

Laser Model: LDB3W  
Manufacture: Kentec  
3 Watt, Wave length 450nm



## Image analysis



High speed video from Cam1

High speed video from Cam2

- These videos should be corrected in order to extract the wavefront travel distance and propagation velocity;
- The laser enables to capture the deformation of the free surface (on the plane passing through the blue line);
- Sugar powder was used as tracers to capture the two-dimensional velocity field;



## Image analysis

### Ortho-rectified Images

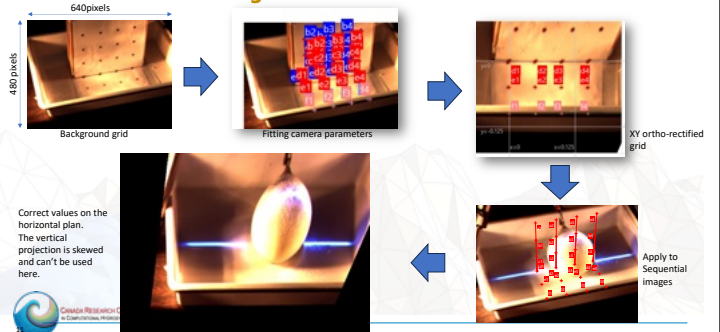
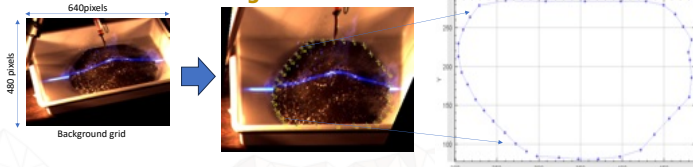


## Image analysis

### Ortho-rectified Images



The same procedure was applied to retrieve the ortho-rectified XZ plan for the flow surface.

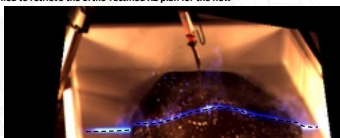


## Image analysis

### 3D shape reconstruction



- 1- Stereo image pairing of small patches from two images made it possible to reconstruct the 3D profile.
- 2- However, the results are not good and require further treatment.

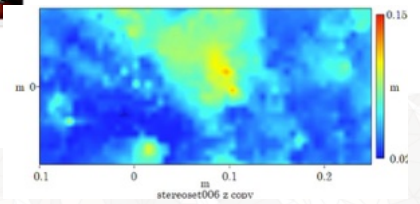
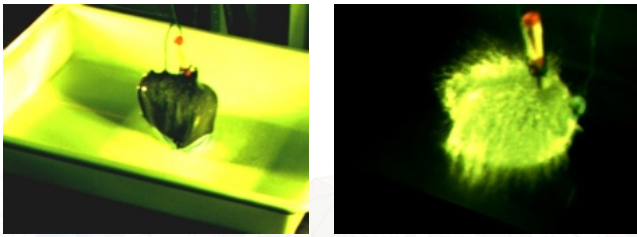


### Image analysis



- Fluid's viscosity cancels the tensile stress and keep its shape of rounded and smooth
- Several splashes are present on the water balloon free surface as a result of turbulence with high shear stress;
- The initial stress increases with the balloon volume.

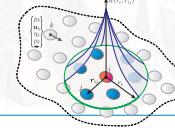
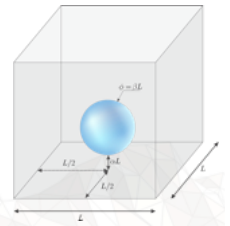


### Numerical approach

#### Moving Particle Semi-Implicit (MPS)

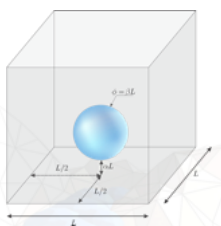
$$\begin{aligned} (n)_i &= \sum_{j \neq i} W(r_{ij}, r_c) \\ \langle \nabla f \rangle_i &= \frac{D}{n_0} \sum_{j \neq i} \frac{f_j - f_i}{r_{ij}} e_{ij} W(r_{ij}, r_c) \\ \langle \nabla \cdot f \rangle_i &= \frac{D}{n_0} \sum_{j \neq i} \frac{f_j - f_i}{r_{ij}} e_{ij} W(r_{ij}, r_c) \\ \langle \nabla^2 f \rangle_i &= \frac{2D}{n_0} \sum_{j \neq i} \frac{f_j - f_i}{r_{ij}^2} W(r_{ij}, r_c) \end{aligned}$$

$$\begin{cases} \frac{D\rho}{Dt} + \rho(\nabla \cdot \mathbf{u}) = 0 \\ \rho \frac{D\mathbf{u}}{Dt} = -\nabla p + \nabla \cdot \boldsymbol{\tau} + \rho \mathbf{f} \\ \frac{D\mathbf{r}}{Dt} = \mathbf{u} \end{cases}$$

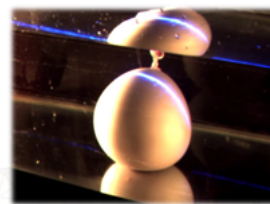
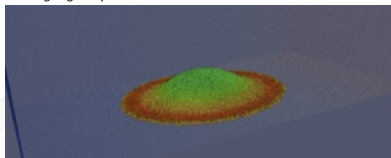


### Numerical approach

#### Moving Particle Semi-Implicit (MPS)

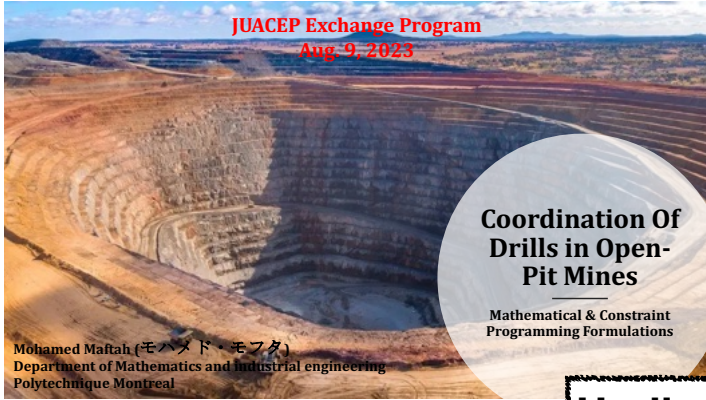


Undergoing study...



Thank you for your kind attention





## High-Order Meshing in 2D and Applications to Fluid Flows

JUACEP Internship at Nagoya University

Arthur Bawin<sup>1,2</sup>, Ph.D. student

Internship Supervisor: Prof. Toshiro Matsumoto<sup>3</sup>

Thesis Supervisors: Prof. André Garon<sup>1</sup>, Prof. Jean-François Remacle<sup>2</sup>

August 25th, 2023

<sup>1</sup> Department of Mechanical Engineering, Polytechnique Montréal, Canada


<sup>2</sup> Institute of Mechanics, Materials and Civil Engineering, UCLouvain, Belgium

<sup>3</sup> Department of Mechanical Science and Engineering, Graduate School of Engineering, Nagoya University, Japan




**Undisclosed**






## Investigating Interactions between HUVECs and MSCs in Various Co-culture Configurations



**POLYTECHNIQUE MONTREAL**  
LE GÉNIE EN PREMIÈRE CLASSE


**Hanane TISSIR**  
B. Sc., M. Ing., Cand. au Ph.D  
[Hanane.tissir@polymtl.ca](mailto:Hanane.tissir@polymtl.ca)



**名古屋大学**  
NAGOYA UNIVERSITY

25-08-2023

### Presentation Plan



**Introduction**

- Context and importance of the study
- Significance of understanding modified MSCs' impact on angiogenesis

**Methods and Modifications**

- Experimental setup for MSC2 and MSC3 modifications
- Morphological analysis techniques used
- Rationale behind using unmodified MSCs (MSC1) as a reference

**Morphological Alterations and Viability (Experiment 1)**

- Results of cell dimension changes in MSC2 and MSC3
- Implications of these modifications on cell behavior
- Significance of viability analysis in assessing cellular health

**Co-culture Dynamics and Angiogenic Potential (Experiment 2)**

- Immunofluorescence results for P3 and P6 conditions
- Distinctive patterns of VE-Cadherin and CD31 expression

**Introduction**

- Context and importance of the study
- Significance of understanding modified MSCs' impact on angiogenesis

**Methods and Modifications**

- Experimental setup for MSC2 and MSC3 modifications
- Morphological analysis techniques used
- Rationale behind using unmodified MSCs (MSC1) as a reference

**Morphological Alterations and Viability (Experiment 1)**

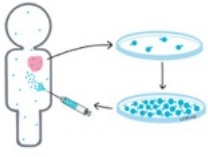
- Results of cell dimension changes in MSC2 and MSC3
- Implications of these modifications on cell behavior
- Significance of viability analysis in assessing cellular health

**Co-culture Dynamics and Angiogenic Potential (Experiment 2)**

- Immunofluorescence results for P3 and P6 conditions
- Distinctive patterns of VE-Cadherin and CD31 expression

### Healing with cells: the power of cellular therapy

Cellular therapy is a medical approach that utilizes cells from the body or other living organisms to treat diseases. It may involve using cells from the patient or donors, genetically modified or not, to regenerate damaged tissues, enhance the immune system, or target cancer cells.




1

### Exploring the potential of stem cell therapy across a range of medical conditions

Stem Cell therapy can be effective in the following bodily conditions:

- Liver Diseases, Cardiology
- Infertility and Cosmetic Procedures
- COPD and other Lung diseases
- Orthopaedics
- Autoimmune disorders
- Neurological conditions
- Ophthalmic diseases
- Chronic Kidney Diseases

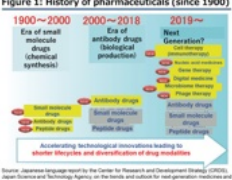


<https://evergoods.com/blog/stem-cell-therapy/>

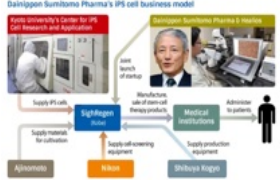
2

### Advances in stem cell research and clinical trials in japan

**Figure 1: History of pharmaceuticals (since 1900)**



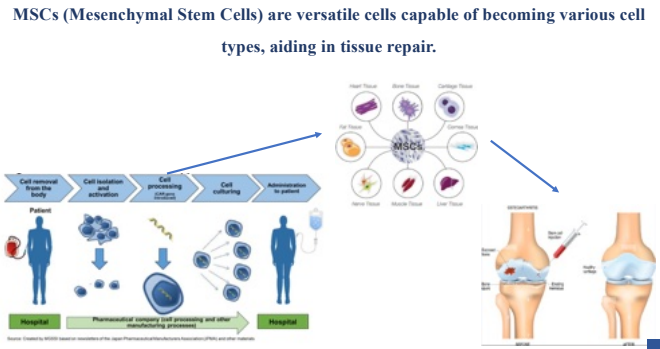
**Dainippon Sumitomo Pharma's IPS cell business model**



Cellular therapy in Japan has rapidly advanced, focusing on utilizing stem cells to treat various diseases. This encompasses applications in regenerative medicine, ophthalmology, oncology, and heart diseases. Japan has established stringent regulations to ensure the safety and efficacy of these therapies

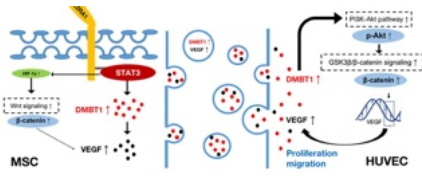
3

### MSCs (Mesenchymal Stem Cells) are versatile cells capable of becoming various cell types, aiding in tissue repair.



4

**HUVECs (Human Umbilical Vein Endothelial Cells) are endothelial cells from umbilical cords, crucial for studying blood vessel formation**



Using HUVECs in co-culture with MSCs allows assessing their ability to promote angiogenesis, a critical process in tissue regeneration. This provides valuable insights into the therapeutic potential of modified MSCs for treating conditions related to vascular insufficiency, such as tissue injuries or cardiovascular diseases

5

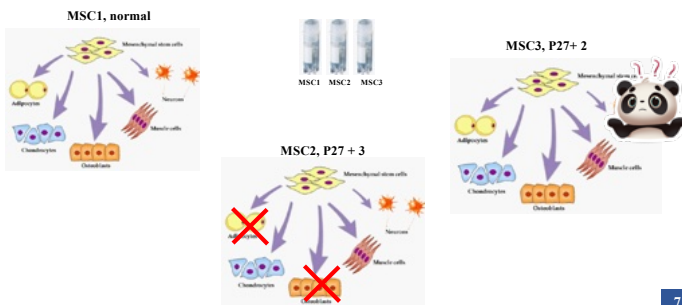
**Exploring modified MSC effects: viability, morphology, and angiogenic potential in co-culture with HUVECs**



- The objective of this study is to investigate the effects resulting from specific modifications applied to MSCs, focusing on their viability, morphology, and angiogenic potential.
- Additionally, the study aims to assess the interactions between these modified MSCs and HUVECs within a co-culture system

6

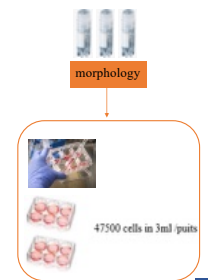
**Three cell populations are being utilized: MSC1 remains unaltered, while both MSC2 and MSC3 have undergone modifications**



7

**Experiment 1 ; compares the morphological changes in MSC2 and MSC3 with reference to MSC1**

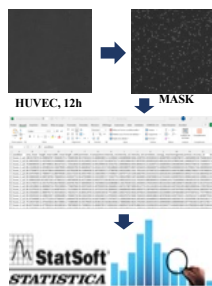
- Cultivate MSCs (MSC1, MSC2, and MSC3) and evaluate their morphological changes.
- Quantify the area of MSCs and determine any significant differences.
- Calculate the Length Width Ratio of MSCs and compare the ratios among the three populations.
- Apply statistical analyses to identify significant variations in morphology.



8

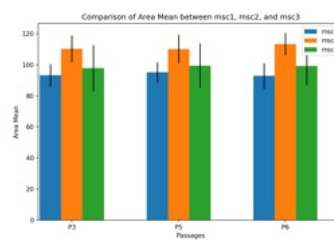
**Microscopic analysis of modified MSCs: morphological insights**

- 1. Image Capture:** Microscopic images were captured over three days with 6-hour intervals, allowing for tracking of MSC changes.
- 2. Digital Analysis:** Using Python, images were processed for 14 parameters, revealing morphological details.
- 3. Statistical Insights:** Through the application of Student's t-tests, comparisons were made among groups, with a focus on the presentation of results for 'area\_mean' and 'Length Width Ratio'.



9

**Cell Area Variation After 24 Hours: Comparing Normal MSC vs. Modified Populations**

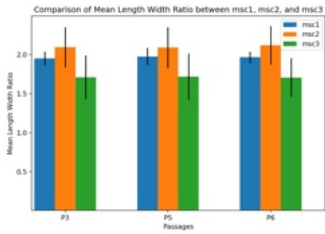


Significant differences in cell areas between the normal population (MSC1) and the modified populations (MSC2 and MSC3).

10

**Length width ratio**

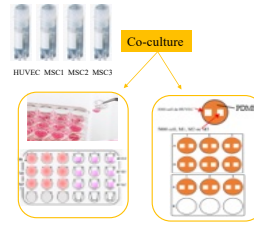
Measures the average of the ratios between the length and width of cells, thereby providing information about the shape and morphology of different cell populations



Both "MSC2" and "MSC3" populations changes in cell shape relative to "MSC1," with variations in the magnitude and direction of alterations across different passages.

11

**Experiment 2 ; involves evaluating angiogenic potential in a co-culture setting**



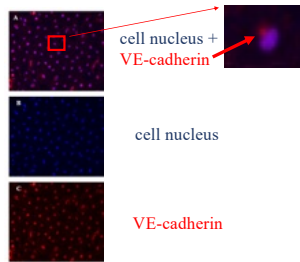
- Establish co-cultures of HUVECs with MSC1, MSC2, and MSC3.
- Allow the co-cultures to incubate for 7 days to enable interactions.
- Perform immunofluorescence staining with DAPI, CD31, and VE-Cadherin markers.
- Examine and compare angiogenic responses among the co-culture groups.

12

**Unveiling viability: Evaluating modified MSCs integrity via HUVEC co-culture and immunofluorescence of CD31 and VE-cadherin**

CD31 and VE-cadherin: Crucial for Blood Vessel Integrity in Co-culture

- Choice of staining: the decision has been made to employ immunofluorescence staining for CD31 and ve-cadherin proteins.
- HUVECs interaction: following a 7-day co-culture with MSCs, staining is applied exclusively to HUVECs.

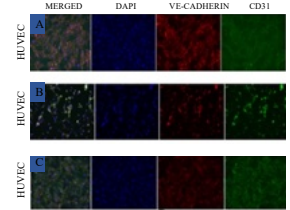


13

**Visualizing HUVEC viability and junctions through immunofluorescence staining**

Immunofluorescence images depict HUVECs cultured for 7 days, stained to highlight nuclei in blue, VE-cadherin in red, and CD31 in green.

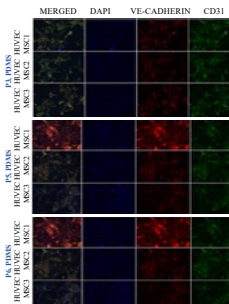
- Uniform nuclear distribution and presence of CD31/VE-cadherin in HUVECs indicated viable cells with intact junctions.



14

**Exploring vascular interactions: influence of modified MSCs on angiogenesis in HUVEC-MSC co-culture via CD31 and VE-cadherin expression**

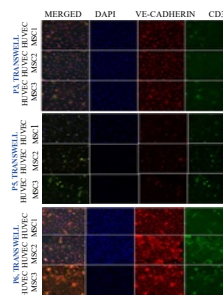
- Uniform Nuclear Distribution of HUVECs.
- The modified MSCs show a reduction in VE-Cadherin expression compared to the normal MSCs
- Reduction in CD31 expression.



15

**Enhanced cellular interactions in transwell co-cultures: exploring spatial influence on HUVEC-MSC dynamics**

- Uniform nuclear distribution
- Distinct VE-cadherin and cd31 mosaic pattern
- Elevated VE-cadherin expression in p6
- Improved cell interaction and structured organization



16

### Conclusion

- ✓ Our exploration of modified MSCs impact on cellular interactions and angiogenesis reveals their potential for organized vascular regeneration.
- ✓ The interplay between morphological changes and spatial arrangement showcases their therapeutic promise.
- ✓ These findings underscore the significance of tailored modifications in advancing regenerative strategies



17



- As my internship at Nagoya University ends, I want to express my sincere thanks. The journey has been rewarding, and I've learned so much.
- I'm grateful for the chance to present our research. It was a team effort, and my colleagues' support and guidance were crucial.
- Their willingness to share knowledge touched me. Their contributions enriched the research and my own learning. I leave with gratitude for the teamwork and knowledge here.
- Thank you for this wonderful experience. I'm excited about the possibility of working together in the future.



### <3> Classes and Events

3-1.	Orientation Sessions, Track A & B....	74
3-2.	Japanese Course Syllabus .....	76
3-3.	Meet-up for JUACEP Students.....	78
3-4.	Hands-on Workshop .....	79
3-5.	Field Trip.....	80
3-6.	The 55 <sup>th</sup> JUACEP Seminar .....	81
3-7.	JUACEP Workshop.....	82

## 3-1. Orientation Sessions for JUACEP Summer Program



### Agenda for Track A

Friday, June 2, 2023

- 14:00     **Reception at ES Hall**
- Check-in. Distribution of the student ID card and Handbook
  - Payment of the admission fee, tuition, campus insurance and Japanese textbook
  - Scholarship
- 14:30     **Orientation at ES Hall**
- Welcome addresses from Prof. Umehara, JUACEP Leader
  - Introduction of Faculty, Staff and the Participants.
- A) Schedule
  - B) Campus map
  - C) Japanese language class
  - D) Meet-up for JUACEP Students
  - E) Hands-on workshop
  - F) Excursion
  - G) Workshop
  - H) Reports and evaluation
  - I) Life information
    - a) Nagoya University ID and Information security training
    - b) University's security department warning
    - c) Medical and health care: Medical services, Health precautions, COVID warning
    - d) Dormitory, Transportations, Accidents, Compliance of law, etc.
- 15:15     **Greetings from Prof. Hara, Director of International Academic Exchange Office**
- 15:30     **Introduction of the Lab Mentors and TAs**
- 15:45     **Photo shooting**
- 16:00     Settlement at each laboratory

## Agenda for Track B



Friday, June 16, 2023

14:00 **Reception at ES Conference room**

- Check-in. Distribution of the student ID card and Handbook
- Payment of the admission fee, tuition, campus insurance and Japanese textbook
- Scholarship

14:30 **Orientation at ES Conference room**

- Welcome addresses from *Prof. Miyazaki, Dean of Graduate School of Engineering* and *Prof. Matsumoto, JUACEP Committee*
- Introduction of Faculty, Staff and the Participants.

- A) Schedule
- B) Campus map
- C) Japanese language class
- D) Meet-up for JUACEP Students
- E) Hands-on workshop
- F) Excursion
- G) Workshop
- H) Reports and evaluation
- I) Life information
  - a) Nagoya University ID and Information security training
  - b) University's security department warning
  - c) Medical and health care: Medical services, Health precautions
  - d) Dormitory, Transportations, Accidents, Compliance of law, etc.

15:30 **Introduction of Lab Mentors and TAs**

16:00 Break

16:30 **Photo shooting and Welcome banquet (with Track A group)**



## 3-2. Japanese Course Syllabus

Course name	Japanese Language									
Teaching staff	Ms. YASUI Sumie									
Course period	June 20 - July 20, 2023									
Weekly timetable	Tuesday 13:45 - 16:15	Thursday 13:45 - 16:15								
Classroom	Engineering Building 3, Minami (EB-3S in the map) 5F Rm.572									
Textbook	<p>“GENKI An Integrated Course in Elementary Japanese” I (The Japan Times)</p> <p>This textbook is a comprehensive approach to developing the four basic language skills (listening, speaking, reading and writing) in order to cultivate overall Japanese-language ability.</p> <p>*Some teaching material will be given in class.</p>									
Course Contents	<p><b>Course outline</b></p> <p>The purpose of this course is to introduce the most essential Japanese words and expressions for everyday life. Students will learn writing system (Hiragana &amp; Katakana), the basic grammar, expressions of Japanese.</p> <p><b>Classroom activities</b></p> <p>Basic communication skills required in everyday life will be taught by introducing new vocabulary, new grammar, and practicing listening, conversation and role-playings.</p> <p><b>Homework and Quiz</b></p> <p>You are expected to submit your homework by the deadline.</p> <p>Quizzes will be given every day in class.</p> <p>1. Hiragana 2. Katakana 3. Dictation 4. Conjugation</p>									
Evaluation	<table> <tr> <td>1. Homework</td> <td>20%</td> </tr> <tr> <td>2. Quizzes</td> <td>30%</td> </tr> <tr> <td>3. Oral exam.</td> <td>50%</td> </tr> <tr> <td></td> <td>100%</td> </tr> </table> <p>More than 80% attendance is required.</p> <p>You will be officially awarded 1 credit of Nagoya University.</p>	1. Homework	20%	2. Quizzes	30%	3. Oral exam.	50%		100%	<p>A<sup>+</sup>=100-95</p> <p>A =94-80</p> <p>B =79-70</p> <p>C =69-65</p> <p>C<sup>-</sup>=64-60</p> <p>F(fail)=59-0</p>
1. Homework	20%									
2. Quizzes	30%									
3. Oral exam.	50%									
	100%									

Course  
schedule

1. 6/20 (Tue)  
Greeting Expressions, Hiragana 1  
Introducing yourself, Noun sentences 1, Occupation, Nationality, Age, Numbers 1-100
2. 6/22 (Thr)  
Classroom expressions, Hiragana 2  
Shopping, Noun sentences 2, Price, Numbers 101-1,000,000
3. 6/27 (Tue)  
Hiragana 3  
Describing where things are, Locations  
Placing an order at a restaurant
4. 6/29 (Thr)  
Hiragana 4  
Talking about your daily life  
Verbal sentences 1, Time reference, Adverbs
5. 7/4 (Tue)  
Hiragana 5  
Invitations, Suggestions, Desires  
Verbal sentences 2, Days/Weeks/Months/Years, Counting
6. 7/6 (Thr)  
Katakana 1  
Talking about your family  
Adjectives, Likes or Dislikes, Degree expressions, Family terms
7. 7/11 (Tue)  
Katakana 2  
Talking about your week-end, Past tense, Time words
8. 7/13 (Thr)  
Katakana 3  
Making a request (Verb-Te-form), Progressive actions,  
Describing your status
9. 7/18 (Tue)  
Asking permission, Prohibition, Negative request  
Describing two things  
Talking about your interests  
Plain form
10. 7/20 (Thr)  
**The Final Examination (speaking)**

### 3-3. Meet-up for JUACEP Students

## Round-Table Discussion with JUACEP participants:

**Information on study abroad in the U.S. & Canada and more!**

16:30 Tue.  
June 27, 2023

at Aerospace Meeting  
Room #347, 3F, EB-2N



We invite the prospective JUACEP participants and engineering students interested in studying abroad to meet our guest students from the U.S and Canada, listen to their short talks, ask questions, and make new friends.

- ❖ To reduce anxieties of your life abroad
- ❖ To know what you need for the beginning of your life abroad
- ❖ To have dependable friends in your life abroad...



Inquiry  
↓  
[office@juacep.engg.nagoya-u.ac.jp](mailto:office@juacep.engg.nagoya-u.ac.jp)  
phone +81-52-789-2799 (内線2799/3179)



Inquiry → [office@juacep.engg.nagoya-u.ac.jp](mailto:office@juacep.engg.nagoya-u.ac.jp)  
phone +81-52-789-2799 (内線2799/3179)  
<https://www.juacep.engg.nagoya-u.ac.jp/>

## Round-Table Discussion for JUACEP Students

2023年6月27日 (火) 16:30～  
工学部2号館3階 航空大会議室

海外留学を考えているみなさん、  
JUACEP留学生と気軽に情報交換しませんか

- ❖ 現地生活での不安を減らしたい...
- ❖ 留学生活を始めるのに必要なものは...
- ❖ 現地で頼れる友達がいたらいいのに...





## 3-4. Hands-on Workshop

*“Disassembly and Assembly of Internal Combustion Engine”*  
July 10<sup>th</sup>, 2023



Date: 13:00 – 16:30, July 10<sup>th</sup>, 2023

Place: Creation Plaza, EI 201

Staff: Prof. Tsuyoshi Inoue, Director of Creation Plaza and CP staffs

Technical staff... Nakakimura, Goto, Isogai, Watanabe and Yamamoto

TA... Amemiya, Kuribara, Nakamura, Tsutsumi, Wang, Kawasaki and Kokuryu

Contents:

1. Opening remarks
2. Introduction to the basis of the Internal Combustion Engine and other engines (History, Characteristics, Operation principle, Demonstration of engines)
3. Disassembling → Assembling → Adjustment
4. Performance test
5. Jet engine demonstration
6. Discussion, questionnaire



### 3-5. Field Trip

Thursday, July 27, 2023

Fee: 2000 yen



Schedule:

Time	Visiting spots	Transportation
9:00	Meeting at Toyoda Auditorium and departure from campus	Hired bus
10:00	Guided tour around Nagoya Port	Chartered ship
12:00	Leaving Nagoya Port and lunch on bus	Hired bus
12:40	[Tentative] Toyota Commemorative Museum of Industry and Technology <a href="https://www.tcmiit.org/english/">https://www.tcmiit.org/english/</a>	
14:30	Leaving the museum	Hired bus
14:50	KIRIN Factory Tours	
16:30	Leaving the facility	Hired bus
17:00	Dinner at GRAN PIATTO	
19:00	Adjournment at Higashiyama campus	5 mins. on foot

\*Schedule above is tentative and may be changed.

\*Wear sports shoes for safety of the tour.



## 3-6. The 55<sup>th</sup> JUACEP Seminar

### **The 55<sup>th</sup> JUACEP Seminar**

第55回 名古屋大学日米加協働教育プログラムセミナー

**11:15-12:30, Wednesday 9 August 2023**  
**TEL Auditorium, 3F, EI Bldg.**

### **Integrated Plasmonic Biosensors: from Critical Care Medicine to Airborne Virus Monitoring**

**Prof. Katsuo Kurabayashi**

**Department of Mechanical and Aerospace Engineering  
Tandon School of Engineering  
New York University, Brooklyn, NY 11201, USA**



**Abstract** Biosensors are devices that combines biological elements with a mechanism to recognize proteins, DNA molecules, or enzymes and produce output optical and electrical signals. Nanoparticle-based biosensors are a type of technology that can detect analyse substances in our body without the need for any labels or additional chemicals. These biosensors are durable, fast, cost-effective, and can easily be integrated into small systems that handle fluids. These biosensors are seen as promising tools for testing diseases right at the point of care, meaning that they can be used in clinics or even at home to quickly diagnose illnesses. However, while they have many advantages, some of these sensors still have limitations when it comes to being both fast and sensitive enough to diagnose critical and life-threatening conditions caused by severe infections, trauma, surgery, or side effects of immunotherapy.

In this talk, the speaker will discuss recent advancements made by his research group and collaborators in developing small biosensors that can perform highly efficient and accurate tests for protein biomarkers. These biosensors are designed to work on a small chip and use a unique atomically thin semiconducting photodetector to detect biomarkers. The speaker's research group has used these biosensors to monitor the levels of sepsis biomarkers and airborne COVID-19 virus particles for critical care medicine and environmental safety.

At the beginning, this talk will briefly introduce the graduate program, international collaborations, and research activities at the New York University Mechanical and Aerospace Engineering Department to the JUACEP student audiences.

**Biography** Katsuo Kurabayashi is a Professor and Chair of Mechanical and Aerospace Engineering at New York University (NYU). Prior to his appointment at NYU, he was a Professor of Mechanical and Electrical Engineering and Computer Science at the University of Michigan, Ann Arbor. He received a B.S. in Precision Engineering from the University of Tokyo, Japan, in 1992, and a M.S. and Ph.D. in Materials Science and Engineering from Stanford University, CA, in 1994 and 1998, respectively. His current research focuses on microfluidic digital immunoassays, optofluidics, nanoplasmonic and biomolecular biosensing, and BioMEMS/microsystems for clinical diagnosis, single-cell study, and analytical chemistry. He has authored and co-authored 180 peer-reviewed papers and holds 11 U.S. patents. He received a 2001 NSF Early Faculty Career Development (CAREER) Award, and the Robert Caddell Memorial Award in 2005, the Pi Tau Sigma Outstanding Professor Award in 2007, the University of Michigan Mechanical Engineering Outstanding Achievement Award in 2013, the Ted Kennedy Award in 2015, and the Wise-Najafi Prize for Engineering Excellence in the Miniature World in 2019 from the College of Engineering at the University of Michigan. He is also a Fellow of the Royal Society of Chemistry (RSC) and the American Society of Mechanical Engineering (ASME).

**Inquiry: JUACEP Office** 日米加協働教育プログラム (Ext. 2799)

JUACEP: Japan-US-Canada Advanced Collaborative Education Program, Graduate School of Engineering

## 3-7. JUACEP Workshop

# The 30th JUACEP Workshop

## 2023 Summer Research Course

Date & time:

9:30~12:30

August 9,  
2023

Venue:

TEL  
Auditorium,  
EI Bldg. 3F  
& Zoom



The participants will deliver presentations (10mins. + Q&A 4mins.) based on the research experience at NU or UCLA.

9:30 – 9:35	Opening address: Prof. S. Hara, Director of International Academic Exchange Office
9:35 – 9:50	(1) Catherine Denisowski: "Development of an Interactive Real Time Android Communication System" Adviser: Assoc. Prof. K. Ogawa, Information & Communication Engineering
9:50 – 10:05	(2) Vi Retault: "Quantum Circuit of Alzette and Applications" Adviser: Prof. T. Iwata, Information & Communication Engineering
10:05 – 10:20	(3) Enzo Luciani "Design of an autonomous glider and prediction of its performances" Adviser: Prof. S. Hara, Aerospace Engineering
10:20 – 10:35	(4) Herman Musumari: "Flow visualization of non-Newtonian fluids - Experimental and Numerical approaches" Adviser: Assoc. Prof. R. Tsubaki, Civil Engineering
10:35 – 10:50	(5) Mohamed Maftah: "Coordination of Drills in Open-Pit Mines: Mathematical & Constraint Programming Formulations", Adviser: Assoc. Prof. T. Sogabe, Applied Physics
10:50~11:05	Completion ceremony  Break time
11:15 – 12:30	Special Guest Talk: Prof. K. Kurabayashi, New York University "Integrated Plasmonic Biosensors: from Critical Care Medicine to Airborne Virus Monitoring"



052-789-2799  
JUACEP Office



# The 30th JUACEP Workshop, Part 2

2023 Summer Research Course Students  
from Polytechnique Montréal

Date & time:

10:00~10:45  
August 25,  
2023

Venue:

TEL  
Auditorium,  
EI Bldg. 3F  
& Zoom



The participants will deliver presentations (10mins. + Q&A 4mins.) based on the research experience at NU.

10:00 – 10:05

Opening address: Prof. Toshiro Matsumoto,  
JUACEP Committee

10:05 – 10:20

(1) Arthur Bawin: “High-order Meshing in Two Dimensions and Applications to Fluid Flows”  
Adviser: Prof. Toshiro Matsumoto,  
Mechanical System Engineering

10:20 – 10:35

(2) Hanane Tissir: “Investigating Interactions between HUVECs and MSCs in Various Co-culture Configurations”  
Adviser: Assoc. Prof. Ryuji Kato, Basic Medicinal Sciences

10:35 – 10:45

Completion ceremony



052-789-2799  
JUACEP Office



## <4> Participation Essays and Questionnaires

4-1. Findings through JUACEP .....85

4-2. Questionnaires .....92

## 4-1. Findings through JUACEP

### My Experience Living in Japan

Vi Retault  
Polytechnique Montréal  
Summer 2023

Supervisor: Tetsu Iwata  
Nagoya University



Friday, June 2nd, 2023. 9 AM. As my Boeing 787 descended onto Chubu Centrair International Airport, the cargo ships departing from the Port of Nagoya seemed almost within reach. Little did I know that I would soon have the opportunity to see them up close, as they were being loaded of containers fetched from an endless, perfectly packed labyrinth of organized logistics. After leaving the airport, armed with my worn-out textbook and timid Japanese skills, I managed to purchase a train ticket that would take me to the buzzing city. It took me instead to the most extraordinary summer of my life.

The first question I was often asked, after how old are you, was why I came to Nagoya, often labeled as the “most boring” city of Japan. But this central hub, home of Japan’s most renowned industries such as Toyota, Mitsubishi, Fuji, Toshiba, Sony, and the list goes on, offered me an authentic view of what living in this country felt like. The city is designed to be as convenient as possible, from a punctual, pristine railway system with high speed trains every ten minutes that will take you anywhere, to konbini open 24/7 with bathrooms and ready made meals, coin lockers, and vending machines strategically located to overcome the summer heat. What struck me the most living there was the unbounded politeness, courtesy and hospitality of the Japanese people.

Throughout my stay, I had the opportunity to embark on numerous trips and meet kind and captivating individuals. Whether it was a simple exchange about the weather or the sharing of life stories, people eagerly engaged in conversation whenever they heard me speaking Japanese. I explored the breathtaking temples and the tranquil gardens of Kyoto, immersing myself in their serene beauty. Climbing Fushimi Inari at the break of dawn, I walked through a mesmerizing path lined with rows of Torii gates that stretched as far as the eye could see, delving into the spiritual realm of the sacred mountain. I got lost in Tokyo’s futuristic streets of Akihabara, while in the narrow streets of Ura-Tenma in Osaka, I discovered hidden izakaya gems. In Nara, I made friends with adorable deer, though I suspect they were fond of me only for the crackers I gave them, because when I ran out, they resorted to chewing on my handbag! My most surreal experience was venturing to Ise, taking the very last train of the day from Nagoya to participate in a Shinto ritual for the summer solstice. At 4 AM, we entered the sea to witness the sun rising above Meoto Iwa, the wedded rocks. Such a wonderful sight!

But my purpose in Japan was not to be merely sightseeing, but rather to immerse myself in the exciting world of quantum computing. I discovered this fascinating research topic and managed to make significant progress towards my PhD, motivated by these awe-inspiring experiences. It’s almost time for me to leave, but I’m already thinking of coming back.

## Findings through JUACEP

**Name:** Mohamed Maftah

**Affiliation at home country:** Department of Mathematics and Industrial Engineering, Polytechnique Montréal

**Participated program:** Summer Course 2023

**Research theme:** Mathematical Optimization

**Advisor at Nagoya Univ:** Prof. Tomohiro Sogabe

**Affiliation at Nagoya Univ.:** Applied Physics | Mathematical Engineering Lab



Participating in the JUACEP program has been truly transformative for me, leaving a lasting impact on both my academic and personal journey. Joining Nagoya University's research community while immersing myself in Japanese culture has been a defining experience.

During my stay, I made significant progress in my PhD project. The research-friendly environment at Nagoya University, along with guidance from mentors and lab mates, fueled innovation, and intellectual growth. Attending presentations by fellow researchers in the mathematical engineering lab twice a week expanded my knowledge and created a sense of shared learning.

Weekends were dedicated to exploring Japan's diverse culture. The efficient subway and train network allowed me to visit cities like Tokyo, Osaka, Gifu, and Inuyama. Museums, temples, parks, and historical sites revealed Japan's rich heritage and traditions.

Engaging with lab mates and peers helped me understand Japanese work culture and collaboration values. This exposure enhanced my cultural sensitivity, global perspective, and interest in learning the Japanese language.

Reflecting on my JUACEP journey, it's clear the program is a milestone shaping my future. Gaining insights from research, academic interactions, and cultural exploration refined my critical thinking and adaptability, essential for my academic pursuits.

Moreover, experiencing different cultures and languages has enhanced my ability to collaborate worldwide, a valuable skill in our interconnected world. The program's impact on my growth and development will continue to influence my journey in academia and beyond.

In conclusion, my time in JUACEP has been all-encompassing, nurturing research, cultural understanding, and a passion for lifelong learning. I'm thankful for the opportunity and excited to contribute to JUACEP's legacy through my ongoing pursuits.



## Findings through JUACEP

**Name:** Catherine Denisowski

**Affiliation at home country:** Electrical and Computer Engineering,  
North Carolina State University

**Participated program:** Summer Course 2023

**Research theme:** Development of an Interactive Real Time Android  
Communication System

**Advisor at Nagoya Univ:** Prof. Ogawa Kohei

**Affiliation at Nagoya Univ.:** Graduate School of Engineering, Information and  
Engineering



Ever since I was in middle school, I have always wanted to study abroad. I wanted to have the opportunity to live in another country and experience another culture, and Japan was one of my top choices due to its opportunities in engineering and rich and unique culture. When I was accepted into the JUACEP program, I was so excited and couldn't wait to go.

My research internship was an incredibly interesting and rewarding project. I worked on developing a system for human-android communication, which allowed a human user to talk to and have a conversation with an android. My work involved using speech recognition, voice activity detection, and response generation with an AI language model to interpret human speech and produce an appropriate response. Throughout my project I was able to not only collaborate and learn from other members in my lab but also get one-on-one support and guidance from my advisor, and this was invaluable for my project's success. Once the base system was completed, it was tested by my lab members and also high school students through the WWL summer lecture and Open Campus events, and it was incredibly rewarding to see the results of my hard work.

When I was not working, I was able to get a glimpse into what life is like in Japan. While there were certain differences in day-to-day life that I was already aware of (such as sorting trash and no tipping), there were smaller differences that I only noticed when I got here. For example, I did not initially realize that people tended to walk on the left side of sidewalks, and I also was surprised that I had to pay my bills at the convenience store. However, I quickly adjusted and did my best to continue exploring. I really enjoyed going to many of the summer festivals, attended a Dragons baseball game at Nagoya Dome, and watched Sumo at the tournament in Nagoya. One activity I particularly enjoyed was karaoke, and I would go many times after work to have a fun and relaxing evening. On the weekends, I explored not only sights in Nagoya such as Nagoya Castle, the aquarium, and the many museums in the city but I also took weekend trips around Japan. These trips included places such as Tokyo, Kyoto, Kamakura, and Nara. These trips were really fun and I was able to see many interesting sights, such as a variety of temples, museums, and even some unique attractions like a monkey park and even the Sanrio theme park!

The events through the JUACEP program itself were incredibly interesting, especially the engine assembly/disassembly workshop and the full day excursion. The port tour, Toyota museum, and Kirin brewery tours were really informative, and it was nice to have another full day to explore Nagoya. I also really enjoyed the Japanese course, and the small class size allowed me to really practice my Japanese directly with our instructor.

This program was an excellent experience, and I can't think of a better way I could have spent my summer. I had a great experience in my lab, as I was able to work on fascinating research and get to know the students in my lab. They were so welcoming and kind to me, and I really enjoyed getting to know them. I was able to experience not only day-to-day life in Japan, but also see the major sights and some more niche ones as well. Additionally, my technical and cultural experiences in this program will be invaluable for my future, especially when it comes to searching for jobs. I am very grateful to have been a part of this program, thank you so much to everyone who made it possible!





## Findings through JUACEP

**Name:** Arthur Bawin

**Affiliation:** Dept. Mechanical Engineering at Polytechnique Montreal (Canada) and Institute of Mechanics, Materials and Civil Engineering at UCLouvain (Belgium)

**Participated program:** Summer Course 2023



**Research theme:** High-order meshing in two dimensions and applications to fluid flows.

**Advisor at Nagoya Univ:** Prof. Toshiro Matsumoto

**Affiliation at Nagoya Univ. (Dept.):** Department of Mechanical Science and Engineering, Graduate School of Engineering

I am grateful for the opportunity to work at Nagoya University. It has been a privilege to immerse myself in the world of research in Japan, and I am leaving with a wealth of unforgettable memories.

While I was already familiar with research, working in a different environment was a refreshing change. The collaboration and exchange of ideas with my Japanese counterparts broadened my horizons and gave me a new perspective on my field of study. One of the highlights of my time here was the warm welcome I received from my colleagues at the laboratory. I felt like a part of the team from day one until the nomikai on the last day of the internship. It was an enriching experience that I will carry with me throughout my academic and professional journey.

During my stay, I had the chance to explore some of Japan's most iconic cities with the other JUACEP interns, including Tokyo, Kyoto, Osaka, and Hiroshima. Each city offered a unique blend of tradition and modernity, and I was able to deepen my appreciation for Japanese culture and history.

Of course, I can't talk about my time in Nagoya without mentioning the food. The culinary delights of Japan are renowned worldwide, and I had the pleasure of savoring some of the most delicious dishes during my stay, including Nagoya's famous hitsumabushi.

Many thanks to the JUACEP program and organizers who made this internship possible and to my colleagues and friends in Nagoya for making me feel at home!

## Findings through JUACEP

**Name:** Enzo

**Affiliation at home country:** Department of Aerospace Engineering, Polytechnique Montréal

**Participated program:** Summer Course 2023

**Research theme:** Educational purpose of designing and building a glider model

**Advisor at Nagoya Univ:** Prof. Susumu Hara

**Affiliation at Nagoya Univ.:** Department of Aerospace Engineering, Graduate School of Engineering, Nagoya University



The JUACEP program was truly a wonderful and life-changing opportunity. Since I began learning Japanese I have been fascinated by this country. I am thankful for having the chance to come here and experience life in Japan, in a great University. The international office staff made a wonderful work to ensure that our arrival went smoothly. The members of my lab were all welcoming and helped me integrate a bit in the Japanese society. I liked working on my project. It was an exciting challenge. I put in practice a lot of my theoretical knowledge in a more practical project. I was really help by one laboratory college that gave me all his practical know-how. That experience was full of lessons.



Even if the work at my lab was interesting, I also took some time to explore Japan. I visited the big cities, Tokyo, Kyoto, Osaka, and obviously Nagoya. I enjoyed taking pictures there, even if not very good at it. Know, I'm preparing for a two week long trip in Kyushu. I am looking forward to it. On top of that, even if the summer is hot in Japan, this also the time of festivals and fireworks. Without the JUACEP program, I might not have had such an opportunity to visit this country.



## Findings through JUACEP

**Name :** Herman Musumari Siaben

**Affiliation at home country (Dept & Univ):** Department of Civil, Geological and Mining Engineering, Polytechnique Montréal, Montréal, Canada

**Participated program:** Summer Course 2023

**Research theme:** Flow visualization of non-Newtonian fluids – The Experimental approach

**Advisor at Nagoya Univ:** Prof. Ryota Tsubaki

**Affiliation at Nagoya Univ. (Dept.):** Department of Civil and Environmental Engineering



“Joining the JUACEP Summer School program has proven to be one of the best decisions I have ever made!”

This program provided me with the opportunity to revisit Japan for the second time and collaborate closely with a remarkably knowledgeable research team led by Professor Ryota Tsubaki. It was a truly unique experience that allowed me to rediscover the beauty of Japan, its rich culture, and its warm-hearted people.

I would like to express my deep appreciation for the exceptional support I received from my advisor. He consistently devoted his time to listening to my ideas and guided me with his profound knowledge and extensive experience. In just a few weeks, I acquired technical skills related to experiments involving PIV (laser) and image analysis and processing using synchronous high-speed cameras. This rapid skill development was both demanding and gratifying, undoubtedly preparing me for my future academic and professional pursuits.

While I had theoretical knowledge on combustion and jet engines, I had never had the chance to gain practical experience that allowed me to comprehend the role of each component within the engine as part of a whole. The hands-on workshop provided an invaluable opportunity to consolidate my previous knowledge, and I only wish we could have more similar opportunities.

I would like to extend my heartfelt gratitude to Tomoko San and Professor Dina Grib for their exceptional organizational skills and support. They made me feel at home right from our initial contact. I recall the challenges I faced in obtaining a train ticket discount, and it was Tomoko San's dedication that made it possible. Thank you for your unwavering support.

Beyond the cherished memories of my travels to various cities, the experiences I gained in Japan will undoubtedly serve as an asset in my future career in Canada.

Lastly, I want to express my sincere thanks to Professor Tsubaki and his wife for welcoming me into their home and for introducing me to the concept of "Ichi-go Ichi-e," which emphasizes the uniqueness of each encounter. This experience has left a lasting impression on me."



## Unveiling Harmony: My Journey of Academic and Cultural Discovery in Japan

**Name:** Hanane TISSIR

**Affiliation at home country:** Biomedical engineering department,  
Polytechnique Montreal

**Participated program:** Summer Course 2023

**Research theme:** Biomedical engineering

**Advisor at Nagoya Univ:** Prof. Ryuji Kato

**Affiliation at Nagoya Univ.:** Graduate School of Pharmaceutical Sciences



My experience with the JUACEP program at Nagoya University has been nothing short of transformative, both academically and personally. Academically, the opportunity to work in the highly developed Laboratory of Cell and Molecular Bioengineering alongside skilled researchers was incredibly enriching. The lab's state-of-the-art facilities and the intellectual rigor have had a profound impact on my professional development.

However, what made the JUACEP experience truly unforgettable was the cultural enrichment that came along with it. The program included organized outings that allowed me to immerse myself in Japanese culture fully. I had the privilege of visiting various museums and cities, each offering a different facet of Japan's rich heritage and technological advancements. These excursions were not just informative but added depth to my understanding of the context in which I was studying and living.

Moreover, my lab mates and other members of the laboratory greatly influenced my perception of Japanese culture. Their professionalism, work ethic, and genuine kindness have left me with an overwhelmingly positive image of the Japanese people. Their willingness to collaborate and share ideas created an atmosphere of mutual respect and enrichment. In summary, the JUACEP program is a perfect blend of rigorous academic pursuit and cultural exploration. I am incredibly grateful for the research skills I have acquired and the cultural insights I have gained. The friendships and connections I've made here are invaluable and have left me excited for the journey ahead in both my career and personal life.



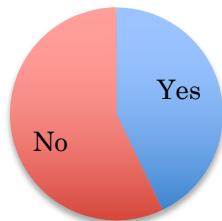


## (b) Questionnaires

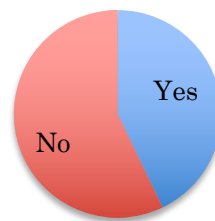
For Q1-4, we asked the same questions BEFORE and AFTER the program.

**Q.1: Are you interested in studying at a Japanese university for PhD?**

Before

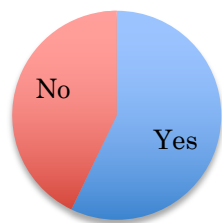


After

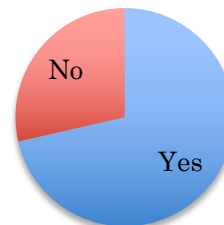


**Q.2: Are you interested in working at a Japanese company in USA?**

Before

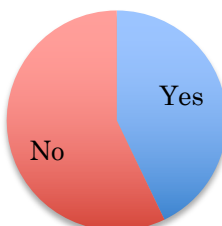


After

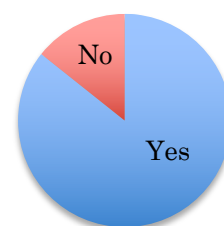


**Q.3: Are you interested in working at a Japanese company in Japan?**

Before

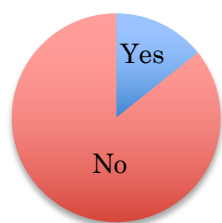


After

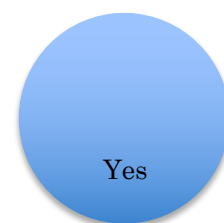


**Q.4: Are you interested in working at a non-Japanese company in Japan?**

Before



After



**Q.5: Which activity did you like? ('Research internship', 'Field trip', 'Engine assembly', 'Japanese course', others)**

- All activities I participated.
- I had a great time during all activities I did.
- I particularly enjoyed the Research Internship program during my time at the JUACEP. Working in the Laboratory of Cell and Molecular Bioengineering provided an incredibly enriching experience, both professionally and personally. I also appreciated the Japanese lectures which added to my understanding of the cultural context in which I was working. This was particularly beneficial in enhancing my overall experience in Japan.
- The combination of rigorous research, a supportive lab environment, and a culturally enriching program made the JUACEP an invaluable experience for me.
- Research internship & Engine assembly.
- I'm always eager to learn more about engineering.

**Q.6: In what did you find difficulty? What could be improved? (Excerpts)**

- A quick resume of the information session could be interesting for people that could not attempt that session. Except that, everything was perfect and the stay at Nagoya went smoothly. Thank you so much for that experience :)
- The program was exceptionally well organized. I would suggest offering several options regarding the hands-on workshop.
- Everything went well during my stay, so it is hard to find improvement points.
- The arrival was on Friday, which is very convenient to meet everybody but then get installed and relax before the work week starts. There was just the right number of common activities with the other JUACEP interns.
- The organizers were very helpful and willing to go above and beyond if ever there was any problem. The engine disassembly was very enjoyable, as I am familiar with the underlying physics, although I could understand that it can be less appealing for students in other fields (even though it remains a great general culture experience!).
- Overall, my experience with the JUACEP program was overwhelmingly positive. However, like any intensive research experience, there were challenges.
- I sometimes had difficulty with more complicated interactions, but this is due to my lack of Japanese language knowledge. Within the JUACEP program, I wish there had been more opportunities to meet and interact with students in other international programs at the university, such as NUPACE or NUSIP. Aside from this, I cannot think of anything else I would improve within the program.
- It was a bit difficult to make friends at the university. The meet-up JUACEP organized with Japanese students interested in studying abroad was very useful for this, but I wish we had those kind of meetings more regularly. I think it would be great to facilitate even more activities between Japanese students and exchange students.

**Q.7: Write comments freely.**

- This program not only allows students to come to NU but also offers them the opportunity to explore Japan and its vast cultural wealth. I believe it would be beneficial if the program could provide grants that fully cover the cost of airfare, especially during the expensive summer season.
- I think it is already summed up! Thank you again for this great Summer!
- I felt very supported throughout my time in Japan and I really enjoyed the program events. My research was a very valuable experience, and I was able to explore Japan in my free time.
- Everything was very good. Thanks!

## <5> Appendices

5-1 Photo Collection.....96

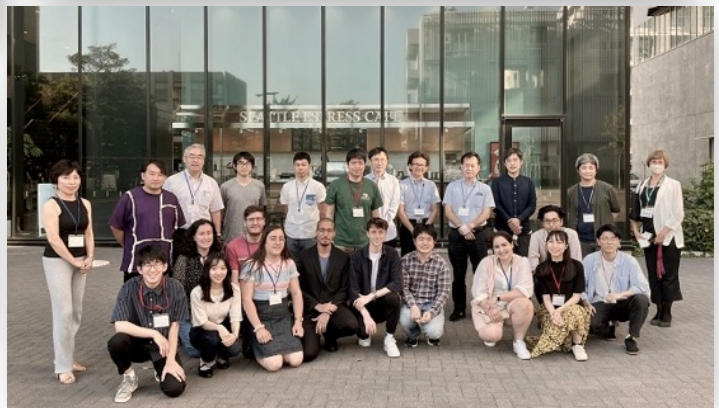
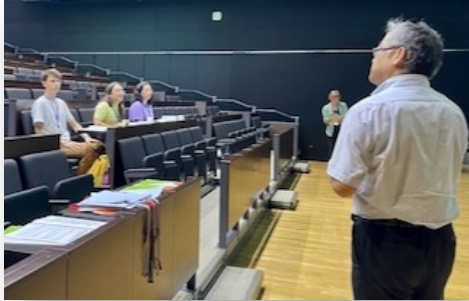
5-2 Building Locations.....99

5-3 Mandatory Deliverables.....100

5-4 Campus Life Information.....101

# 5-1. Photo collection

Orientations and Welcome Banquet, June 2 and 17



Meet-up, June 27



Japanese Language Class



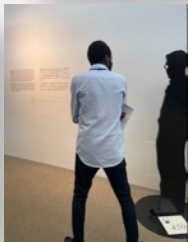
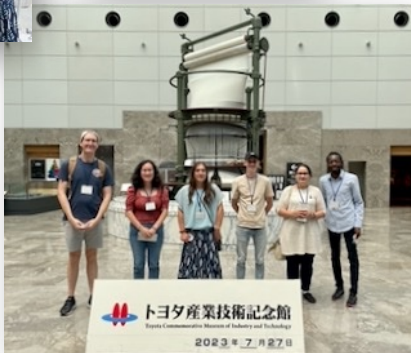




Engine Disassembly/Assembly Workshop, July 10

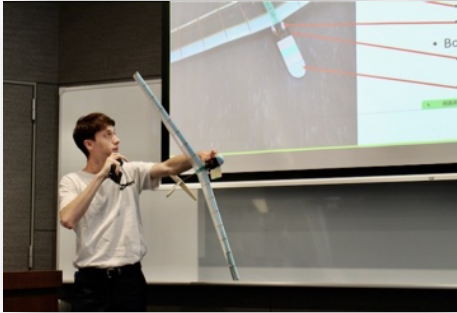
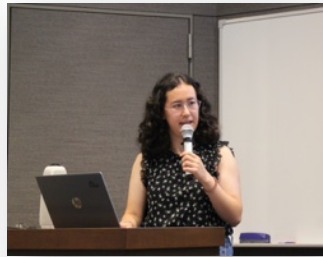


Excursion: Nagoya Port, Toyota Commemorative Museum and Kirin Factory, July 27

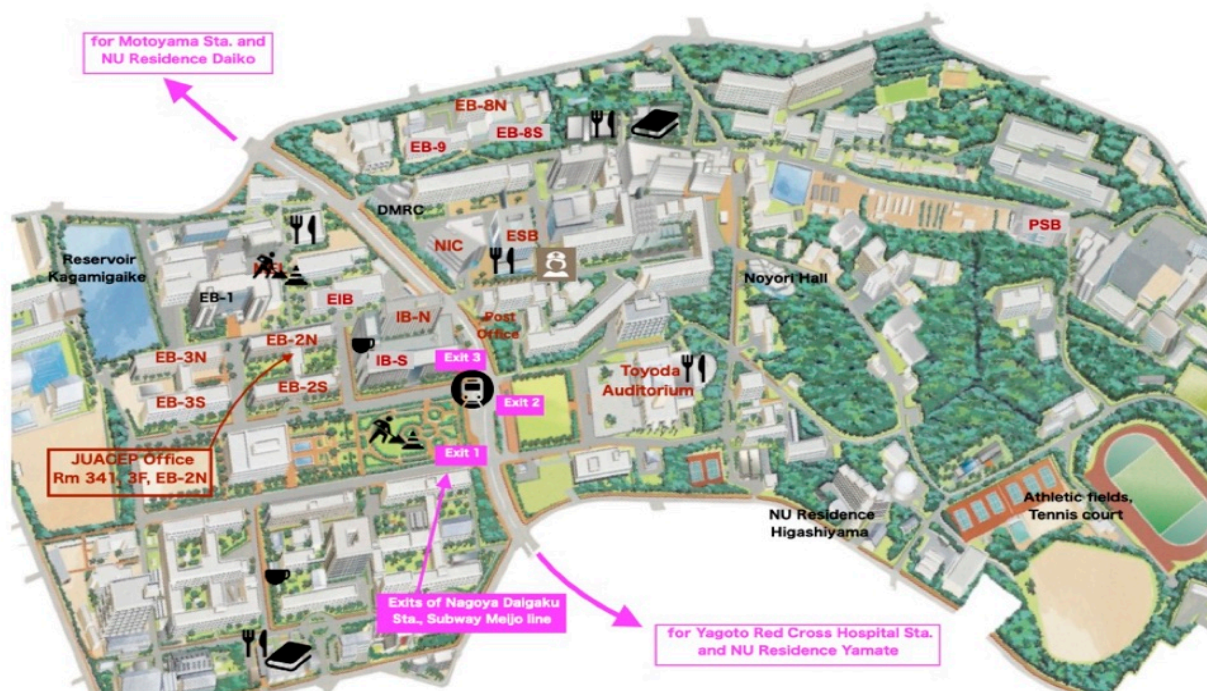




Final Workshops and Farewell Banquet,  
August 9 and 25



## 5-2. Building Locations



Bldg. icon on the map	Building name (in Japanese)	Important places for JUACEP	Lab locations for JUACEP students
EB-2N	Engineering Building 2 North (Kougakubu ni-gou-kan, Kita)	<ul style="list-style-type: none"> <li>JUACEP Office, Room 341, 3F for Stipend on July 3 &amp; Aug. 4</li> <li>Round-table Discussion on June 27 at Room 347, 3F</li> </ul>	Matsumoto Lab, 3F, for Arthur
EB-2S	Engineering Building 2 South (Kougakubu ni-gou-kan, Minami)		Hara Lab, 4F for Enzo
EB-3S	Engineering Building 3 South (Kougakubu san-gou-kan, Minami)	Japanese class at Room 572, 5F	Sogabe Lab, 4F for Mohamed
EB-9	Engineering Building 9 (Kougakubu kiu-gou-kan)		Tsubaki Lab, 2F for Herman
IB-N	Integrated Building North (IB Kita-kan)		Iwata Lab, 9F for Vi
IB-S	Integrated Building South (IB Minami-kan)		Ogawa Lab, GF for Catherine
PSB	Pharmaceutical Science Building		Kato Lab, 3F, for Hanane
ESB	Engineering & Science Building (E-S kan)	Orientations of June 2&16 at ES Conference Room, GF	
EIB	Emergent/Innovative Building (E-I kan)	Hands-on Exercises, July 10, Creation Plaza, 201, 2F	
Toyoda Auditorium	(Toyoda koudou)	Meeting point for the Field Trip, July 27, 9:00am	
Post Office		Money withdrawal, Postal affairs	
	Cafeteria/Convenience Shop		
	Café		
	Book Store		
	Subway Station	Nagoya Univ.: Nagoya Daigaku Sta. Dormitory Daiko: Sunadabashi Sta.	
	Health Administration Office	Open hours: 9:00–12:00, 13:00–17:00, Mon.–Fri. (052)789-3970	



## 5-3. Mandatory Deliverables

★ All of following templates can be downloadable at

<https://www.juacep.engg.nagoya-u.ac.jp/downloads/index.html>

### 1. JUACEP Independent research report

See Appendix-1.

Deadline: **August 10, 2023 for Track A**

**August 30, 2023 for Track B**

Send to... office@juacep.engg.nagoya-u.ac.jp

### 2. JUACEP Research presentation slides

We will collect the PowerPoint/PDF slides at the workshop site on **August 9 from Track A students** and **August 25 from Track B students**. Also, we would appreciate you sending us a backup copy beforehand.

**Evaluation:** your final score is calculated by the points of the research report (1~50pts.) and the presentation at the workshop (1~50pts.) evaluated by your Nagoya Supervisor.

A <sup>+</sup> : 100~95
A : 94~80
B : 79~70
C : 69~65
C <sup>-</sup> : 64~60
F(fail) : 59~0

You will be officially awarded credits from Nagoya University and the transcript to be airmailed to your home university in September 2023.

#### Important:

- JUACEP will publish the participants' research reports and the presentation slides on the website and booklet. When you submit the report, Please LET US KNOW IF YOUR SUPERVISOR PERMITS THE PUBLICATION.
- If you are planning to transfer the credits, kindly discuss it with your home university office and submit the transcript to JUACEP Office.

### 3. Findings through JUACEP

See Appendix-2.

Deadline: **August 10, 2023 for Track A**

**August 30, 2023 for Track B**

Send to... office@juacep.engg.nagoya-u.ac.jp

Please write freely about your experience in Japan inserting pictures.

### 4. JASSO Scholarship obligatory questionnaires, H-1

See Appendix-3. There are "Pre-arrival" part which you already submitted and "After the program" part which you have to submit until **August 9 (Track A)** or **August 25 (Track B)**.

Send to... office@juacep.engg.nagoya-u.ac.jp

\* Please note that all program participants will be processed at the same time, so late submission will affect the certification process for others.

## 5-4. Campus Life Information

### [Housing]

#### **International Residence Daiko (on Daiko campus)**

Address: 1-1-18, Daiko Minami, Higashi-ku, Nagoya 461-0047, Japan

Office Phone: (052)737-8470

Resident Assistant office: rm. 228

WiFi is available.

Please follow the residential guidelines.

### [NU ID & information security]

#### **Student ID Card**

A student ID card is issued upon your arrival. You can use the university libraries with it. The card lets you get student discounts at museums, theatres and so on. This card is delivered at the orientation.

#### **Internet on Campus**

Wireless Internet connection (NUWNET) is available on campus as far as your Nagoya University ID is valid. To connect, at the beginning you have to access to 'Information and Communications Headquarters' <<https://ist.nagoya-u.ac.jp/portal> > using your ID and a default password that are shown in a sealed card delivered at the orientation, then take the online "Information Security Training" and "Information Security Check". To pass the check, you must score at least 80% or repeat the test until you clear 80%. Please do all of required steps described in the web like changing password, otherwise acquired wireless connection will be expired in a week.

See: <https://ist.nagoya-u.ac.jp/>

#### **University Security Department Warning**

Copyright infringement using P2P software is prohibited. University has been strongly warning to all of faculty, staff and students not to use P2P software like Gntella, Share, Winny, WinMX, Xunlei, and so on. It can be easily detected and reflects discredit on University and oneself who used it.

Please never use P2P in University, nor PC in which P2P is installed accessing to University network. You will be detected and warned.

### [Everyday Life]

#### **Refuse Disposal at Nagoya University**

A sorting system for refuse disposal is used at Nagoya University. There are trash bins for "combustible refuse", "incombustible refuse", and recycle bins for "empty bottles", "empty cans", and "PET bottles" all over campus. Recycle companies collect papers and magazines. Used paper products such as used copy paper are collected and recycled. Students are kindly requested to be mindful when they throw away their rubbish and to use the correct bins to help waste reduction and the reuse of recyclable materials.

Also please follow the manners ruled in each laboratory.

#### **Public Transportation of Nagoya City**

1. MANACA マナカ is a pre-paid IC card that can be used for subway/ city bus/ most of train companies through Japan. It is also used at many shops, vending machines, restaurants, and so on.
2. The Student/Commuter Railway Pass allows you to take unlimited rides between stations on the specified route. (Only the person registered on the card may use this pass.)

We recommend to purchase it or add it to your Manaca at a subway station counter by filling out a form and presenting your Student ID Card.

A 3-month Student Railway pass between *Nagoya Daigaku* station and *Sunada-Bashi* or *Nagoya Dome-mae Yada* station will cost you JPY 15,680 (for your reference, round trip will cost you JPY 480 daily.)

3. ONE-DAY TICKETS allow for unlimited rides of city traffic for a day. One-day tickets for all bus, subway, and bus & subway routes are available. Ticket, Donichi-Eco-Kippu, that can be used on Saturdays, Sundays, holidays and the 8th of every month can be also purchased. These tickets include a discounted admission fee for some tourist facilities in Nagoya city such as Nagoya Castle or the Tokugawa Museum.

They can be purchased at any subway station. For further information, refer to the website:

<http://www.kotsu.city.nagoya.jp/>

(3) Besides the city-running transportation, trains and buses of JR, Meitetsu, Kintetsu, Aonami-sen will make your passage easier in/around Nagoya City.

Useful Links:

The following websites provide information on available transport services, time-tables, etc. HYPERDIA:  
<http://www.hyperdia.com/en/>

### **If involved in a Traffic Accident.**

If you are involved in a traffic accident, remain calm and do the following:

1. Dial 119 for an ambulance.
2. Move any dangerous including vehicles, off the road to prevent other accidents.
3. Report the accident immediately, even if it is small, to a nearby police station and obtain a report of the accident.
4. Write down the license plate number of the car concerned as well as the name, address and age of the driver, after requesting to see his/her driver's license.
5. If there are witnesses, write down their names, addresses and telephone numbers.
6. Make detailed notes of the accident and take photographs, if possible.
7. See a doctor, even if you think that you are all right, because sometimes symptoms can take time to occur.
8. Consult your insurance company as soon as possible.

Smartphone zombies often cause accidents. Many cases are especially happened between bikers and walkers and some come fatal. Refrain from using mobile during walking.

### **Compliance with Japanese Law**

During your stay in Japan, anyone who commits a crime, misdemeanor or any other illegal act, will be subject to legal procedures according to Japanese Law. Nagoya University also takes strict disciplinary measures against such person, and may expel the person from university.

#### **1. Prohibition of Narcotics**

In Japan, the possession and sale, for personal use or otherwise, of all narcotics and any illegal substances are strictly prohibited. If offered, refuse them. If leaving Japan temporarily, never agree to look after a stranger's luggage at the airport.

#### **2. Drinking and Smoking Restrictions**

In Japan, people aged under 20 are not allowed to drink or smoke. Smoking is not allowed in many places, including stations, public facilities and within the campus. Nagoya city has special zones where smoking on the street is banned. If found smoking there, you will be fined.

Driving a car, riding a motorcycle or bicycle after drinking any amount of alcohol is a serious offence in Japan, and can also cause accidents. Never drive after drinking. Those who accept a ride in a car that is driven by a drunk driver or those who offer alcohol to a driver are all subject to punishment under Japanese law.

#### **3. Others**

Whilst inside a shop, removing product wrapper and price tag or putting product into the pocket or the bag before actually paying for them are easily treated as a shoplift in Japan. Talking loudly on the street in the midnight should be refrain.

### **Safety Guide**

Japan is not as safe as most people think. There is the risk of crime anywhere in the world, including Japan. Please pay attention to safety and security for yourself and your belongings in any scenes as you do in the US.

### **Culture Shock**

Although "culture shock" is generally understood as a temporary shock felt when confronted by different cultural customs, ways of thinking and behavior patterns, it actually refers to a psychological state of depression caused by a succession of failure experiences in unfamiliar social situations. Culture shock is temporary, and everybody goes through it to some extent in the process of cultural adaptation. General symptoms of culture shock include negative feelings such as: losing self- confidence, feeling depressed, attributing all failure to yourself, feeling that nobody understands you, feeling inadequate, etc. Accordingly, you may lose all motivation to talk with Japanese people or to attend classes. Most of these psychological reactions are, again, very natural in the process of cultural adaptation. Please take time to cope with each single event in your life and to talk with friends, teammates and supervisor, and you will be able to overcome these emotions sooner or later.

### **Differences in "Academic Culture"**

It is widely accepted that different values, behavioral and communication patterns exist from culture to culture. However, we often fail to realize that there are also differences in "academic culture", such as

expected roles of academic advisers and students, classroom communication, evaluation criteria, etc. Such differences can also be a major cause of your stress. For example, the relationship between academic adviser and advisee is considered particularly important at the graduate level education in Japan. Some knowledge of the Japanese academic culture will help you achieve your goal more smoothly.

### **Cope with Stress**

If you feel pressured by stress or lose confidence in your ability to study, you should think about releasing yourself from these negative emotions. Achieving good results in your studies may take a certain amount of time, and ought to be viewed as an accumulative process. Sometimes, you will need to take a break. If you feel tired, do not push yourself too hard and try to enjoy some of your favorite foods, recreation, and physical exercise. It is also recommended that you talk with your friends, academic adviser, or international students' advisors/counselors. Moreover, please do not consider the process of cultural adaptation solely as a cause of stress; you can learn tremendously about various cultures, including your own, from this process.

<Visit the Global Engagement Center Support Team (Advising & Counseling Services)>

If you feel that you cannot deal with stress or feel a sense of isolation or frustration, do not hesitate to ask for help from international counselors at the Global Engagement Center Support Team. There is an international student counselor who will support your personal and psychological concerns. A discussion with an international student counselor can help achieve a useful perspective on culture shock and insights into Japanese culture.

Global Engagement Center Support Team (7th floor, West Wing of IB Bldg.)

<https://acs.iee.nagoya-u.ac.jp>

### **Harassment**

Nagoya University has set up a Harassment Consultation Center to prevent and eliminate the occurrence of any kinds of harassment, such as sexual harassment and academic harassment. Professional counselors deal with inquiries with utmost respect for their clients' feelings and wishes. For English language consultation, you may visit the representative at the Education Center for International Students (ECIS). All consultation will be kept confidential.

Nagoya University Harassment Consultation Center (Appointments by fax or E-mail)

Tel: (052) 789-5806 (9:30-16:00)

Fax: (052) 789-5968

[sh-help@adm.nagoya-u.ac.jp](mailto:sh-help@adm.nagoya-u.ac.jp)

<http://www.sh-help.provost.nagoya-u.ac.jp/english.html>

Contact person at each School (including ECIS)

## **[Medical & Health Care]**

### **Medical Services**

If you suffer from continuous headaches, a loss of appetite, or you cannot sleep well, etc., you should seek the advice of a doctor before the condition gets serious. These symptoms may be signs of fatigue or exhaustion. They may also be psychological or psychosomatic symptoms, which are treatable by specialist doctors. In addition to taking care of your own health, please pay attention to your friends' health and encourage them to see a doctor, if they are feeling unwell.

**(1) The Health Administration Office** See Building Location map.

Students can undergo physical examinations, receive health advice, first-aid and arrange psychiatric counseling at this facility. There is no charge for using any of these services.

Appointments are necessary for psychiatric counseling services. Please call the office,

Tel: (052) 789-3970 or email to [hokekan@htc.nagoya-u.ac.jp](mailto:hokekan@htc.nagoya-u.ac.jp)

### **[Office Hours for Health Services]**

Treatment	Time	Mon	Tue	Wed	Thu	Fri
Physical Examinations & First-Aid	10:00 - 11:30	○	○	○	○	○
	13:30 - 16:30	○	○	○	○	○
Psychiatric Counseling	10:00 - 12:00	○	○	○	○	○
	13:30 - 16:30	○	○	-	○	○

## (2) Calling an Ambulance

Telephone 119 or press the RED button on a public phone for connection. Free of charge.  
This number is also used for requesting fire engine.

## Precautions for Food Poisoning and Infectious Diseases

Great care should be taken with regard to eating habits during the extreme summer weather in Japan. To avoid food spoilage, check the expiration date before buying food, apply heat to raw foods and be careful not to keep food in the refrigerator for an excessive amount of time. To guard against food poisoning, always wash culinary items with hot water.

Also follow the basic hygienic rules to avoid being infected.

World Health organization: <http://www.who.int/en/>

### [Hospitals around Nagoya University]

<b><i>Nagoya Daini Red Cross Hospital (Yagoto Nisseki)</i></b>	Address: 2-9 Myoken-cho, Showa-ku, Nagoya Tel: (052) 832-1121 Mon-Fri: 8:00-11:00 Closed on Sat, Sun, holidays
<b><i>Watanabe Clinic [Internal medicine]</i></b>	Address: 2F Nihonchouzai Yamate-dori Bldg, 3-8-1 Yamate-dori, Showa-ku, Nagoya Tel: (052) 861-3450 Mon-Sat: 9:00-12:00 Mon, Wed-Fri: 16:00-18:00 Closed on Sun, holidays
<b><i>Kai Clinic [Internal medicine, Urology]</i></b>	Address: 32-2 Myoken-cho, Showa-ku, Nagoya Tel: (052) 836-9136 Mon-Sat: 9:00-12:00 Mon-Wed, Fri: 18:00-20:30 Closed on Sun, holidays
<b><i>Yamate Dermatologist</i></b>	Address: 2F Habitation Yamate, 2-9-1 Yamate-dori, Showa-ku Tel: (052) 836-4115 Mon, Tue, Thu-Sat: 9:30-12:30 Mon, Tue, Thu, Fri: 16:30-19:30 Sat: 14:30-17:30 Closed on Wed, Sun, holidays
<b><i>Fujimi Dentist</i></b>	Address: 139 Yagotohujimi, Showa-ku, Nagoya Tel: (052) 835-3200 Mon-Wed, Fri, Sat: 9:30-12:30 Mon-Wed, Fri, Sat: 14:00-19:00 Closed on Thu, Sun, holidays

Copyright © JUACEP 2024 All Rights Reserved

Published in January 2024

Japan-US-Canada Advanced Collaborative Education Program (JUACEP)

Graduate School of Engineering

Nagoya University

Furo-cho, Chikusa-ku, Nagoya 464-8603, Japan

[office@juacep.engg.nagoya-u.ac.jp](mailto:office@juacep.engg.nagoya-u.ac.jp)

<https://www.juacep.engg.nagoya-u.ac.jp>

